From
The Department of Neuropathology, University of Tübingen
and
German Center for Neurodegenerative Diseases (DZNE), Tübingen

Mechanisms of FUS-associated neurodegeneration: Effects of post-translational modifications of FUS

A **Master thesis**
submitted to the faculty of
the Technical University of Graz
in partial fulfillment of the requirements for the degree of

Master of Science

by
Claudia Wallnöfer

Graz, January 2013

1st Supervisor:
Prof. Dr. med. Manuela Neumann
Department of Neuropathology, University of Tübingen and German Center for Neurodegenerative Diseases (DZNE) Tübingen

2nd Supervisor:
Chiara Valori, PhD
Department of Neuropathology, University of Tübingen and German Center for Neurodegenerative Diseases (DZNE) Tübingen

The experiments presented in this Masterthesis were performed at the Institute of Neuropathology, University Hospital Zürich and at the Department of Neuropathology, University of Tübingen and German Center of Neurodegenerative Diseases (DZNE) Tübingen.

Acknowledgments

This Masterthesis would not have been possible without the support and the help of people around me, to only some of whom it is possible to give particular mention here.

I wish to thank, first and foremost, my 1st supervisor Prof. Manuela Neumann, for the possibility to do my Masterthesis in her research group. Especially for her help, patience and the excellent atmosphere during work.

I would like to thank Chiara Valori, for her help, support and friendship. She was always there cheering me up and patiently corrected my writing.

Many thanks also to Jay Tracy, Thorsten Läufer, Petra Frick and other workers at the Institute of Neuropathology/Zurich and DZNE Tubingen.

I cannot find words to express my gratitude to my brother, Stefan Wallnöfer, who was always willing to help me with great patience.

A special thanks also to my sisters, Kathrin and Judith Wallnöfer, who caused me to laugh in good and bad times.

Finally, I would like to thank my parents, Klaus and Christine Wallnöfer, and my grandparents, Alois and Marianne Haaser. They were always supporting me, stood me by in good and bad times and were the one who enabled me to study and going abroad.

THANK YOU

Abstract

Frontotemporal dementia and amyotrophic lateral sclerosis are two neurodegenerative diseases which are, in a subset of cases, characterized by abnormal cytoplasmic aggregations of FUS, a protein that is normally nuclear. Until now, the pathomechanisms which lead to cytoplasmic FUS inclusions are unknown.

In attempt to gain more insights into factors affecting FUS localization, my Masterthesis aimed at determining the impact of phosphorylation and dephosphorylation on the subcellular distribution of FUS. I used site directed mutagenesis to produce FUS expression vectors with phospho- and dephosphomimicking mutations for all the sites where phosphorylation has been previously described. Then I used them to transfect different cell lines and I monitored the localisation of the variant proteins by immunofluorescence.

In HEK 293 cells, the phosphomimicking FUS variants S61D, S84D, S185D and S186D are significantly mislocalised into the cytoplasm. Furthermore, also the dephosphomimicking FUS variants of S185A and S186A showed significantly enhanced cytoplasmic localisation.

Moreover, in HeLa cells all four variants showed a mislocalisation of FUS into the cytoplasm, but this mislocalisation was only significant for the phosphomimicking variants S185D and S186D and for the dephosphomimicking variant S185A.

These results suggest that modifications on specific residues may lead to FUS cytoplasmic localisation in a subgroup of cells, thus supporting the possibility that abnormal post-translational modifications of FUS might be involved in the pathogenesis of FUS-proteinopathies.

Table of Contents

1 Introduction

1.1 Frontotemporal Dementia and Amyotrophic Lateral Sclerosis

Frontotemporal dementia (FTD) is the second most common cause of dementia after Alzheimer disease (AD) and it was described the first time by Arnold Pick in 1892 (Bird et al., 2003). Compared to Alzheimer disease, FTD does not lead to memory and orientation ability impairment, but it is characterized by changes in personality and behaviour and linguistic problems. Due to that, the FTD diagnosis groups three clinical subtypes, behavioural variant of FTD (bvFTD), progressive non fluent aphasia (PNFA) and semantic dementia (SD) (Bird et al., 2003).

FTD occurs often in patients younger than 65 years and can be verified in 15-20 % of patients with dementia (Bird et al., 2003). The incidence is estimated of approximately 3,5-4,1 per 100.000 people between 45 to 64 years and the prevalence is estimated of 10-20 per 100.000 people (Rosso et al., 2003). FTD affects men and women with the same frequency. Most patients die 6-8 years after the first symptoms (Hodges et al., 2003).

Although most FTD cases are sporadic, mutations in several genes may cause familial FTD. It is known that mutations in the genes encoding the microtubule associated protein tau *(MAPT) (Hutton et al., 1998)*, progranulin *(GRN)* (Baker et al., 2006, Cruts et al., 2006), valosin containing protein *(VCP)* (Watts et al., 2004) and charged multivescular body protein 2b *(CHMP2B)* (Skibinski et al., 2005) lead to autosomal inheritance . Some families show also a genetic linkage to a locus on chromosome 9p. This elusive mutation has recently been unravelled as an hexanucleotide expansion in a non-coding region of the gene *C9orf72* (DeJesus-Hernandez et al., 2011, Renton et al., 2011).

The neuropathology is characterized by atrophy in the frontal and temporal lobes (frontotemporal lobar degeneration, FTLD), gliosis and abnormal protein aggregations, also known as protein inclusions.

The molecular classification of FTLD is based on the identity of the distinctive protein in the aggregates (Figure 1) (Mackenzie et al., 2010a).

Around 50% of FTLD cases are characterized by accumulations of the TAR-DNA binding protein 43 (FTLD-TDP), ~ 40% are characterized by accumulations of the protein Tau (FTLD-Tau), 9% are characterized by accumulations of the protein FUS (FTLD-FUS) and in 1% of the cases the pathological protein is unknown (FTLD-UPS) (Diehl-Schmid et al., 2009, Mackenzie et al., 2009, Neumann et al., 2009a, Mackenzie et al., 2010a).

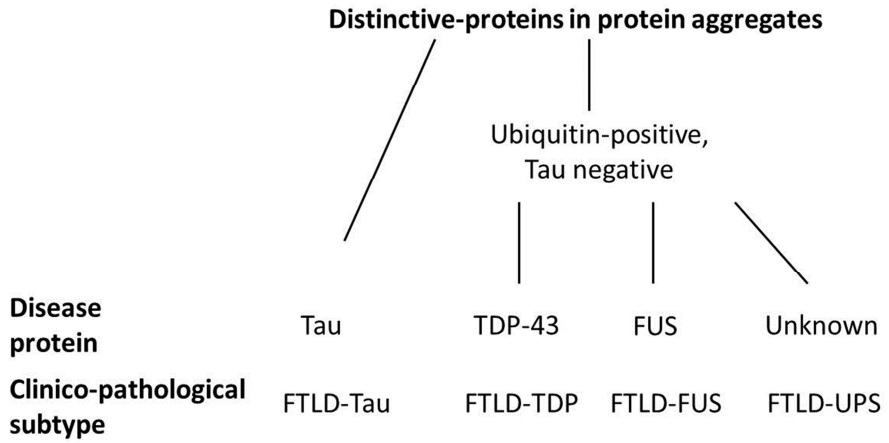

Figure 1. Molecular classification of Frontotemporal lobar degeneration (FTLD).
The molecular classification is based on the identity of the distinctive-protein in the protein aggregates. Around 40% of the protein aggregates are positive for the protein Tau. In the remaining cases the protein aggregates are ubiquitin positive but Tau-negative. 50% of them are positive for TDP-43 (FTLD-TDP), 9% are characterized by the protein FUS (FTLD-FUS) and in 1% of the cases the distinctive pathological protein is unknown.

Amyotrophic lateral sclerosis (ALS) is the most common neuromuscular disease affecting motor neurons. ALS develops mainly in the cerebral cortex, with a loss of the upper motor neurons (UMN), in the brainstem and in the spinal cord, with a loss of the lower motor neurons (LMN). The loss in motor neurons leads to muscle weakness and wasting as well as spasticity and dysphagia (Mitchell and Borasio, 2007).
Patients with ALS have a combination of signs of UMN degeneration, like hyperreflexia and muscular spasticity, and of LMN degeneration, such as muscular atrophy and fasciculations. In most of the patients (two-third) ALS begins in the muscles of the arms or the legs, in one-third of the patients ALS begins in the muscles of the tongue, pharynx and larynx, the one that are needed for speaking and swallowing (Shoesmith et al., 2007, Chio et al., 2009).

ALS mainly occurs in patients between 55 and 60 years and affects more men than women (Ferraiuolo et al., 2011). The average disease course is 3-5 years, after the first symptoms, and patients die due to respiratory failure (Chio et al., 2009). The incidence of ALS has been estimated of 1,5-2,7 per 100.000 people in western countries and the prevalence is estimated of 2,7-7,4 per 100.000 people (Worms, 2001).
As for FTLD, most cases of ALS are classified as sporadic ALS (~90%, SALS), approximately 5-10% of the patients have a positive family history (FALS).
It is known that mutations in genes like *Cu/Zn superoxide dismutase (SOD1), alsin (ALS2), senataxin (SETX), VAMP (vesicle associated membrane protein) associated protein B*

(VAPB), dynactin 1 (DCTN1), angiogenin (ANG), optineurin (OPTN), ubiquilin 2 (UBQLN2), TAR-DNA binding protein (TARDBP) and *fused in sarcoma (FUS)* can lead to FALS (van Langenhove et al., 2012).
As described already in patients with FTLD, 30% of patients with ALS carry also a mutation in the *C9ORF72* gene (DeJesus-Hernandez et al., 2011, Renton et al., 2011).

The neuropathology of ALS is heterogeneous and is characterized by degeneration of motor neurons with ubiquitin positive protein accumulations and reactive gliosis. Most of the ALS cases (>90%) are characterized by accumulations of the protein TDP-43 (ALS-TDP) (Neumann et al., 2006). In ALS patients with a mutation in the *FUS* gene, FUS positive but TDP-43 negative inclusions were observed (ALS-*FUS*) (Kwiatkowski et al., 2009). Another protein is SOD-1, SOD-1 positive inclusions were demonstrated in patients with a mutation in the *SOD-1* gene (ALS-SOD) (Bruijn et al., 1998).

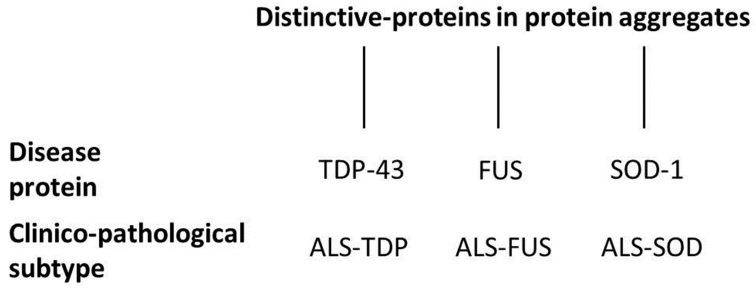

Figure 2. Molecular classification of Amyotrophic lateral sclerosis.
The molecular classification is based on the identity of the distinctive-protein in the protein aggregates. Most of the cases are positive for the protein TDP-43 (ALS-TDP). Some of the cases are positive for the protein FUS (ALS-*FUS*). The third protein is SOD-1, this protein is aggregated in ALS patients with a mutation in the *SOD-1* gene.

1.2 FUS

FUS is a 526 amino acid protein, encoded by 15 exons, ubiquitously expressed and firstly discovered as fusion protein in human cancers (Aman et al., 1996). It is also called TLS (translocated in liposarcoma) or hnRNP P2 (heterogeneous ribonucleoprotein P2) (Crozat et al., 1993, Rabbitts et al., 1993, Calvio et al., 1995). As shown in Figure 3, FUS consists of a 165 amino acids N-terminal domain which is enriched in glutamine (Q), glycine (G), serine (S) and tyrosine (T). Then there is a glycine rich domain with 102 amino acids and an RNA recognition motif (RRM) of 86 amino acids and containing a nuclear export signal. This is followed by multiple arginine glycine-glycine (RGG) repeats (99 amino acids), a zinc finger

motif (31 amino acids) and a C-terminal domain (19 amino acids) (Law et al., 2006). This C-terminal domain is highly conserved and contains a non-classical proline-tyrosine nuclear localisation signal (PY-NLS), which is recognized by transportin (Dormann et al., 2010).

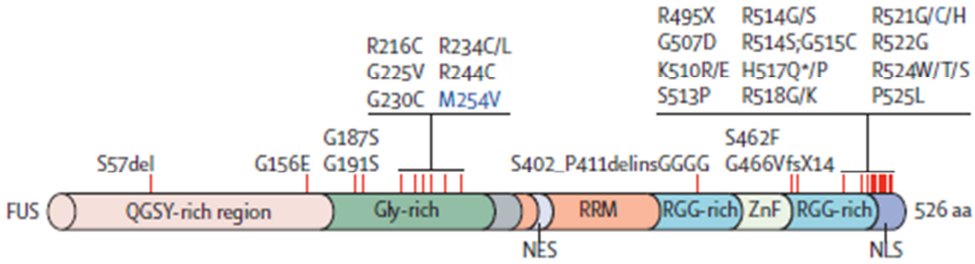

Figure 3. Schematic overview of protein domains of FUS and identified gene mutations associated with ALS and FTLD.
FUS consist of a N-terminal domain, with a glutamine-glycine-serine-tyrosine rich region (QGSY-rich region), followed by a glycine rich domain (Gly-rich). Than FUS contains a RNA recognition motif (RRM), which includes the nuclear export signal (NES). This is followed by multiple arginine-glycine-glycine repeats (RGG-rich), a zinc finger motif (ZnF) and the C-terminal domain, which encodes for a non-classical nuclear localisation signal (NLS). This figure further summarises all identified mutations in *FUS*. Mutations colored in black have been found only in patients with ALS and mutations highlighted in blue have been found also in patients with FTD. Reference: modified from Mackenzie et al. 2010b

FUS is a member of the FET/TET family of multifunctional DNA/RNA binding proteins. Other members of this family are the Ewing Sarcoma protein (EWS), the TATA-binding protein associated factor 15 (TAF15) and the Drosophila Cabeza/SARF protein (Tan and Manley, 2009, Lagier-Tourenne et al., 2010).

As a DNA/RNA binding protein, it can bind RNA, single-stranded DNA and double stranded DNA. It is thought that FUS binds to a GGUG RNA-motif with its zinc finger domain and not with its RRM domain (Lerga et al., 2001, Iko et al., 2004).

FUS is expressed in the nucleus as well as in the cytoplasm and shuttles between those two compartments. In neurons there is a lower level of FUS in the cytoplasm compared to the nucleus and in glia cells FUS is only found in the nucleus (Zinszner et al., 1997, Andersson et al., 2008).

1.2.1 Physiological role of FUS

Until now, the physiological role of FUS is not completely understood although it has been implicated in many biological processes like transcription, RNA maturation, splicing, mRNA transport and translation, micro-RNA processing and DNA repair (Figure 4) (Lagier-Tourenne et al., 2010, Lanson and Pandey, 2012).

There are many different mechanisms as to how FUS is involved in transcription regulation. It binds the DNA-domain of specific nuclear hormone receptors, such as steroid, thyroid or retinoid receptors (Powers et al., 1998). Furthermore it influences the initiation of transcription by interacting with subunits of the RNA polymerase II and the TFIID complex (transcription factor IID), which is a part of the RNA polymerase II preinitiation complex (Bertolotti et al., 1996, Yang et al., 2000). Finally, FUS also binds gene-specific transcription factors, such as the NF-κB subunit p65 and therewith co-activates NF-κB and Sp-1, a transcription factor in B-lymphocyte differentiation (Hallier et al., 1998, Uranishi et al., 2001). However FUS can also inhibit the transcription of genes, for example the transcription of RNAP III genes, though FUS binds the TATA binding protein (TBP) and TFIIIB, a complex which recruits and assembles the polymerase III at the transcription start (Tan and Manley, 2010).

As previously mentioned, FUS is also called hnRNP P2 and it is a subunit of a heterogeneous ribonucleoprotein complex, the H complex. This complex of proteins and RNA prevents the transport of not completely processed pre-mRNA into the cytoplasm. FUS is part of the spliceosome machinery (Rappsilber et al., 2002) and it was found at the 5'splice sites and at the 3'splice sites of pre-mRNA of FUS, so a role in splicing regulation was hypothesized (Wu and Green, 1997, Kameoka et al., 2004). In keeping with this, FUS interacts with different splicing factors, like the serine/arginine-rich proteins SC35 and TASR (Yang et al., 1998, Lerga et al., 2001), hnRNP A1 and C1/C2 (Lerga et al., 2001, Meissner et al., 2003), PTB (polypyrimidine tract-binding protein), or YB-1 (Chansky et al., 2004). In 2008, a group reported that FUS plays also a role in alternative splicing, like in H-ras pre-mRNA splicing (Camats et al., 2008).

More recently, several mRNA and pre-mRNAs have been identified as FUS targets by different groups using cross-linking immunoprecipitation (CLIP) followed by high-troughput sequencing. On a first study performed on HEK293 cells expressing either wild type or mutant FUS (FUS-R521G and FUS-R521H) Hoell et al. could show that wild type FUS binds RNA transcripts at multiple positions and the binding regions are predominantly located in the intronic regions of pre-mRNAs. Furthermore, the RNA-binding properties of mutant FUS are altered and mutant FUS binds a different set of target RNAs (Hoell et al., 2011). Another group investigated the FUS mRNA interaction pattern in neurons and they could show that binding sites of FUS are widespread to and around alternatively spliced exons and it binds

specific binding sites with secondary structures. Moreover, in the promoter region FUS binds to the antisense RNA strand thereby downregulating the transcription of the coding sense RNA strand (Ishigaki et al., 2012). Using iCLIP in mouse brain, Rogelj et al. could demonstrate that FUS binds nascent RNA with a saw-tooth binding pattern. The binding sites are enriched in pentamers containing GGU motifs and are located over the whole length of the nascent RNA. They could also show that FUS is bound to the pre-mRNA as long as the splicing mechanism is active (Rogelj et al., 2012). Furthermore, it has been demonstrated in mouse brain that FUS can bind to the RNA of more than 5500 genes and if FUS is depleted it can influence RNA processing by changing the expression levels of more than 600 mRNAs and by changing the splicing pattern of more than 350 mRNAs (Lagier-Tourenne et al., 2012).

FUS interacts with the RNase III enzyme Drosha, which leads to the initiation of micro-RNA maturation. This finding leads to the suggestion that FUS is also involved in micro-RNA processing (Gregory et al., 2004).
FUS is located in the nucleus as well in the cytoplasm and shuttles between those two compartments. Therefore FUS could also be involved the subcellular location, translation and degradation of mRNA.
Some years ago, different groups reported that FUS is located in RNA-transporting granules in neurons, which translocate RNAs to dendritic spines in response to post synaptic activity. Thus, suggesting that FUS may play a role in neuronal plasticity through modifying mRNA transport and translation in neurons (Belly et al., 2005, Fujii et al., 2005). FUS associates with the NMDAR (*N*-methyl-D-aspartate receptor)-adhesion proteins signalling complex, thus regulate mRNA translation at excitatory synaptic sites (Husi et al., 2000, Belly et al., 2005, Selamat et al., 2009). Nd1-L is an actin-stabilizing protein and is involved in regulation of actin filament assembling during cytokinesis. FUS binds to Nd1-L mRNA and thereby may plays a role in actin reorganization in spines (Fujii and Takumi, 2005).

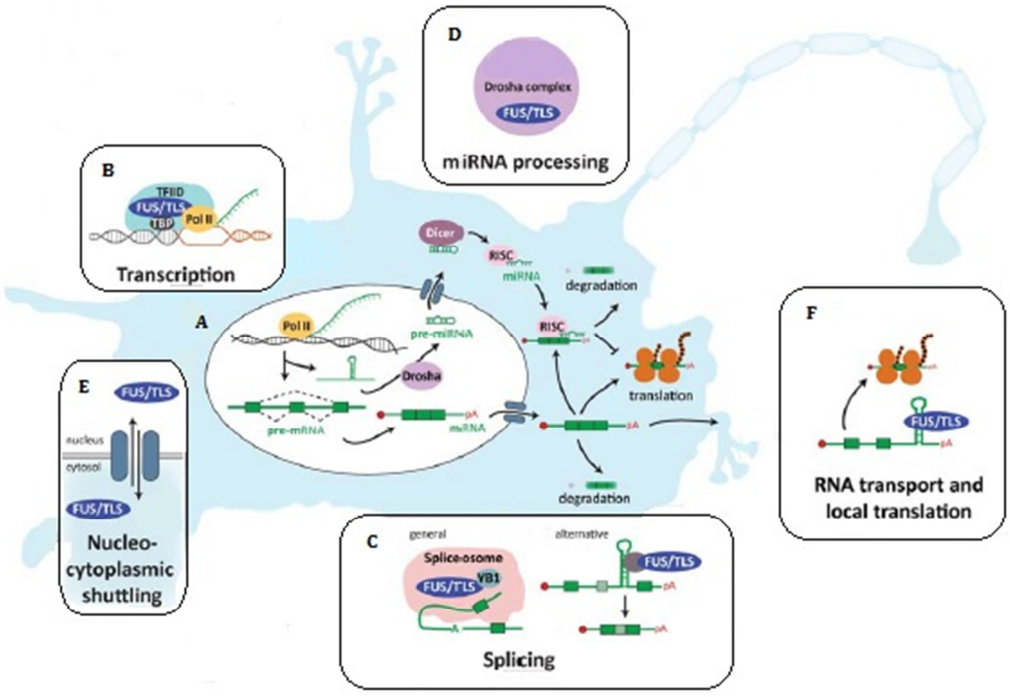

Figure 4. Physiological roles of FUS.
(A) FUS is involved in RNA processing: transcription, translation and/or degradation. (B) FUS can influence the initiation of the transcription by interacting with subunits of the RNA pol II and the TFIID complex. (C) It is involved in general and alternative splicing. FUS is part of the spilceosome and binds specific splicing factors. Alternative splicing: involved in splicing of H-ras mRNA. (D) FUS interacts with Drosha, which leads to the initiation of micro-RNA maturation. (E) FUS is located in the nucleus as well in the cytoplasm and shuttles between those two compartments. (F) Its located in RNA-transporting granules that transport RNA to dendritic spines, is involved in mRNA translation at excitatory synaptic sites and binds the actin-stabilizing protein Nd1-L. Reference: modified from Lagier-Tourenne et al. 2010

1.2.2 FUS-Proteinopathies

Histopathological analysis of human post-mortem brain and spinal cord of FTLD-FUS and ALS-*FUS* patients shows the presence of abnormal protein accumulations, also called inclusions, in neurons and glia cells (Kwiatkowski et al., 2009, Vance et al., 2009). Those inclusions are immunoreactive for FUS, GRP78/BiP (78 kDa glucose-regulated protein/binding immunoglobuline protein), p62 and ubiquitin (Vance et al., 2009). The distribution and morphology of FUS protein aggregates is different between specific types of ALS-*FUS* and FTLD-FUS (Figure 5) (Mackenzie et al., 2010b).

In unaffected cells, FUS staining is almost exclusively nuclear, whereas a reduction in nuclear immunoreactivity can be observed in inclusion bearing cells (Neumann et al., 2009a). However, this redistribution does not lead to complete nuclear FUS depletion, in contrast to what occurs in FTD-TDP, where TDP-43 appears completely redistributed from the nucleus to cytoplasmic inclusion in affected cells (Neumann et al., 2009a).

Moreover, in sequential extraction experiments, FUS is shifted towards the insoluble protein fractions in post-mortem material from FTD-FUS patients, while routine biochemical analysis so far have not revealed additional post-translational changes like truncations or higher-molecular weight species of FUS (Neumann et al., 2009a, Neumann et al., 2011).

FTLD-FUS

FTLD-FUS can be divided into atypical FTLD-U, neuronal intermediate filament inclusion disease (NIFID) and basophilic inclusion body disease (BIBD) (Mackenzie et al., 2011b). FTLD-FUS occurs mainly sporadic, there are no data about FTD associated with *FUS* mutations and analyses of genomic DNA, cDNA and mRNA have so far excluded *FUS* mutations (Neumann et al., 2009a, Neumann et al., 2009b, Urwin et al., 2010).

The pathology of the most frequent FTLD-FUS subtype, atypical FTLD-U, is characterized by neuronal intranuclear inclusions, with different morphology, such as elongated straight, curved or twisted filamentous. In a few cases inclusions have a ring-like structure (Figure 5). They are mainly visible in the frontotemporal neocortex and the hippocampus, and to a lesser degree in the striatum, thalamus and brainstem (Neumann et al., 2009a).

ALS-*FUS*

In the last years, several mutations in the *FUS* gene were associated to ALS cases with FUS pathology and overall, 3-4 % of all FALS cases are due to a mutation of the *FUS* gene (Kwiatkowski et al., 2009, Vance et al., 2009). Post-mortem analysis of brain and spinal cord from patients with ALS shows a severe loss of motor neurons in the spinal cord and to a lesser extent in the brainstem, which shows also demyelination of the corticospinal tracts. Cytoplasmic FUS inclusions are present in the motor neurons of the spinal cord and in dystrophic neurites, the morphology differs between filamentous and granular cytoplasmic inclusions (Figure 5). FUS inclusions can be also observed in other regions, like brainstem, striatum, thalamus and substantia nigra (Rademakers et al., 2010).

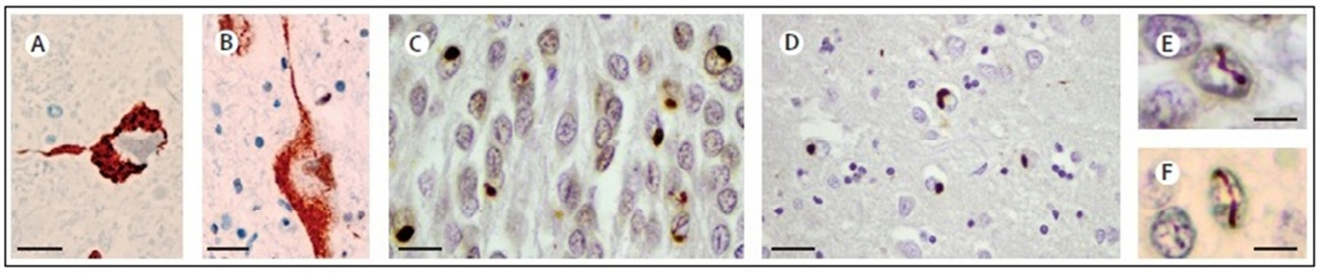

Figure 5. Pathological characteristics of ALS-*FUS* and FTLD-FUS.
FUS immunohistochemistry on specific paraffin-embedded tissues of ALS-*FUS* and FTLD-FUS. In ALS-*FUS* with the Arg521Cys mutation characteristic inclusions with filamentous (A) and granular (B) morphology can be observed. In atypical FTLD-U, a subtype of FTLD-FUS, different FUS positive cytoplasmic inclusions can be observed. In picture C cytoplasmic inclusions are visible in dentate granule cells and in picture D in the frontal cortex. The pictures E and F show characteristic vermiform intranuclear inclusions. Scale bars: 15 µm (A,B), 20 µm (C), 30 µm (D), 8µm (E,F). Reference: modified from Mackenzie et al. 2010b

1.2.3 *FUS* mutations

As already mentioned, ALS with FUS pathology is usually associated with mutations of the *FUS* gene. Until now, around 40 different mutations (Figure 3) have been identified in 4% of familial ALS and in a few sporadic ALS cases (<1%) (van Langenhove et al., 2012). Most of them show an autosomal dominant inheritance pattern, but there is one mutation (H517Q) which shows a recessive pattern (Kwiatkowski et al., 2009). Mutations can be found in families from all over the world and are mostly missense mutations. Most of them are located in the C-terminal domain, especially in the NLS. Another cluster of mutations in the *FUS* gene can be found in exons 3, 5, and 6 which encode for the glycine-rich region (Gly-rich). However, mutations in the Gly-rich region occur more often in sporadic ALS cases than in FALS.

In 2010, Dormann et al. could show that C-terminal *FUS* mutations, like the severe mutation P525L in the NLS of FUS, lead to a disruption of the nuclear localisation motif and thereby to an impaired transportin-mediated nuclear import and a redistribution of FUS to the cytoplasm (Dormann et al., 2010).

Some other mutations are in-frame insertions and deletions and are located in the Gly-rich region, which is encoded by exons 5 and 6, for those functional consequences are not known yet.

Despite the variability of disease onset in patients carrying a *FUS* mutation from 13 years up to 70 years, also within the same families, there is a correlation between the age of onset and nuclear import impairment (Dormann et al., 2010). Patients with the severe P525L mutation, which leads to a greater nuclear import impairment in cultured cells, have a juvenile disease onset (<30 years) and have a faster disease progression than patients with the R521C mutation

(Baumer et al., 2010, Dormann et al., 2010, Yan et al., 2010, Mackenzie et al., 2011a) thus suggesting that nuclear import impairment is a key event in the pathogenesis of FUS-proteinopathies.

1.3 Post-Translational Modifications (PTM) of proteins

The function of a protein can be finely tuned by several post-translational modifications (PTMs), chemical alterations that regulate their activity, localisation and the interaction with other molecules, like proteins, cofactors and lipids.
One of the most important and better characterized PTMs is phosphorylation (Pawson, 2002).

1.3.1 Phosphorylation

Phosphorylation is a reversible PTM that can take place on amino acids containing a hydroxyl group in their side chain, namely serine, threonine and tyrosine. The enzymes that catalyse this reaction are called kinases and use adenosine triphosphate (ATP) as a cofactor and donor of the phosphate group. The reverse reaction, dephosphorylation, is catalysed by phosphatases and leads to hydrolytic removal of the phosphate group (Figure 6).

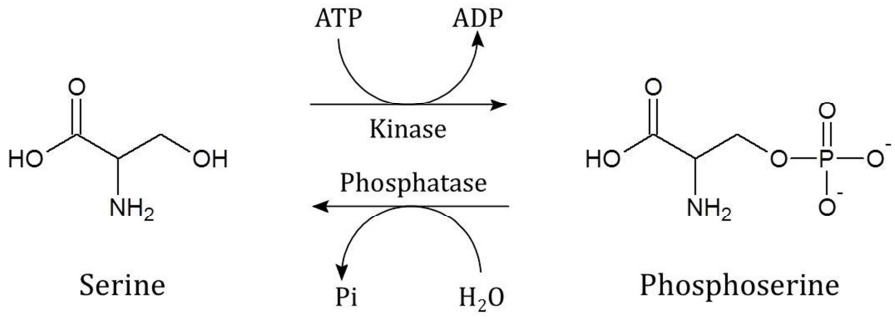

Figure 6. Phosphorylation of serine.
The hydroxyl group of serine is phosphorylated by kinases, using the phosphate group from adenosine triphosphate (ATP). Dephosphorylation is catalysed by phosphatases, which leads to a hydrolytic removal of the phosphate group. Analogue reactions modify the hydroxyl group of threonine and tyrosine. Figure was made with the software ChemSketch.

Phosphorylation is a widely used PTM as it can regulate protein function and activity, either by activation or inactivation of different proteins, though it causes conformational changes in the protein and through that the activity can be regulated (Cohen, 2000, Ubersax and Ferrell, 2007, Thermo Fisher Scientific, 2012).

In neurons, phosphorylation plays an important role in many different signal transduction cascades leading to synaptic plasticity, the cellular basis of cognitive functions. In particular, phosphorylation of receptors of glutamate, the main excitatory neurotransmitter, modulates their activity, thus changing early postsynaptic response. Moreover, gene transcription and protein synthesis are also regulated by phosphorylation of specific signalling components, such as cyclic AMP response element-binding protein (CREB) in gene transcription and the cytoplasmic polyadenylation element binding protein (CPEB) in protein synthesis by the enzyme Ca^{2+}/CaMKII (Berridge, 2012).

1.3.2 Post-translational modifications of FUS

From cell culture and *in vitro* data it is known that FUS can be phosphorylated at serine 26, 42, 61, 84 and 131 by the serine/threonine kinases ATM (ataxia-telangiectasia mutated) (Gardiner et al., 2008), as response to agents causing double-strand breaks, at serine 257 by PKCB iso 2, a serine/threonine kinase of the protein kinase C family (PKC family) (Perrotti et al., 2000) and also at other sites (Table 4). However, the potential role of phosphorylation in the pathogenesis of FUS-proteinopathies has not been investigated so far.

Another important FUS PTM is arginine methylation. In the last years, many groups demonstrated that FUS is dimethylated on arginines in the arginine-glycine-glycine (RGG) domains (Boisvert et al., 2003, Rappsilber et al., 2003, Du et al., 2011). More recently, it has been demonstrated that inhibition of arginine methylation can rescue cytoplasmic mislocalisation of mutant FUS (Tradewell et al., 2012) by enhancing its affinity for transportin (Dormann et al., 2012). Furthermore, FUS inclusions of ALS patients contain methylated FUS, whereas FUS in inclusion of FTLD-patients is not methylated (Dormann et al., 2012).

2 Objectives

Cytoplasmic accumulation of FUS seems to be a key event in the pathogenesis of FUSopathies. In ALS-*FUS*, mutations disrupting the NLS are the cause of this terminal event. Conversely, the mechanisms leading to cytoplasmic accumulation in sporadic conditions are currently unknown.

In the absence of *FUS* mutations, I thus speculated that a post-translational modification can affect FUS localisation in FTLD-FUS and, on the basis of this, the aim of my Masterthesis is to determine the impact of FUS phosphorylation/dephosphorylation on its subcellular distribution. Therefore, I generated by site directed mutagenesis a series of expression vectors to obtain phospho- and dephosphomimicking FUS variants based on described phosphorylation sites of FUS (Table 4). Then, these expression vectors were used to transiently transfect HEK293 cells in order to monitor the subcellular distribution of the encoded proteins by immunofluorescence. The variants with altered subcellular distribution in HEK293 cells were further investigated in HeLa cells to validate the results in a different cell line.

3 Material and Methods

3.1 Generation of FUS expression vectors with phosphomimicking and dephosphomimicking mutations

3.1.1 FUS phosphorylation sites

As preliminary bioinformatic work, I gathered information about known phosphorylation sites from the portal www.phosphosites.org. To mimic phosphorylation at serine and threonine, the negative charge of the phosphate group is mimicked by the carboxy group of an aspartic acid, while the mutation to alanine will resemble the dephosphorylated status. For tyrosine, a proper phosphomimetic amino acid does not exist (Anthis et al., 2009), therefore only mutation to phenylalanine is produced to mimic dephosphorylation.

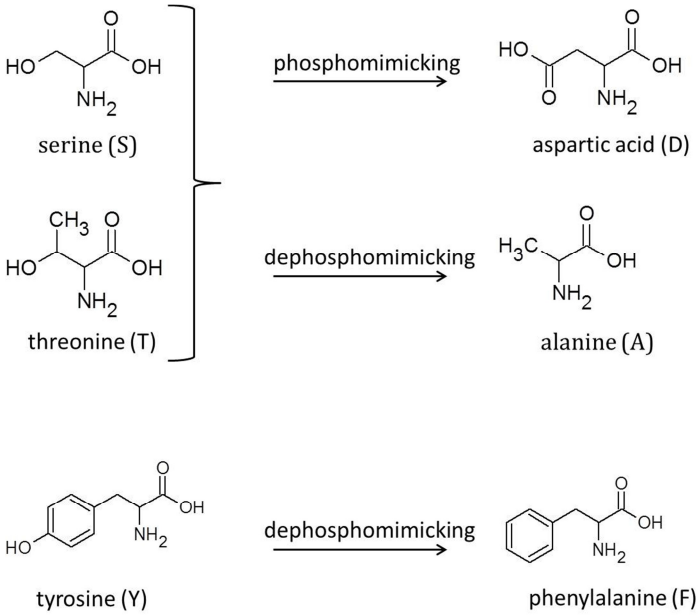

Figure 7. Structures of the amino acids, which were used to establish phosphomimicking and dephosphomimicking FUS expression vectors.
The amino acids serine (S) and threonine (T) will be exchanged to aspartic acid (D) to mimic phosphorylation and to alanine (A) to mimic dephosphorylation. For the amino acid tyrosine (Y), no proper phosphomimetic amino acid exists, therefore the amino acid will be only changed to phenyalanine (F) to mimic dephosphorylation.

3.1.2 Site directed mutagenesis

To generate phosphomimicking and dephosphomimicking FUS expression vectors, the QuickChange® Site-directed mutagenesis Kit was used (Stratagene). FUS expressions vectors were generated from the plasmid pcDNA5/FRT encoding HA-tagged wildtype FUS (pcDNA5/FRT-HA-hFUS wt) according to manufacturer's instructions. The important features of the vector are illustrated in Figure 8.

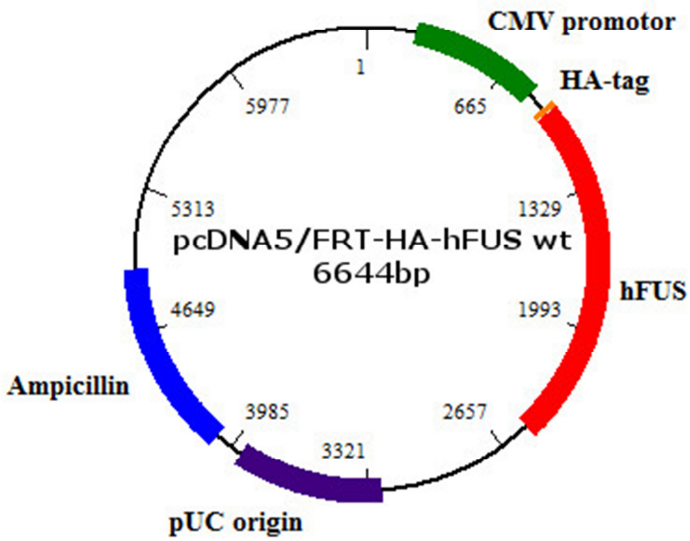

Figure 8. Important properties of the plasmid pcDNA5/FRT-HA-hFUS wt.
FUS expression vectors with phosphomimicking and dephosphomimicking mutations were generated from the plasmid pcDNA5/FRT-HA-hFUS wt by using Site-directed mutagenesis. This plasmid consists of a CMV promoter for high expression levels in mammalian cells, a N-terminal HA-tag for detection of mutated FUS with an HA-specific antibody, human FUS cDNA wild type sequence, Ampicillin resistance gene for selection and a pUC origin (origin of replication of the bacterial plasmid) for the replication.

All forward and reverse primers for mutagenesis were designed by using Stratagenes web-based QuickChange® Primer Design Program. The primers listed in Table 1 and Table 2 were synthetized by Microsynth (Balgach, Switzerland).

Primername	Sequence
S26D fwd	5'-gggcagggctatgaccagcagagcagtcag-3'
S26D rev	5'-ctgactgctctgctggtcatagccctgccc-3'
S42D fwd	5'-cagagttacagtggttatgaccagtccacggacacttc-3'
S42D rev	5'-gaagtgtccgtggactggtcataaccactgtaactctg-3'
S61D fwd	5'-gctattcttcttatggccaggaccagaacacaggctatg-3'
S61D rev	5'-catagcctgtgttctggtcctggccataagaagaatagc-3'
S84D fwd	5'-gcggctatggcagtgaccagagctcccaatc-3'
S84D rev	5'-gattgggagctctggtcactgccatagccgc-3'
S131D fwd	5'-gagtgggagctacgaccagcagcctagctatg-3'
S131D rev	5'-catagctaggctgctggtcgtagctcccactc-3'
S183D fwd	5'-ctatggccaagatcaatccgacatgagtagtggtggtggc-3'
S183D rev	5'-gccaccaccactactcatgtcggattgatcttggccatag-3'
S185D fwd	5'-caagatcaatcctccatggatagtggtggtggcagtgg-3'
S185D rev	5'-ccactgccaccaccactatccatggaggattgatcttg-3'
S186D fwd	5'-gccaagatcaatcctccatgagtgatggtggtggcag-3'
S186D rev	5'-ctgccaccaccatcactcatggaggattgatcttggc-3'
S221D fwd	5'-ggcaggggtggcgatggtggcggcgg-3'
S221D rev	5'-ccgccgccaccatcgccacccctgcc-3'
S257D fwd	5'-ggtggcatgggcggagatgaccgtggtggc-3'
S257D rev	5'-gccaccacggtcatctccgcccatgccacc-3'
S277D fwd	5'-ccaaggatcacgtcatgacgacgaacaggataattcagac-3'
S277D rev	5'-gtctgaattatcctgttcgtcgtcatgacgtgatccttgg-3'
T286D fwd	5'-aggataattcagacaacaacgacatctttgtgcaaggcctgg-3'
T286D rev	5'-ccaggccttgcacaaagatgtcgttgttgtctgaattatcct-3'
S462D fwd	5'-ggggaccaggtggcgatcacatgggggta-3'
S462D rev	5'-tacccccatgtgatcgccacctggtcccc-3'

Table 1. Specific forward and reverse primers to produce phosphomimicking mutations.
Nucleotides in red allow introducing the desired mutations.

Primername	Sequence
S26A fwd	5'-cccgggcagggctatgccagcaga-3'
S26A rev	5'-tctgctgggcatagccctgcccggg-3'
S42A fwd	5'-gacagcagagttacagtggttatgccagtccacgga-3'
S42A rev	5'-tccgtggactggcataaccactgtaactctgctgtc-3'
S61A fwd	5'-ctattcttcttatggccaggccagaacacaggctatgga-3'
S61A rev	5'-tccatagcctgtgttctggcctggccataagaagaatag-3'
S84A fwd	5'-gactggcggctatggcagtgccagagctcc-3'
S84A rev	5'-ggagctctggcactgccatagccgccagtc-3'
S131A fwd	5'-cagagtgggagctacgccagcagcctagcta-3'
S131A rev	5'-tagctaggctgctggcgtagctcccactctg-3'
S183A fwd	5'-tggccaagatcaatccgccatgagtagtggtgg-3'
S183A rev	5'-ccaccactactcatggcggattgatcttggcca-3'
S185A fwd	5'-caagatcaatcctccatggctagtggtggtggcagtgg-3'
S185A rev	5'-ccactgccaccaccactagccatggaggattgatcttg-3'
S186A fwd	5'-gccaagatcaatcctccatgagtgctggtggtggcag-3'
S186A rev	5'-ctgccaccaccagcactcatggaggattgatcttggc-3'
S221A fwd	5'-ggcaggggtggcgctggtggcggcgg-3'
S221A rev	5'-ccgccgccaccagcgccacccctgcc-3'
Y232F fwd	5'-ggcggtggtggtttcaaccgcagcagt-3'
Y232F rev	5'-actgctgcggttgaaaccaccaccgcc-3'
S257A fwd	5'-gtggcatgggcggagctgaccgtggtgg-3'
S257A rev	5'-ccaccacggtcagctccgcccatgccac-3'
S277A fwd	5'-caaggatcacgtcatgacgccgaacaggataattcag-3'
S277A rev	5'-ctgaattatcctgttcggcgtcatgacgtgatccttg-3'
T286A fwd	5'-gataattcagacaacaacgccatctttgtgcaaggcc-3'
T286A rev	5'-ggccttgcacaaagatggcgttgttgtctgaattatc-3'
S462A fwd	5'-ggaccaggtggcgctcacatggggg-3'
S462A rev	5'-cccccatgtgagcgccacctggtcc-3'
Y468F fwd	5'-gctctcacatgggggtaacttcggggatgatc-3'
Y468F rev	5'-gatcatccccgaagttacccccatgtgagagc-3'
Y479F fwd	5'-gtggtggcagaggaggcttgatcgaggc-3'
Y479F rev	5'-gcctcgatcaaagcctcctctgccaccac-3'
Y484F fwd	5'-atgatcgaggcggcttccggggcc-3'
Y484F rev	5'-ggccccggaagccgcctcgatcat-3'

Table 2. Specific forward and reverse primer to produce dephosphomimicking mutations.
Nucleotides in red allow introducing the desired mutations.

For the PCR reaction, 15 ng plasmid as DNA template and 125 ng primers were used, the other PCR components were used according to manufacturer's instructions. In Table 3, PCR cycling parameters are described.

Temperature	Time	Cycles
95°C	30 seconds	1
95°C	30 seconds	
60°C	1 minute	16
68°C	7 minute	
68°C	3 minute	1
4°C	endless	

Table 3. PCR cycling parameters

To digest the original parental DNA template, the reaction mixture was incubated with the enzyme DpnI for 1 hour. Then, 1 µl of DpnI-treated DNA was used to transform XL1-Blue supercompetent cells by heat shock at 42°C for 45 seconds. After adding 500µl S.O.C. medium (Super Optimal broth with Catabolite repression medium, Invitrogen) the liquid culture was incubated at 37°C for 1 hour at 220 rpm and finally, spread onto two agar plates. To ensure optimal colony densities, two different amounts of culture were plated, in particular 150 µl were spread on the first plate and the remaining culture (~ 300 µl) on the second plate. Both were then incubated at 37°C over night. Agar plates were prepared by dissolving and autoclaving 16 g LB Agar (Invitrogen) in 500 ml dH_2O. To select for transformed XL-1 Blue cells, ampicillin (50 µg/ml) was added after heat sterilization.

3.1.3 Plasmid DNA purification (Miniprep)

For plasmid DNA purification, overnight cultures were prepared. Therefore, single colonies were inoculated in 3 ml LB Medium (Invitrogen, 500 ml: 10 g LB Broth Base + 500 ml dH_2O) with Ampicillin (50 µg/ml) and incubated overnight at 37°C with shaking at 220 rpm.
The culture was centrifuged at 4600 rpm for 15 min at 4°C to obtain a bacterial pellet used for subsequent plasmid DNA purification with the Qiagen Miniprep Kit according to Manufactor's instructions.
Finally, yield and purity of the purified plasmid DNA were measured with a UV/Vis NanoDrop spectrophotometer.

3.1.4 Sequencing

To confirm the presence of the desired mutation and to exclude randomly introduced mutations, selected plasmids were sent to the in-house sequencing service. The following primers were used for sequencing: CMV forward 5'-CGCAAATGGGCGGTAGGCGTG-3' and BGH reverse 5'-TAGAAGGCACAGTCGAGG-3'. The chromatograms were analysed with the program CLC Main Workbench 6.

3.1.5 Plasmid DNA purification (Midiprep)

To produce higher amounts of plasmid DNA for transfection, a small amount of each frozen bacterial culture was inoculated as described in 3.1.3 in 50 ml LB Medium and allowed to grow overnight at 37°C under shacking. Once recovered the bacteria by centrifugation, the plasmid DNA was purified from the pellet with Qiagen Hispeed Plasmid Midi Kit according to Manufactor's instructions.

3.2 Cell culture

3.2.1 Cell culture

T-Rex^{TM}-Human embryonic kidney (HEK) 293 cells (Invitrogen) and Human cervical carcinoma cells (HeLa) were cultured in Dulbecco's modified Eagle's medium supplemented with 10 % foetal calf serum (FCS, Invitrogen) and penicillin/ streptomycin (100 units penicillin and 0,1 mg streptomycin per ml; Sigma Aldrich). Medium for the HeLa cells was additionally supplemented with 2 mM Glutamax (Invitrogen). HEK293 and HeLa cells were grown in a humidified 5 % CO_2 atmosphere at 37°C to 90 % confluence.

To maintain the culture, the cells had then to be harvested and seeded at a lower density in a new flask. Therefore the cells were incubated with 0,05 % Trypsin and 0,5 mM EDTA (Gibco) until they detached from the cell culture flask. To stop the reaction, 3 fold amount of cell culture medium was used. 1/10 of the resulting cell suspension was plated into a new cell culture flask.

3.2.2 Transfection

For transfection, HEK293 cells and HeLa cells were used. 40.000 cells were seeded in 24-well plates containing a glass coverslip and allowed to recover overnight. To achieve cell adhesion on glass, the coverslips were pretreated with 50 µg/ml poly-L-lysin solution (Sigma-Aldrich) overnight.

Transfection of HEK293 cells

Transfection was carried out with Calcium-phosphate method. For each well, 600 ng of plasmid DNA in 35 µl of transfection mix was used.

Each transfection was performed in duplicate and the transfection mix was prepared in small excess to ensure the availability of the exact quantity in each well. Briefly, 40 µl of transfection mix were prepared by adding 1.37 µg plasmid DNA diluted in 20 µl 0.25 M $CaCl_2$ drop wise to 20 µl of HBS 2x (Hepes buffered saline: 280 mM NaCl, 100 mM HEPES, 1.5 mM Na_2HPO_4, pH 7.1) followed by incubation for 15 min at room temperature. Then 35 µl were added dropwise to each well and incubated for 7-8 hours at 37°C. Media was finally replaced by fresh medium and the cells were incubated for 72 hours.

Transfection of HeLa cells

Transfection was carried out with Effectene Transfection Reagent (Qiagen) according to Manufactor's instructions. Therefore 200 ng of plasmid DNA was used. After adding the transfection mix to each well, the cells were incubated for 7-8 hours at 37°C. Afterwards the medium was replaced by fresh medium and the cells were incubated for 72 hours.

3.2.3 Double-Immunofluorescence

Antibodies

As primary antibody a rat monoclonal anti-HA antibody (clone 3F10, provided by Dr. Elisabeth Kremmer, Helmholtz Center Munich; 1:500) was used. Secondary antibody was the goat anti rat Alexa Fluor 594 (Invitrogen, 1:500).

Staining procedure

For immunofluorescence, the cells were briefly rinsed with phosphate buffered saline (PBS) than fixed with 4 % formaldehyde (Sigma-Aldrich) in PBS for 15 min at room temperature. After 3 washes with PBS for 5 min, the cells were permeabilized for 5 min with 0.25 % Triton X (Sigma-Aldrich) in PBS to enhance the antibody penetration across the membrane. Then cells were briefly washed with PBS and subsequently incubated for 1 hour in blocking buffer (0.1 % TritonX + 2 % FBS in PBS) to block all unspecific binding sites. After this, cells were incubated with the primary antibody diluted in blocking buffer for 3 hours at room temperature or overnight at 4°C and washed 3 times for 5 min with PBS. Incubation with the secondary antibody diluted in blocking buffer was performed for 1 hour at room temperature and washed again 3 times for 5 min with PBS. To visualize the nuclei, cells were incubated

for 10 min with 1 µg/ml of the nuclear die Höchst33342 in PBS and washed 3 times for 5 min with PBS. Coverslips were mounted onto glass slides using fluorescence mounting medium (Dako).

Images were taken utilising Olympus BX-UCB fluorescence microscope and pictures were made with the cooled CCD color camera F-View *II* (Soft imaging system). For image analysis, the software analysis^D was used.

3.2.4 Data collection and statistics

To establish whether FUS variants lead to a different subcellular distribution, the percentage of transfected cells showing cytoplasmic immunoreactivity was calculated. For each construct, the experiment was performed two times independently and within each experiment transfection was carried out in duplicates. For each experiment with HEK293 cells, 5 images were taken randomly and approximately 100-200 transfected cells were counted and evaluated, while for each experiment with HeLa cells, 10 images were taken randomly and approximately 100 transfected cells were counted and evaluated. Furthermore, in each experiment, transfection with the plasmid encoding for FUS wild type was performed as control. Statistical analysis of the results was then performed by one-way analysis of the variance test (ANOVA) followed by Bonferroni post hoc test for comparison between groups using the software's Microsoft EXEL and GraphPad Prism 5. Significance level was set at $p<0.05$.

4 Results

4.1 FUS phosphorylation sites

The portal www.phosphosites.org was used to search for known phosphorylation sites of FUS and the results of this bioinformatic work are summarized in Table 4.

site	references	kinases	phosphomimetic	dephosphomimetic
S26	Gardiner et al., 2008	ATM	S-> D	S-> A
S42	Gardiner et al., 2008	ATM	S-> D	S-> A
S61	Gardiner et al., 2008	ATM	S-> D	S-> A
S84	Gardiner et al., 2008	ATM	S-> D	S-> A
S131	Gardiner et al., 2008	ATM	S-> D	S-> A
S183	http://www.phosphosite.org/siteAction.do?id=15426462		S-> D	S-> A
S185	http://www.phosphosite.org/siteAction.do?id=15426465		S-> D	S-> A
S186	http://www.phosphosite.org/siteAction.do?id=15426467		S-> D	S-> A
S221	a) (Rigbolt et al., 2011) b) http://www.phosphosite.org/siteAction.do?id=12217072		S-> D	S-> A
Y232	http://www.phosphosite.org/siteAction.do?id=5872884			Y-> F
S257	(Perrotti et al., 2000)	PKCB	S-> D	S-> A
S277	a) (Mayya et al., 2009) b) http://www.phosphosite.org/siteAction.do?id=1232881		S-> D	S-> A
T286	a) (Hsu et al., 2011) b) (Mayya et al., 2009)		T-> D	T-> A
S462	(Wu et al., 2010)		S-> D	S-> A
Y468	a) http://www.phosphosite.org/siteAction.do?id=27185 b) (Jorgensen et al., 2009)			Y-> F
Y479				Y-> F
Y484	http://www.phosphosite.org/siteAction.do?id=4118620			Y-> F

Table 4. Specific sites of FUS of which expression vectors with phosphomimetic and dephosphomimetic mutations were produced.
ATM (ataxia-telangiectasia mutated) is a serine/threonine protein kinase. PKCB iso 2 is a AGC kinase of the PKC family. S= serine, T= threonine, Y= tyrosine, A= alanine, D= aspartic acid, F= phenylalanine

4.2 Generation of phospho- and dephosphomimicking FUS expression vectors

FUS expression vectors were produced by site directed mutagenesis, followed by cloning and DNA purification with a Miniprep kit as described in material and methods. Figure 9 describes the typical results of DNA quality and concentration measured by Nanodrop. For efficient transfection, protein contamination should be low, therefore the ratio of the

absorbance at 260 nm (wavelength of absorbance for nucleic acid) to 280 nm (wavelength of absorbance for protein) should be above 1.8.

Report | Test type: Nucleic Acid | 23.02.2012 10:48 | Exit

Report Name | Report Full Mode: Ignore

Sample ID	User ID	Date	Time	ng/ul	A260	A280	260/280	260/230	Constant	Cursor Pos.	Cursor abs.	340 raw
003-cl.1	Default	23.02.2012	10:41	561.18	11.224	5.900	1.90	2.27	50.00	230	4.952	0.053
003-cl.2	Default	23.02.2012	10:42	-2.67	-0.053	-0.036	1.48	0.93	50.00	230	-0.058	-0.036
003-cl.2-2nd	Default	23.02.2012	10:43	556.71	11.134	5.846	1.90	2.24	50.00	230	4.961	0.093
003-cl.3	Default	23.02.2012	10:44	382.88	7.658	4.218	1.82	1.80	50.00	230	4.264	7.684
003-cl.3-2nd	Default	23.02.2012	10:45	578.73	11.575	6.084	1.90	2.29	50.00	230	5.060	-0.483
003-cl.4	Default	23.02.2012	10:46	688.82	13.776	5.280	2.61	2.94	50.00	230	4.691	28.700
003-cl.4-2nd	Default	23.02.2012	10:47	592.08	11.842	6.189	1.91	2.25	50.00	230	5.264	0.010

Figure 9. DNA concentration of S26D measured with UV/Vis Spectrophotometer.
After site directed mutagenesis 4 clones were picked, the DNA with the Qiagen Miniprep Kit purified and DNA concentration measured. For all 4 clones the ratio of the absorbance is above 1.8. S26D is used in this figure as a representative for all the other expression vectors.

All 4 clones have DNA concentration between 550 ng/µl and 690 ng/µl. The ratio for the quality of the DNA is above 1.8 for all clones.

After the measurement of the DNA concentration, the samples were sent for sequencing to confirm the specific exchange of the desired nucleotide. In Figure 10 the resulting chromatogram for the plasmid FUS S26D clone 1 is shown, as an example of the type of analysis performed for all other plasmids. The nucleotides highlighted in pink display a conflict with the wild type FUS sequence thus indicating a mutation from TC in the wild type to GA in the mutant. This implicates that the analysed plasmid correctly encodes the desired aspartic acid (genetic code GAC) instead of a serine (genetic code TCC) at position 26.

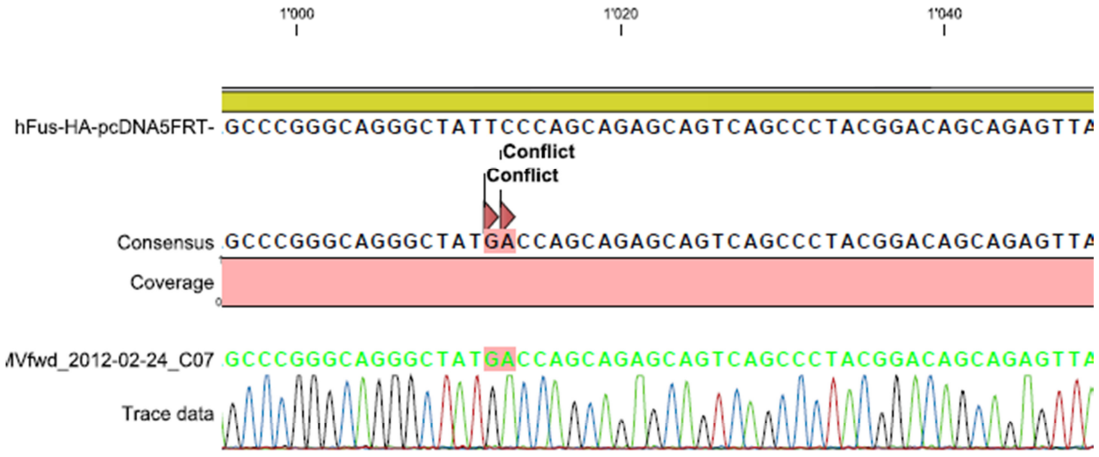

Figure 10. Sequencing of FUS expression vector S26D.
The sequence of the produced FUS expression vector S26D was matched with the sequence of the wild type FUS expression vector. The letters in pink are showing the 2 amino acids which got changed.

The expression vectors with the specific mutations and with no other conflicts were used for cell culture experiments.

4.3 Analyses of subcellular localization of phosho- and dephosphomimicking FUS expression vectors in cell culture

4.3.1 HEK293 cells

To test whether phosphorylation has an effect on the subcellular distribution of FUS, I transiently transfected HEK293 cells with the plasmid encoding wild type FUS and with the plasmids with phosphomimicking and dephosphomimicking mutations. As described in Materials and Methods, cells were stained and visualized with a fluorescence microscope to calculate the percentage of cells showing cytoplasmic FUS immunoreactivity.

As expected HA-tagged wild type FUS (HA-FUSwt) is localised almost exclusively in the nucleus, I could observe only in 4 % of transfected cells FUS in the cytoplasm (Figure 11A and B).

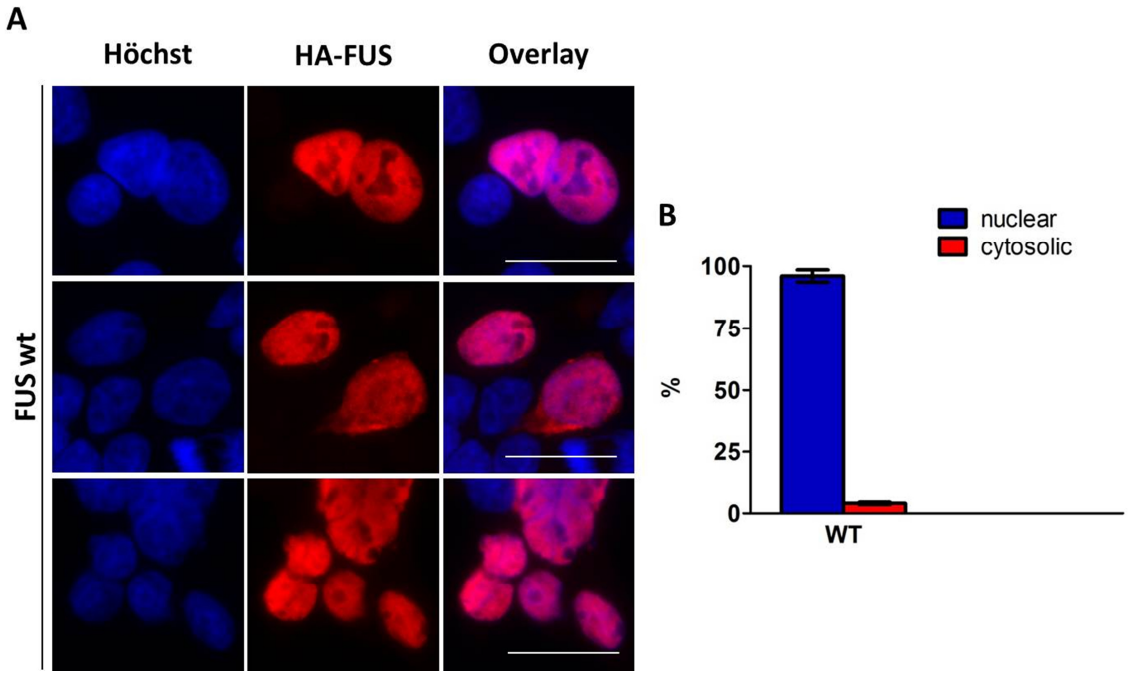

Figure 11. Double immunofluorescence and statistic of HEK293 cells transfected with HA-tagged wild type FUS.
A. Double immunofluorescence. Representative pictures of HEK293 cells transfected with HA-tagged wild type FUS expression vector for 72 hours. Cells were stained with an HA-specific antibody (red) and with "Höchst" to visualize the nuclei (blue). Stained cells were analysed with a fluorescent microscope. HA-FUSwt is located mostly in the nucleus in few cells HA-FUSwt is translocated into the cytoplasm. Scale bar, 25 µm
B. Quantification of transfected cells on the basis of the location of HA-tagged wild type FUS. Transfection was carried out two times and of each, 5 images were taken randomly and 246 transfected cells were counted. Counted cells were divided on the basis of the HA-FUS protein localisation into nuclear and cytoplasmic. Bars represent the mean percentage of cells of HA-FUS in the cytoplasm and nucleus. Error bars indicate standard deviation.

The following figures show the results obtained transfecting all generated expression vectors. HA-FUSwt which is shown in Figure 11 was used as a reference and all expression vectors were compared with this reference.

The first investigated amino acids were serine 26 (S26, Figure 12) and serine 42 (S42, Figure 13). Both proteins with either phosphomimicking or dephosphomimicking mutation are located almost exclusively nuclear only a few cells showed a translocation of the mutated FUS into the cytoplasm.

In a second series of experiments, I examined the impact of mutations on sites serine 61 (S61) and serine 84 (S84). Interestingly, both HA-FUS S61D and S84D are localized in the cytoplasm in a significantly higher number of cells, rather than HA-FUSwt (Figure 14A-D, Figure 15A-D), a phenomenon that does not occur in the corresponding dephosphomimicking

proteins. The significance level for the difference between HA-FUSwt and HA-FUS S61D is $p < 0.001$ and for HA-FUSwt and HA-FUS S84D is $p < 0.05$.

In cells transfected with expression vectors of the sites serine 131 (S131) and serine 183 (S183) HA-tagged FUS is located mostly in the nucleus, there were only a few cell which showed a translocation into the cytoplasm (Figure 16A,B and Figure 17A,B). The quantitative and statistical analysis of those two sites demonstrates that the population of cells expressing cytoplasmic HA immunoreactivity does not vary between phosphomimetic and dephosphomimetic mutations in comparison with HA-FUSwt (Figure 16C,D and Figure 17C,D).

Figure 18 and Figure 19 represent the transfection with the expression vectors of serine 185 (S185) and serine 186 (S186). Phosphomimetic as well as dephosphomimetic mutation of S185 and S186 results in an excessive mislocalisation of HA-FUS into the cytoplasm upon in 40-50 % of the transfected cells. In comparison with HA-FUSwt this mislocalisation in to the cytoplasm is significant for the phospho- and dephosphomimetic mutation of HA-FUS S185 ($p < 0.0001$) and HA-FUS S186 ($p < 0.0001$).

Figure 20 to Figure 28 demonstrate that all the other phosphomimicking and dephosphomimicking FUS variants at the sites S221, Y232, S257, S277, T286, S462, Y468, Y479 and Y484 show that HA-tagged FUS is located almost exclusively in the nucleus. Only in a few cells a mislocalisation of HA-FUS into the cytoplasm is visible, though this mislocalisation occurs not more often than in HA-FUSwt.

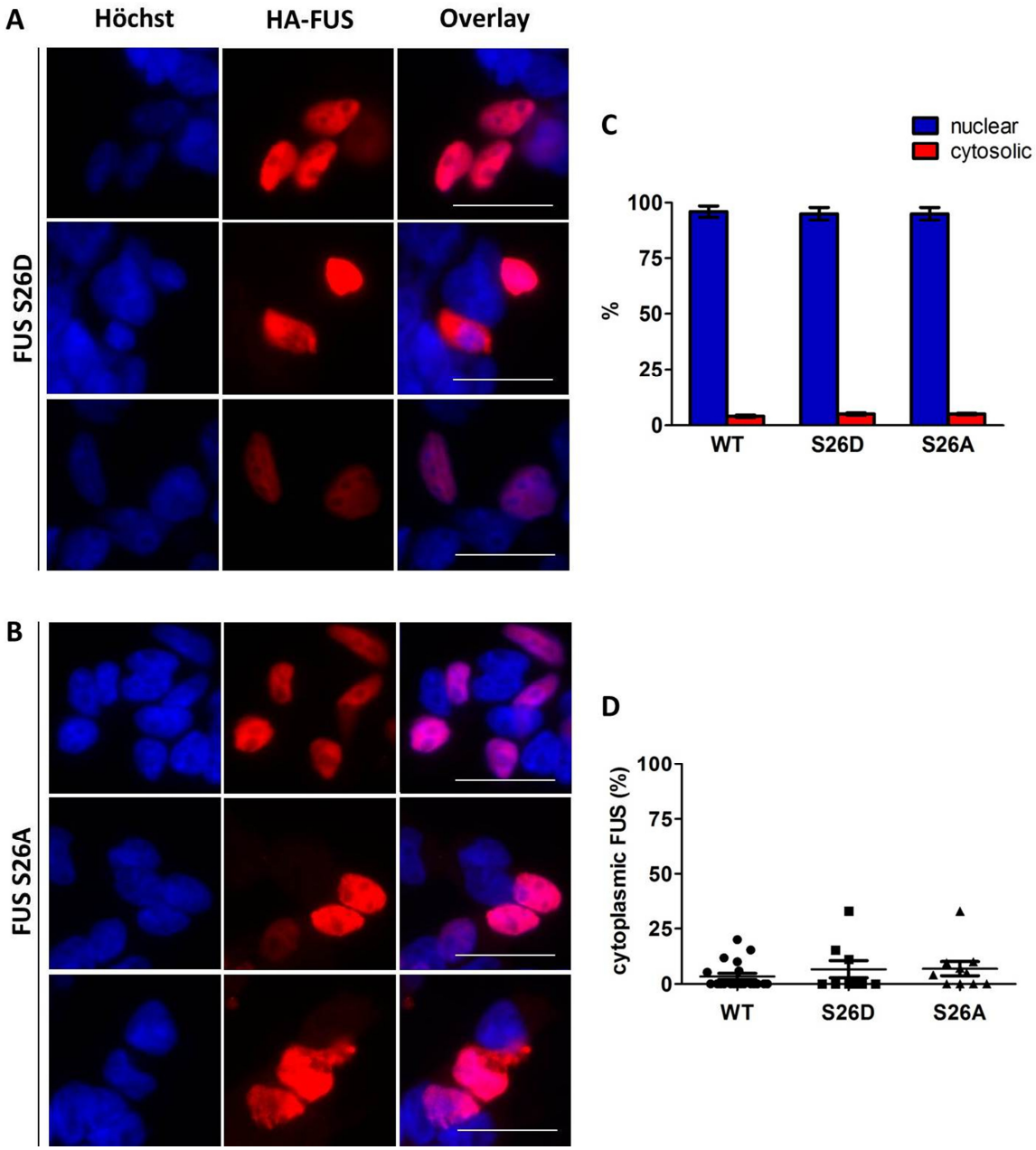

Figure 12. Double immunofluorescence and statistics of HEK293 cells transfected with HA-FUS S26D and FUS S26A.

A and B. Double immunofluorescence. Representative pictures of HEK293 cells transfected with HA-tagged FUS expression vector S26D and S26A for 72 hours. Cells were stained with an HA-specific antibody (red) and with "Höchst" to visualize the nuclei (blue). Stained cells were analysed with a fluorescent microscope. HA-FUS S26D and S26A are located mostly in the nucleus in few cells HA-FUS S26D and S26A are mislocated into the cytoplasm. Scale bar, 25 µm **C. Quantification of transfected cells on the basis of the location of HA-tagged FUS.** Transfection was carried out two times and of each, 5 images were taken randomly and of HA-FUS S26D 100 transfected cells and of HA-FUS S26A 174 transfected cells were counted. Counted cells were divided on the basis of the HA-FUS protein localisation into nuclear and cytoplasmic. Bars represent the mean percentage of cells of HA-FUS in the cytoplasm and nucleus. Error bars indicate standard deviation. **D. Statistical analysis of cytoplasmic HA-tagged FUS.** Counted cells were divided on the basis of the HA-FUS protein localisation into nuclear and cytoplasmic. Transfected cells with a cytoplasmic HA-FUS localisation were analysed with one-way ANOVA and Bonferroni post hoc test. Significance level was set at $p<0.05$ and error bars indicate standard deviation. The difference between HA-FUSwt and HA-FUS S26D and S26A is not significant.

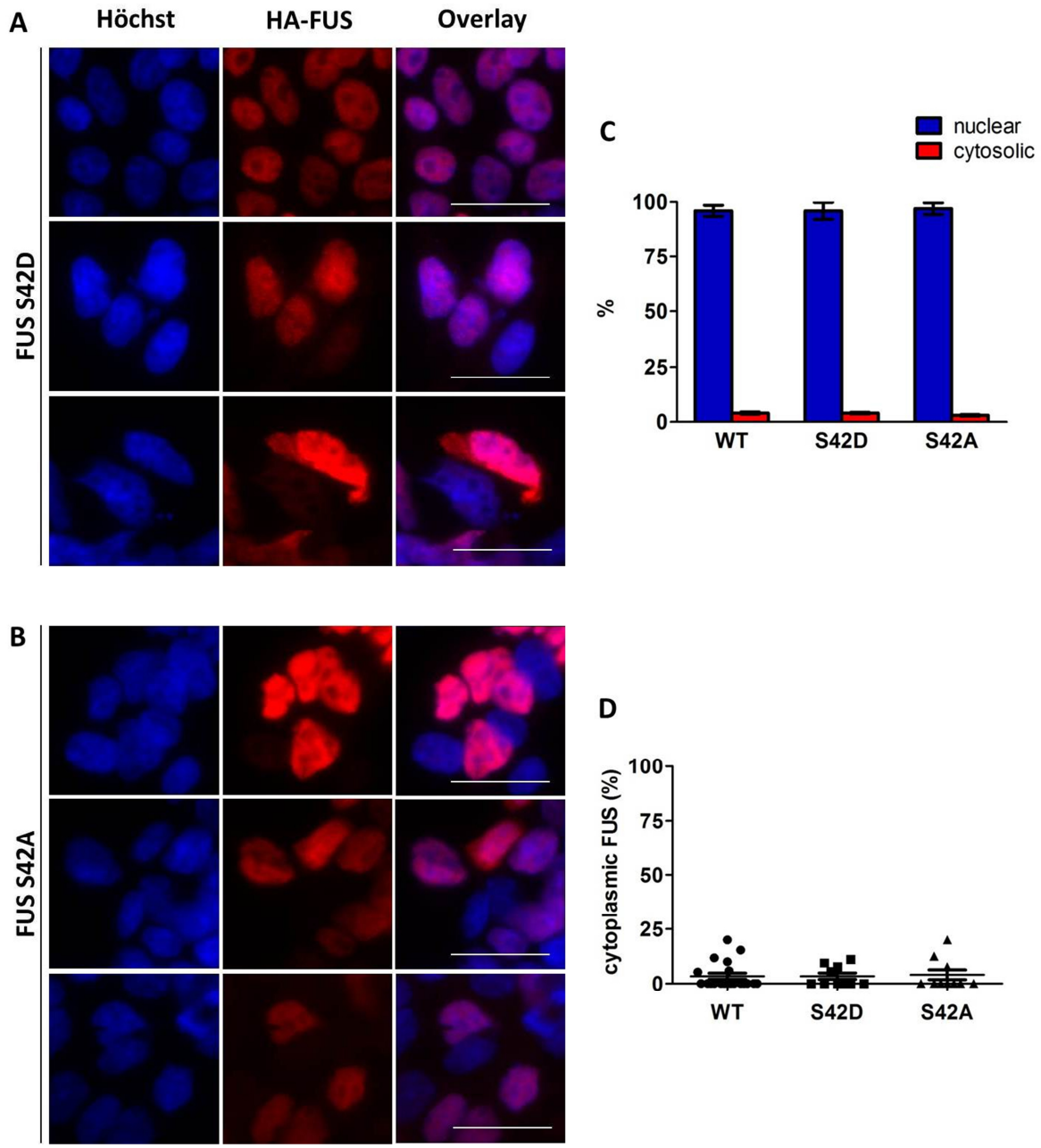

Figure 13. Double immunofluorescence and statistics of HEK293 cells transfected with HA-FUS S42D and FUS S42A.

A and B. Double immunofluorescence. Representative pictures of HEK293 cells transfected with HA-tagged FUS expression vector S42D and S42A for 72 hours. Cells were stained with an HA-specific antibody (red) and with "Höchst" to visualize the nuclei (blue). Stained cells were analysed with a fluorescent microscope. HA-FUS S42D and S42A are located mostly in the nucleus in few cells HA-FUS S42D and S42A are mislocated into the cytoplasm. Scale bar, 25 µm **C. Quantification of transfected cells on the basis of the location of HA-tagged FUS.** Transfection was carried out two times and of each, 5 images were taken randomly and of HA-FUS S42D 130 transfected cells and of HA-FUS S42A 125 transfected cells were counted. Counted cells were divided on the basis of the HA-FUS protein localisation into nuclear and cytoplasmic. Bars represent the mean percentage of cells of HA-FUS in the cytoplasm and nucleus. Error bars indicate standard deviation. **D. Statistical analysis of cytoplasmic HA-tagged FUS.** Counted cells were divided on the basis of the HA-FUS protein localisation into nuclear and cytoplasmic. Transfected cells with a cytoplasmic HA-FUS localisation were analysed with one-way ANOVA and Bonferroni post hoc test. Significance level was set at $p<0.05$ and error bars indicate standard deviation. The difference between HA-FUSwt and HA-FUS S42D and S42A is not significant.

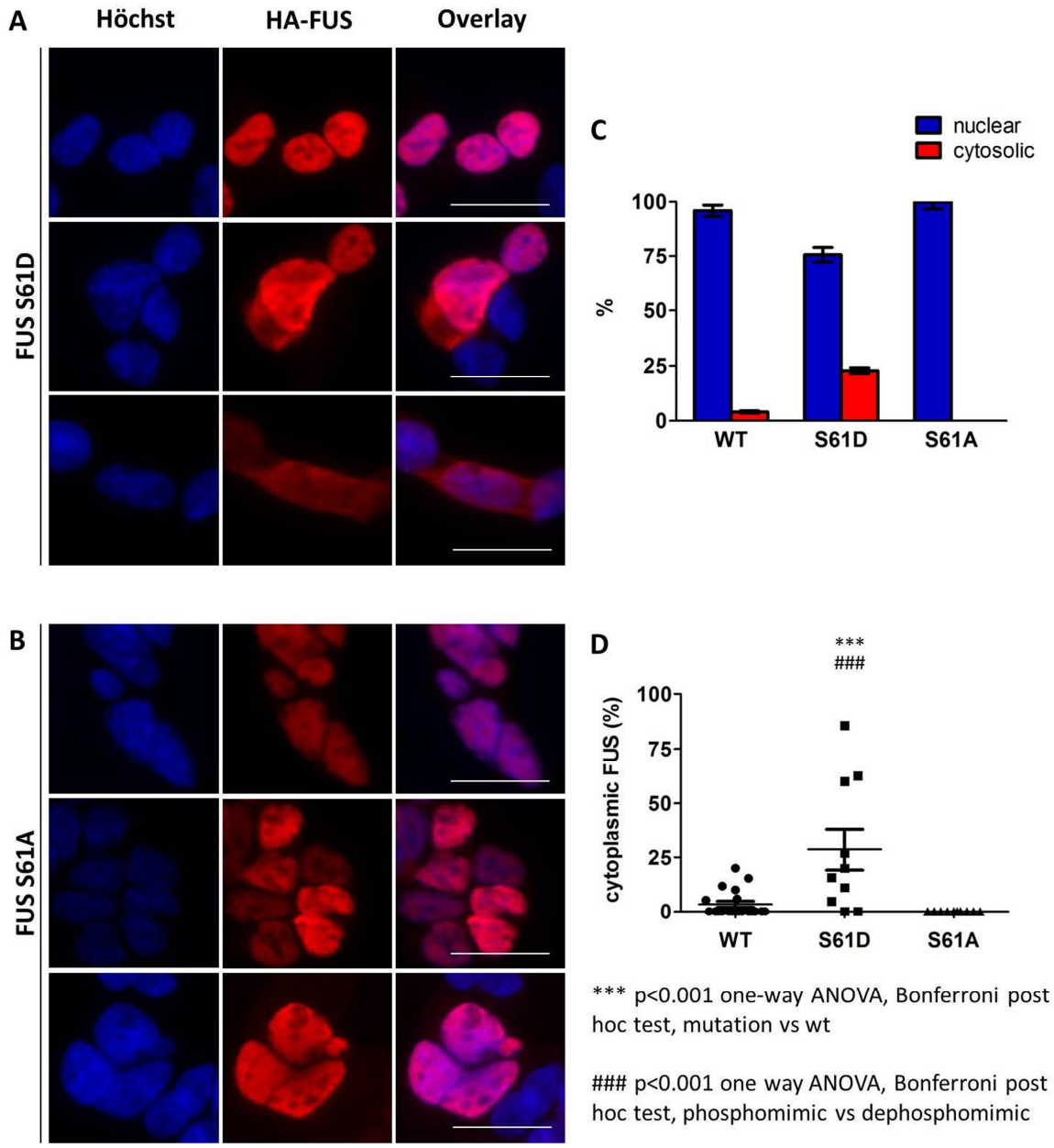

Figure 14. Double immunofluorescence and statistics of HEK293 cells transfected with HA-FUS S61D and FUS S61A.

A and B. Double immunofluorescence. Representative pictures of HEK293 cells transfected with HA-tagged FUS expression vector S61D and S61A for 72 hours. Cells were stained with an HA-specific antibody (red) and with "Höchst" to visualize the nuclei (blue). Stained cells were analysed with a fluorescent microscope. HA-FUS S61D shows cytoplasmic localisation and in a few cell nuclear localisation. HA-FUS S61A is located exclusively in the nucleus. Scale bar, 25 µm **C. Quantification of transfected cells on the basis of the location of HA-tagged FUS.** Transfection was carried out two times and of each, 5 images were taken randomly and of HA-FUS S61D 131 transfected cells and of HA-FUS S61A 155 transfected cells were counted. Counted cells were divided on the basis of the HA-FUS protein localisation into nuclear and cytoplasmic. Bars represent the mean percentage of cells of HA-FUS in the cytoplasm and nucleus. Error bars indicate standard deviation. **D. Statistical analysis of cytoplasmic HA-tagged FUS.** Counted cells were divided on the basis of the HA-FUS protein localisation into nuclear and cytoplasmic. Transfected cells with a cytoplasmic HA-FUS localisation were analysed with one-way ANOVA and Bonferroni post hoc test. Significance level was set at $p<0.05$ and error bars indicate standard deviation. HA-FUS S61D shows a significantly higher mislocalisation into the cytoplasm compared to HA-FUSwt and the dephosphomimicking partner HA-FUS S61A.

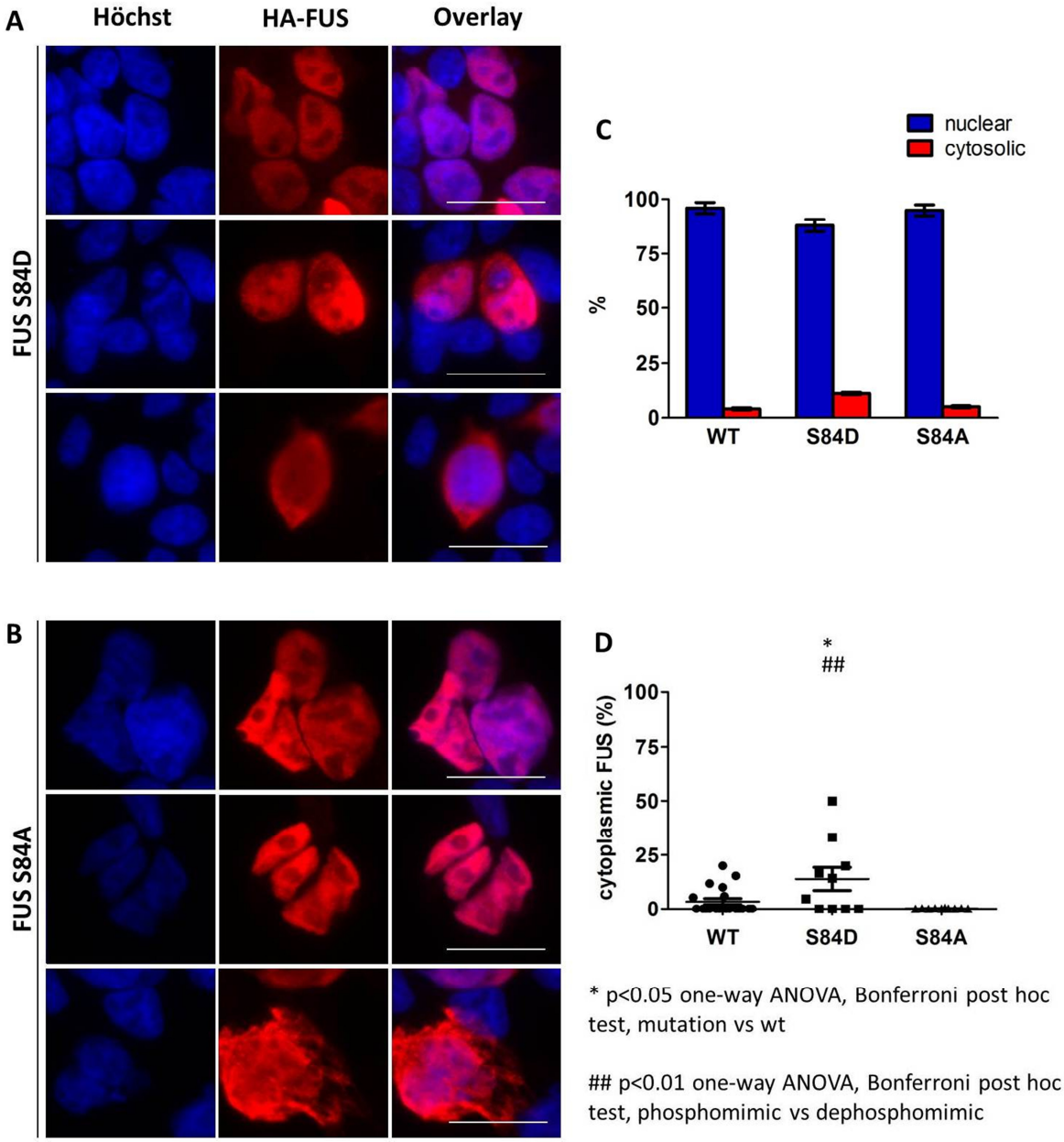

Figure 15. Double immunofluorescence and statistics of HEK293 cells transfected with HA-FUS S84D and FUS S84A.

A and B. Double immunofluorescence. Representative pictures of HEK293 cells transfected with HA-tagged FUS expression vector S84D and S84A for 72 hours. Cells were stained with an HA-specific antibody (red) and with "Höchst" to visualize the nuclei (blue). Stained cells were analysed with a fluorescent microscope. HA-FUS S84D is located in the cytoplasm and in the nucleus. HA-FUS S84A is almost exclusively located in the nucleus only in a few cells location in the cytoplasm. Scale bar, 25 µm **C. Quantification of transfected cells on the basis of the location of HA-tagged FUS** Transfection was carried out two times and of each, 5 images were taken randomly and of HA-FUS S84D 99 transfected cells and of HA-FUS S84A 155 transfected cells were counted. Counted cells were divided on the basis of the HA-FUS protein localisation into nuclear and cytoplasmic. Bars represent the mean percentage of cells of HA-FUS in the cytoplasm and nucleus. Error bars indicate standard deviation. **D. Statistical analysis of cytoplasmic HA-tagged FUS.** Counted cells were divided on the basis of the HA-FUS protein localisation into nuclear and cytoplasmic. Transfected cells with a cytoplasmic HA-FUS localisation were analysed with one-way ANOVA and Bonferroni post hoc test. Significance level was set at $p<0.05$ and error bars indicate standard deviation. HA-FUS S84D shows a significantly higher mislocalisation into the cytoplasm compared to HA-FUSwt and the dephosphomimicking partner HA-FUS S84A.

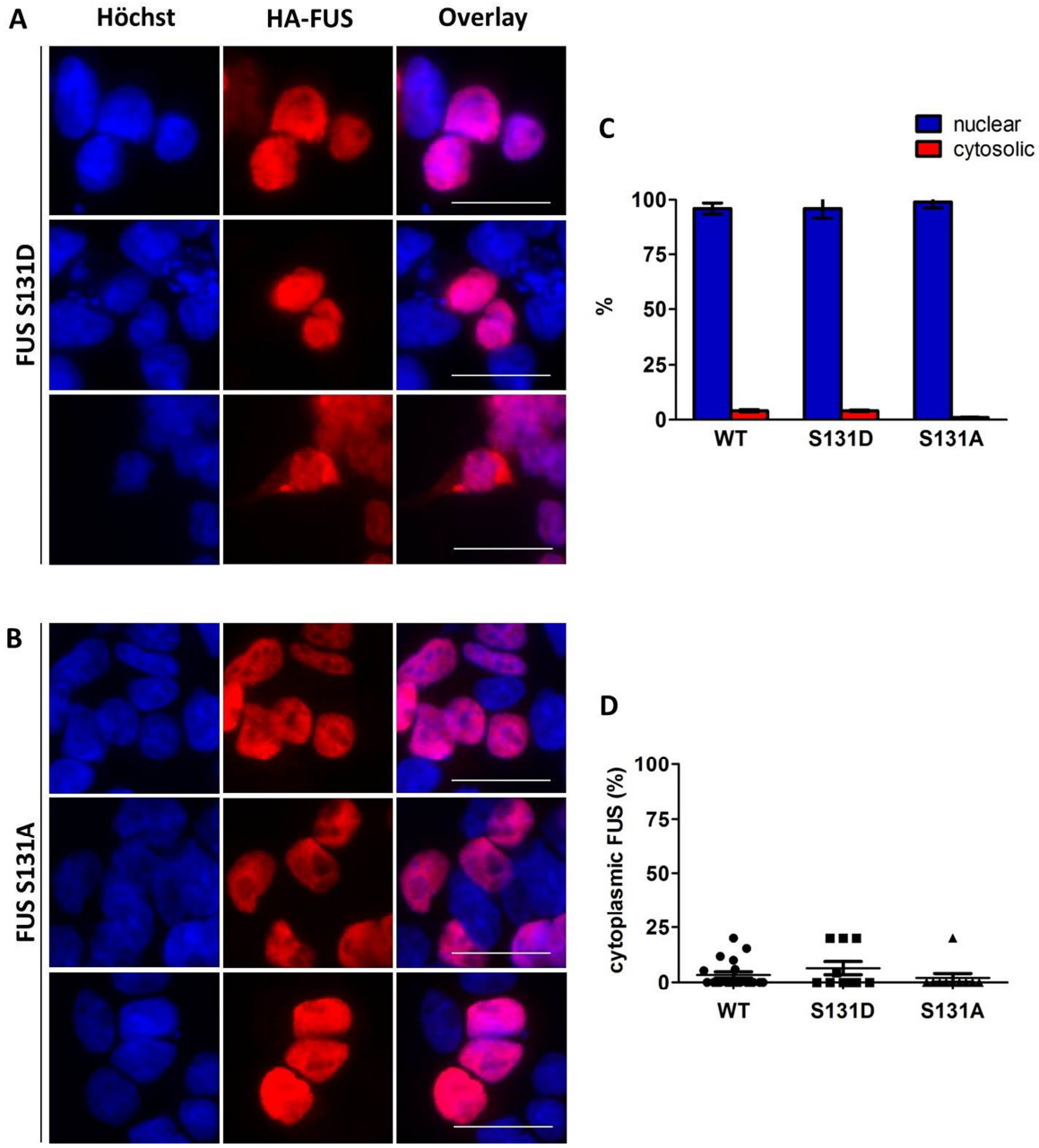

Figure 16. Double immunofluorescence and statistics of HEK293 cells transfected with HA-FUS S131D and FUS S131A.

A and B. Double immunofluorescence. Representative pictures of HEK293 cells transfected with HA-tagged FUS expression vector S131D and S131A for 72 hours. Cells were stained with an HA-specific antibody (red) and with "Höchst" to visualize the nuclei (blue). Stained cells were analysed with a fluorescent microscope. HA-FUS S131D and S131A are located almost exclusively in the nucleus in few cells HA-FUS S131D and S131A are mislocated into the cytoplasm. Scale bar, 25 µm **C. Quantification of transfected cells on the basis of the location of HA-tagged FUS.** Transfection was carried out two times and of each, 5 images were taken randomly and of HA-FUS S131D 121 transfected cells and of HA-FUS S131A 80 transfected cells were counted. Counted cells were divided on the basis of the HA-FUS protein localisation into nuclear and cytoplasmic. Bars represent the mean percentage of cells of HA-FUS in the cytoplasm and nucleus. Error bars indicate standard deviation. **D. Statistical analysis of cytoplasmic HA-tagged FUS.** Counted cells were divided on the basis of the HA-FUS protein localisation into nuclear and cytoplasmic. Transfected cells with a cytoplasmic HA-FUS localisation were analysed with one-way ANOVA and Bonferroni post hoc test. Significance level was set at $p<0.05$ and error bars indicate standard deviation. The difference between HA-FUSwt and HA-FUS S131D and S131A is not significant.

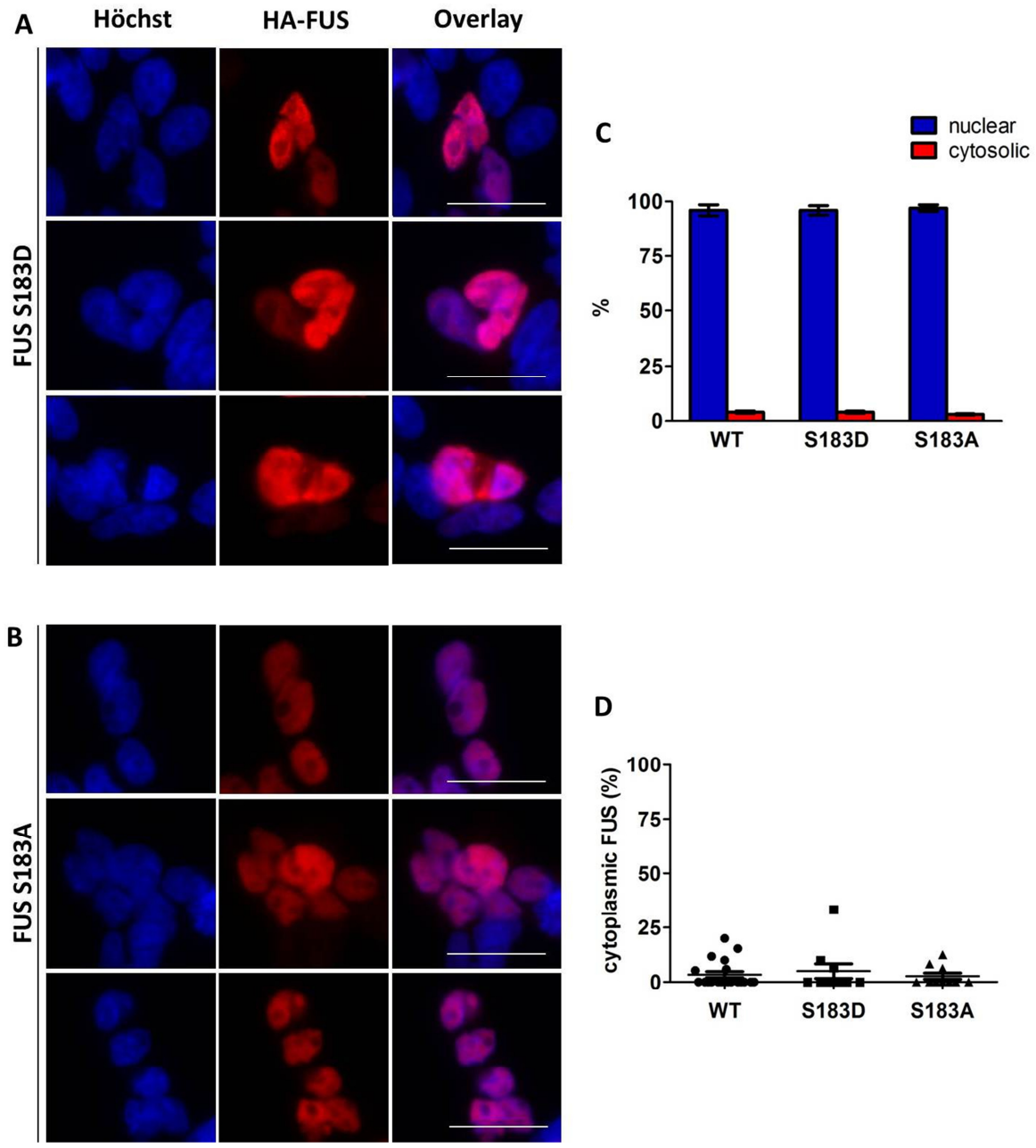

Figure 17. Double immunofluorescence and statistics of HEK293 cells transfected with HA-FUS S183D and FUS S183A.

A and B. Double immunofluorescence. Representative pictures of HEK293 cells transfected with HA-tagged FUS expression vector S183D and S183A for 72 hours. Cells were stained with an HA-specific antibody (red) and with "Höchst" to visualize the nuclei (blue). Stained cells were analysed with a fluorescent microscope. HA-FUS S183D and S183A are located mostly in the nucleus in few cells HA-FUS S183D and S183A are mislocated into the cytoplasm. Scale bar, 25 µm **C. Quantification of transfected cells on the basis of the location of HA-tagged FUS.** Transfection was carried out two times and of each, 5 images were taken randomly and of HA-FUS S183D 134 transfected cells and of HA-FUS S183A 141 transfected cells were counted. Counted cells were divided on the basis of the HA-FUS protein localisation into nuclear and cytoplasmic. Bars represent the mean percentage of cells of HA-FUS in the cytoplasm and nucleus. Error bars indicate standard deviation. **D. Statistical analysis of cytoplasmic HA-tagged FUS.** Counted cells were divided on the basis of the HA-FUS protein localisation into nuclear and cytoplasmic. Transfected cells with a cytoplasmic HA-FUS localisation were analysed with one-way ANOVA and Bonferroni post hoc test. Significance level was set at $p<0.05$ and error bars indicate standard deviation. The difference between HA-FUSwt and HA-FUS S183D and S183A is not significant.

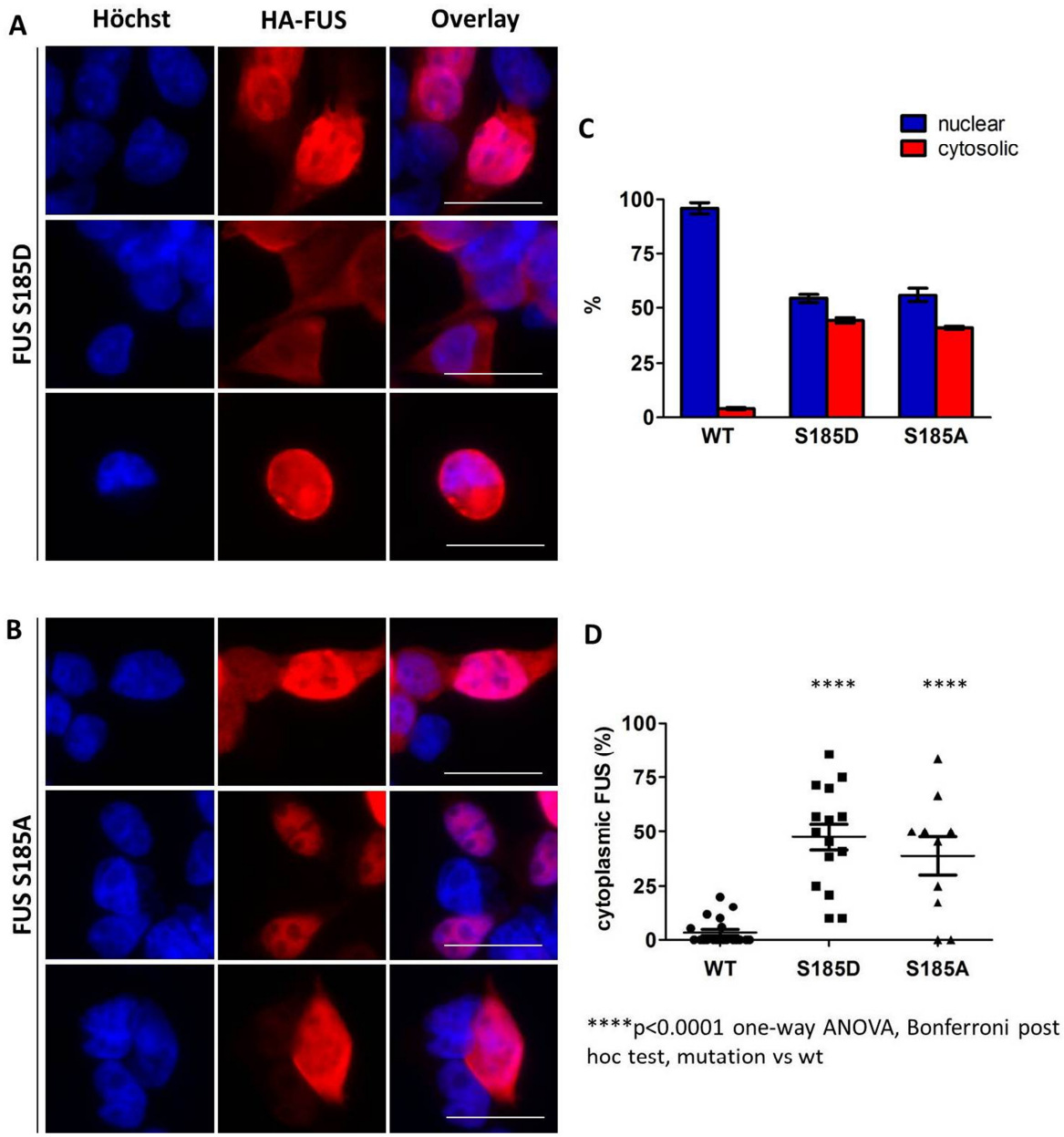

Figure 18. Double immunofluorescence and statistics of HEK293 cells transfected with HA-FUS S185D and FUS S185A.

A and B. Double immunofluorescence. Representative pictures of HEK293 cells transfected with HA-tagged FUS expression vector S185D and S185A for 72 hours. Cells were stained with an HA-specific antibody (red) and with "Höchst" to visualize the nuclei (blue). Stained cells were analysed with a fluorescent microscope. Nearly half of the transfected cells show a mislocalisation of HA-FUS S185D and S185A into the cytoplasm in the other cells HA-FUS S185D and S185A are located in the nucleus. Scale bar, 25 µm **C. Quantification of transfected cells on the basis of the location of HA-tagged FUS.** Transfection was carried out two times and of each, 5 images were taken randomly and of HA-FUS S185D 158 transfected cells and of HA-FUS S185A 105 transfected cells were counted. Counted cells were divided on the basis of the HA-FUS protein localisation into nuclear and cytoplasmic. Bars represent the mean percentage of cells of HA-FUS in the cytoplasm and nucleus. Error bars indicate standard deviation. **D. Statistical analysis of cytoplasmic HA-tagged FUS.** Counted cells were divided on the basis of the HA-FUS protein localisation into nuclear and cytoplasmic. Transfected cells with a cytoplasmic HA-FUS localisation were analysed with one-way ANOVA and Bonferroni post hoc test. Significance level was set at $p<0.05$ and error bars indicate standard deviation. HA-FUS 185D and S185A show a significantly higher mislocalisation of HA-FUS into the cytoplasm than HA-FUSwt.

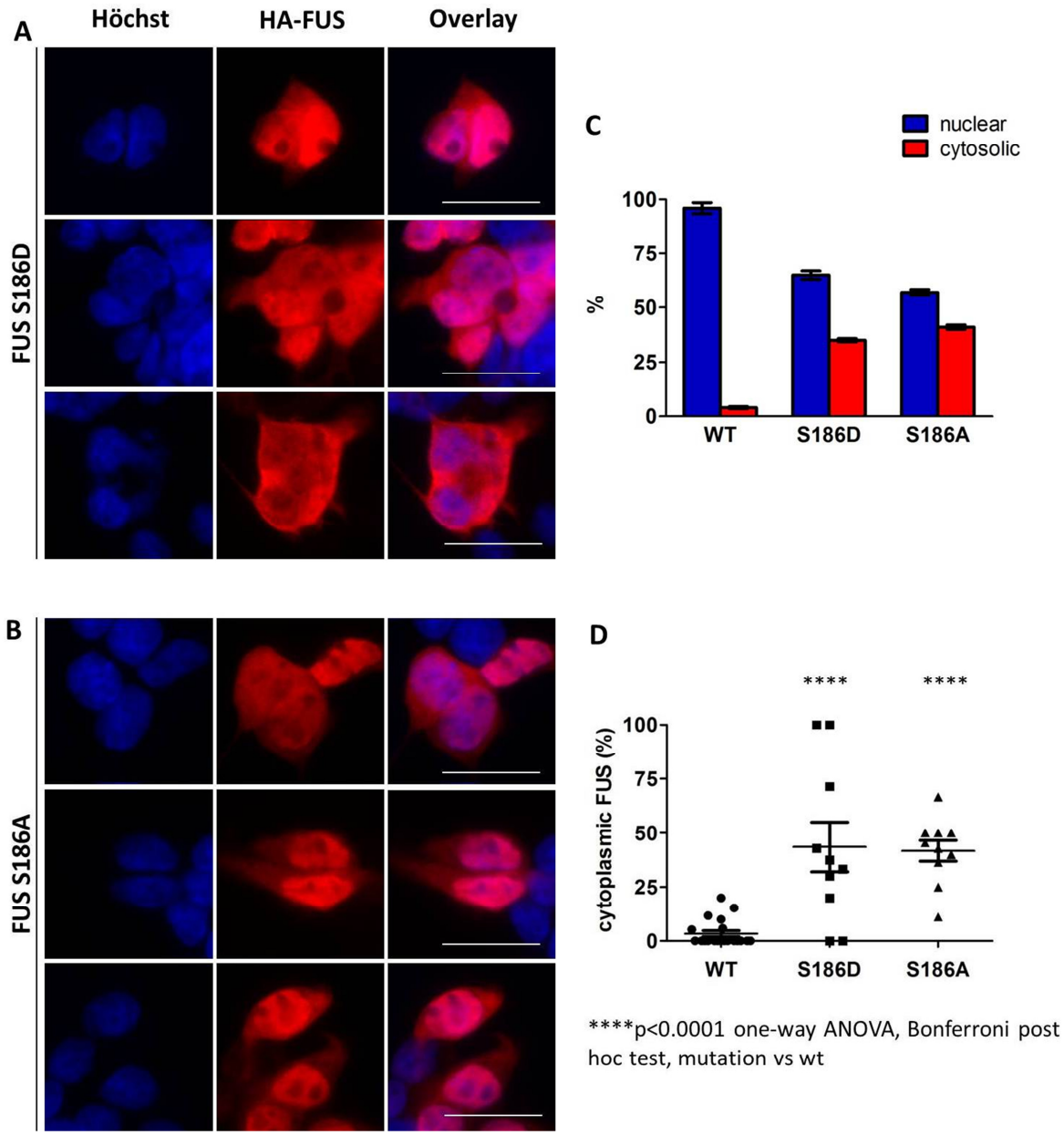

Figure 19. Double immunofluorescence and statistics of HEK293 cells transfected with HA-FUS S186D and FUS S186A.

A and B. Double immunofluorescence. Representative pictures of HEK293 cells transfected with HA-tagged FUS expression vector S186D and S186A for 72 hours. Cells were stained with an HA-specific antibody (red) and with "Höchst" to visualize the nuclei (blue). Stained cells were analysed with a fluorescent microscope. Nearly half of the transfected cells show a mislocalisation of HA-FUS S186D and S186A into the cytoplasm in the other cells HA-FUS S186D and S186A are located in the cytoplasm. Scale bar, 25 µm **C. Quantification of transfected cells on the basis of the location of HA-tagged FUS.** Transfection was carried out two times and of each, 5 images were taken randomly and of HA-FUS S186D 72 transfected cells and of HA-FUS S186A 121 transfected cells were counted. Counted cells were divided on the basis of the HA-FUS protein localisation into nuclear and cytoplasmic. Bars represent the mean percentage of cells of HA-FUS in the cytoplasm and nucleus. Error bars indicate standard deviation. **D. Statistical analysis of cytoplasmic HA-tagged FUS.** Counted cells were divided on the basis of the HA-FUS protein localisation into nuclear and cytoplasmic. Transfected cells with a cytoplasmic HA-FUS localisation were analysed with one-way ANOVA and Bonferroni post hoc test. Significance level was set at $p<0.05$ and error bars indicate standard deviation. HA-FUS 186D and S186A show a significantly higher mislocalisation of HA-FUS into the cytoplasm than HA-FUSwt.

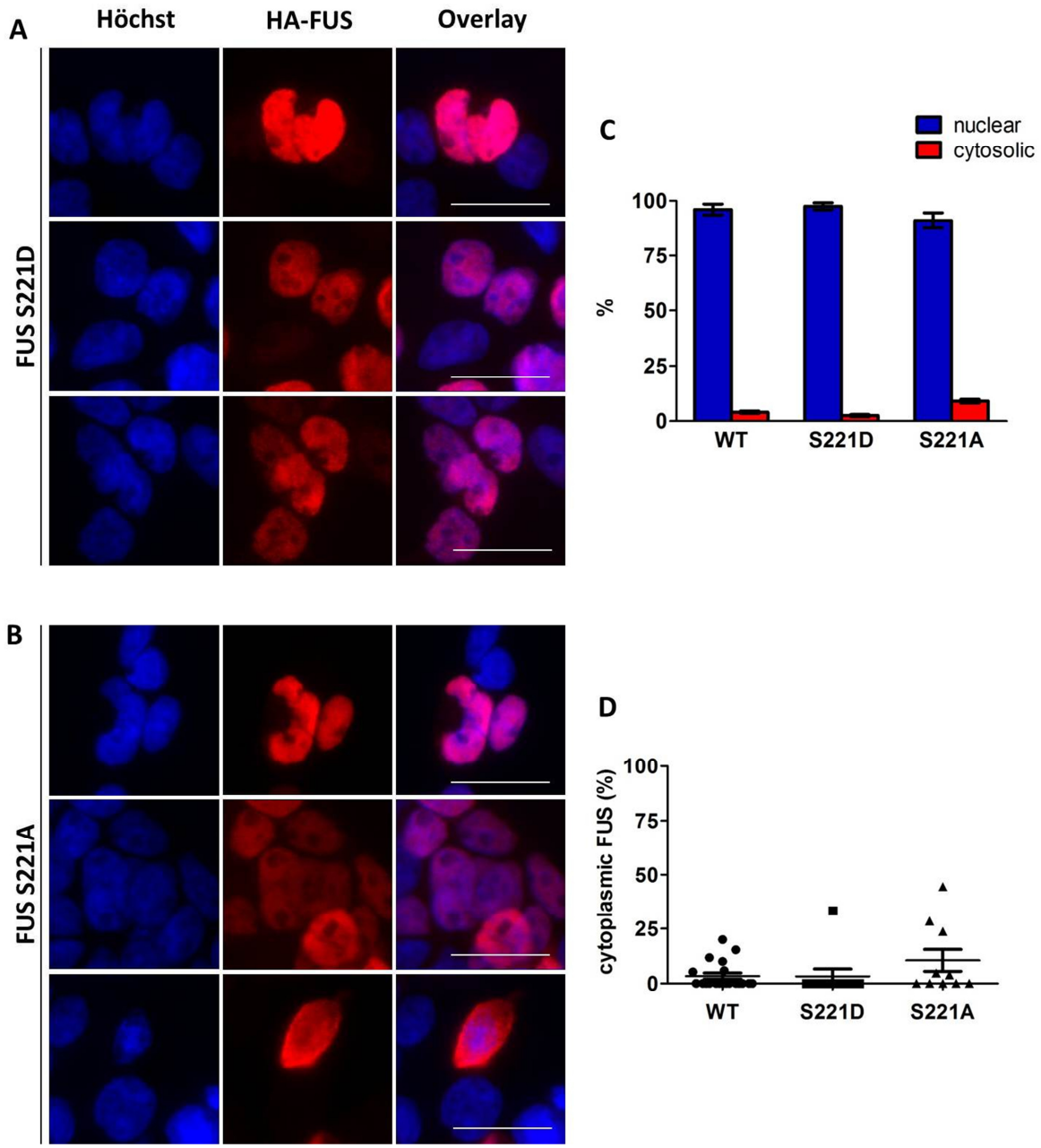

Figure 20. Double immunofluorescence and statistics of HEK293 cells transfected with HA-FUS S221D and FUS S221A.

A and B. Double immunofluorescence. Representative pictures of HEK293 cells transfected with HA-tagged FUS expression vector S221D and S221A for 72 hours. Cells were stained with an HA-specific antibody (red) and with "Höchst" to visualize the nuclei (blue). Stained cells were analysed with a fluorescent microscope. HA-FUS S221D and S221A are located mostly in the nucleus in few cells HA-FUS S221D and S221A are mislocated into the cytoplasm. Scale bar, 25 µm **C. Quantification of transfected cells on the basis of the location of HA-tagged FUS.** Transfection was carried out two times and of each, 5 images were taken randomly and of HA-FUS S221D 120 transfected cells and of HA-FUS S221A 145 transfected cells were counted. Counted cells were divided on the basis of the HA-FUS protein localisation into nuclear and cytoplasmic. Bars represent the mean percentage of cells of HA-FUS in the cytoplasm and nucleus. Error bars indicate standard deviation. **D. Statistical analysis of cytoplasmic HA-tagged FUS.** Counted cells were divided on the basis of the HA-FUS protein localisation into nuclear and cytoplasmic. Transfected cells with a cytoplasmic HA-FUS localisation were analysed with one-way ANOVA and Bonferroni post hoc test. Significance level was set at $p<0.05$ and error bars indicate standard deviation. The difference between HA-FUSwt and HA-FUS S221D and S221A is not significant.

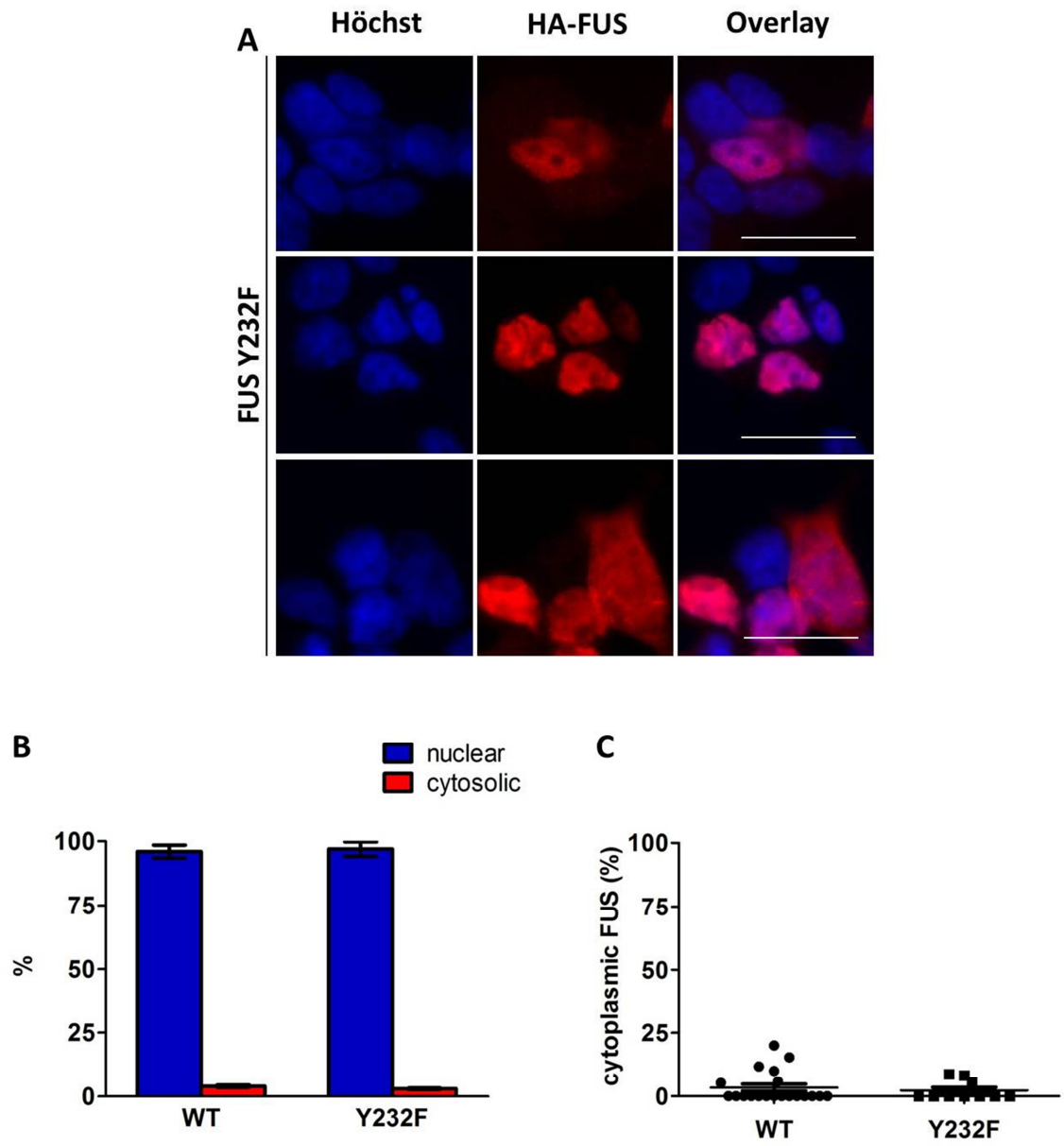

Figure 21 A. Double immunofluorescence and statistics of HEK293 cells transfected with HA-FUS Y232F. A. Double immunofluorescence. Representative pictures of HEK293 cells transfected with HA-tagged FUS expression vector Y232F for 72 hours. Cells were stained with an HA-specific antibody (red) and with "Höchst" to visualize the nuclei (blue). Stained cells were analysed with a fluorescent microscope. HA-FUS Y232F is located mostly in the nucleus in few cells HA-FUS Y232F is mislocated into the cytoplasm. Scale bar, 25 μm **B. Quantification of transfected cells on the basis of the location of HA-tagged FUS.** Transfection was carried out two times and of each, 5 images were taken randomly and of HA-FUS Y232F 155 transfected cells were counted. Counted cells were divided on the basis of the HA-FUS protein localisation into nuclear and cytoplasmic. Bars represent the mean percentage of cells of HA-FUS in the cytoplasm and nucleus. Error bars indicate standard deviation. **C. Statistical analysis of cytoplasmic HA-tagged FUS.** Counted cells were divided on the basis of the HA-FUS protein localisation into nuclear and cytoplasmic. Transfected cells with a cytoplasmic HA-FUS localisation were analysed with one-way ANOVA and Bonferroni post hoc test. Significance level was set at $p<0.05$ and error bars indicate standard deviation. The difference between HA-FUSwt and HA-FUS Y232F is not significant.

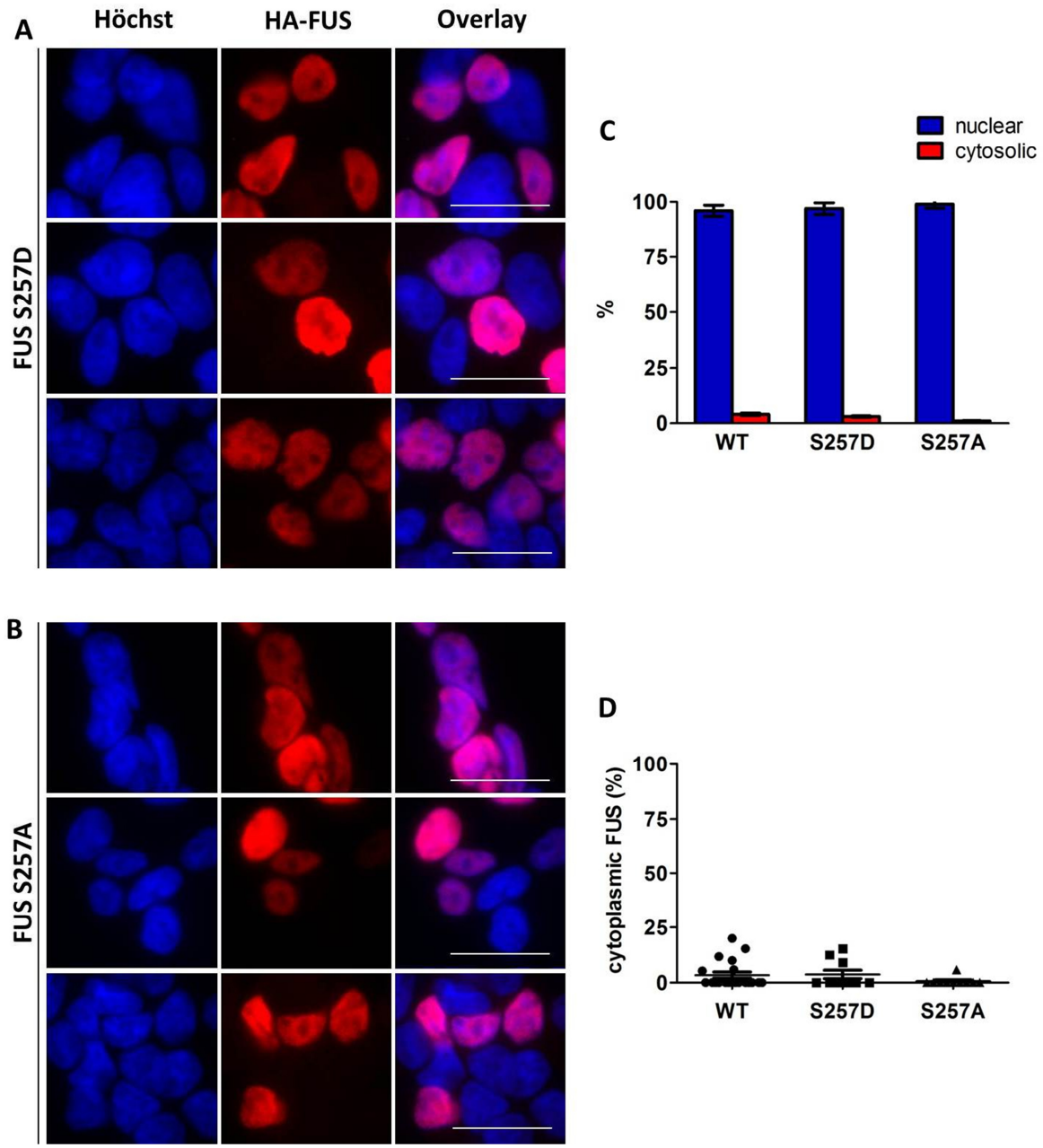

Figure 22. Double immunofluorescence and statistics of HEK293 cells transfected with HA-FUS S257D and FUS S257A.

A and B. Double immunofluorescence. Representative pictures of HEK293 cells transfected with HA-tagged FUS expression vector S257D and S257A for 72 hours. Cells were stained with an HA-specific antibody (red) and with "Höchst" to visualize the nuclei (blue). Stained cells were analysed with a fluorescent microscope. HA-FUS S257D and S257A are located mostly in the nucleus in few cells HA-FUS S257D and S257A are mislocated into the cytoplasm. Scale bar, 25 µm **C. Quantification of transfected cells on the basis of the location of HA-tagged FUS.** Transfection was carried out two times and of each, 5 images were taken randomly and of HA-FUS S257D 118 transfected cells and of HA-FUS S257A 112 transfected cells were counted. Counted cells were divided on the basis of the HA-FUS protein localisation into nuclear and cytoplasmic. Bars represent the mean percentage of cells of HA-FUS in the cytoplasm and nucleus. Error bars indicate standard deviation. **D. Statistical analysis of cytoplasmic HA-tagged FUS.** Counted cells were divided on the basis of the HA-FUS protein localisation into nuclear and cytoplasmic. Transfected cells with a cytoplasmic HA-FUS localisation were analysed with one-way ANOVA and Bonferroni post hoc test. Significance level was set at $p<0.05$ and error bars indicate standard deviation. The difference between HA-FUSwt and HA-FUS S257D and S257A is not significant.

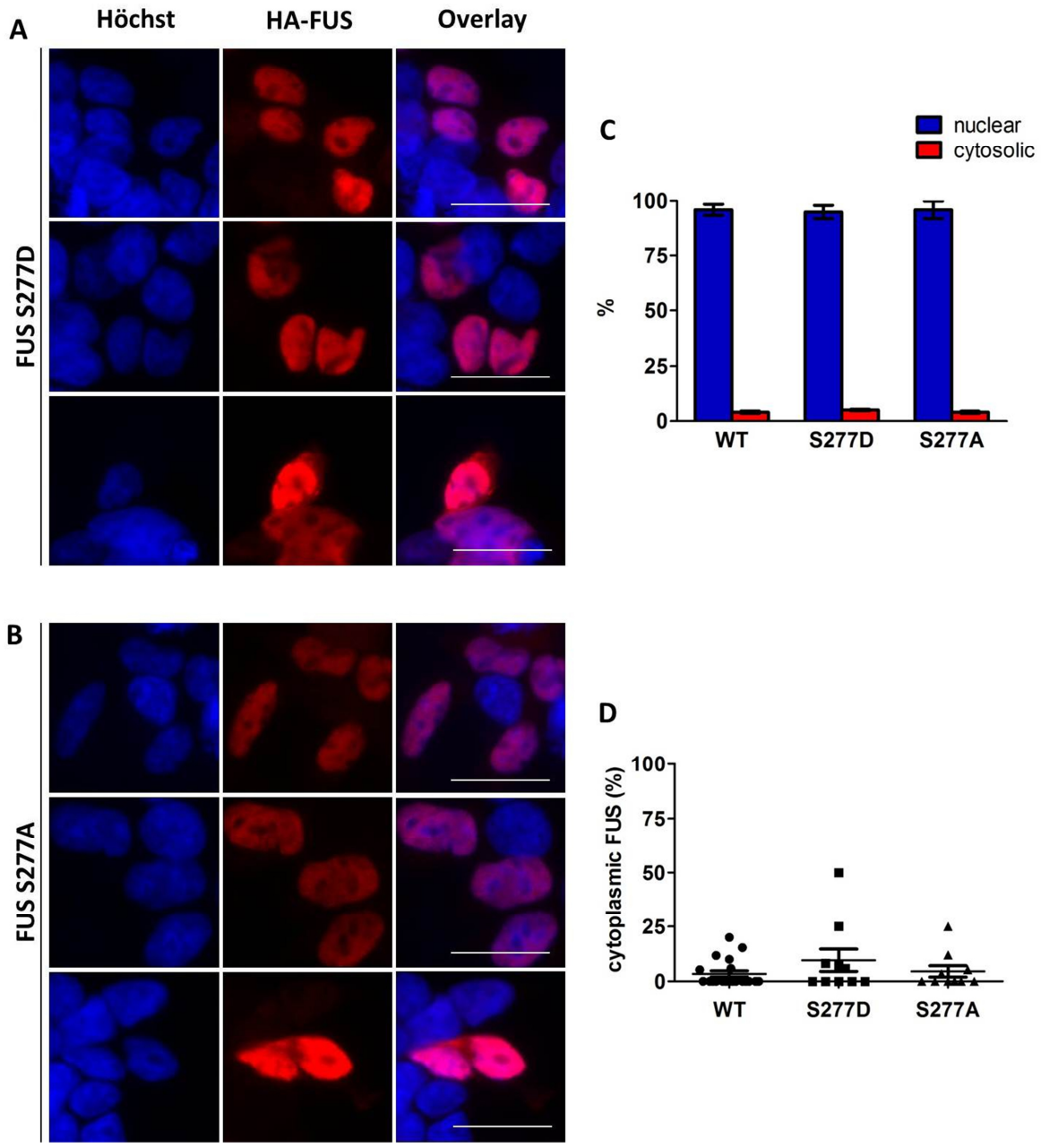

Figure 23. Double immunofluorescence and statistics of HEK293 cells transfected with HA-FUS S277D and FUS S277A.

A and B. Double immunofluorescence. Representative pictures of HEK293 cells transfected with HA-tagged FUS expression vector S277D and S277A for 72 hours. Cells were stained with an HA-specific antibody (red) and with "Höchst" to visualize the nuclei (blue). Stained cells were analysed with a fluorescent microscope. HA-FUS S277D and S277A are located mostly in the nucleus in few cells HA-FUS S277D and S277A are mislocated into the cytoplasm. Scale bar, 25 µm **C. Quantification of transfected cells on the basis of the location of HA-tagged FUS.** Transfection was carried out two times and of each, 5 images were taken randomly and of HA-FUS S277D 128 transfected cells and of HA-FUS S277A 168 transfected cells were counted. Counted cells were divided on the basis of the HA-FUS protein localisation into nuclear and cytoplasmic. Bars represent the mean percentage of cells of HA-FUS in the cytoplasm and nucleus. Error bars indicate standard deviation. **D. Statistical analysis of cytoplasmic HA-tagged FUS.** Counted cells were divided on the basis of the HA-FUS protein localisation into nuclear and cytoplasmic. Transfected cells with a cytoplasmic HA-FUS localisation were analysed with one-way ANOVA and Bonferroni post hoc test. Significance level was set at $p<0.05$ and error bars indicate standard deviation. The difference between HA-FUSwt and HA-FUS S277D and S277A is not significant.

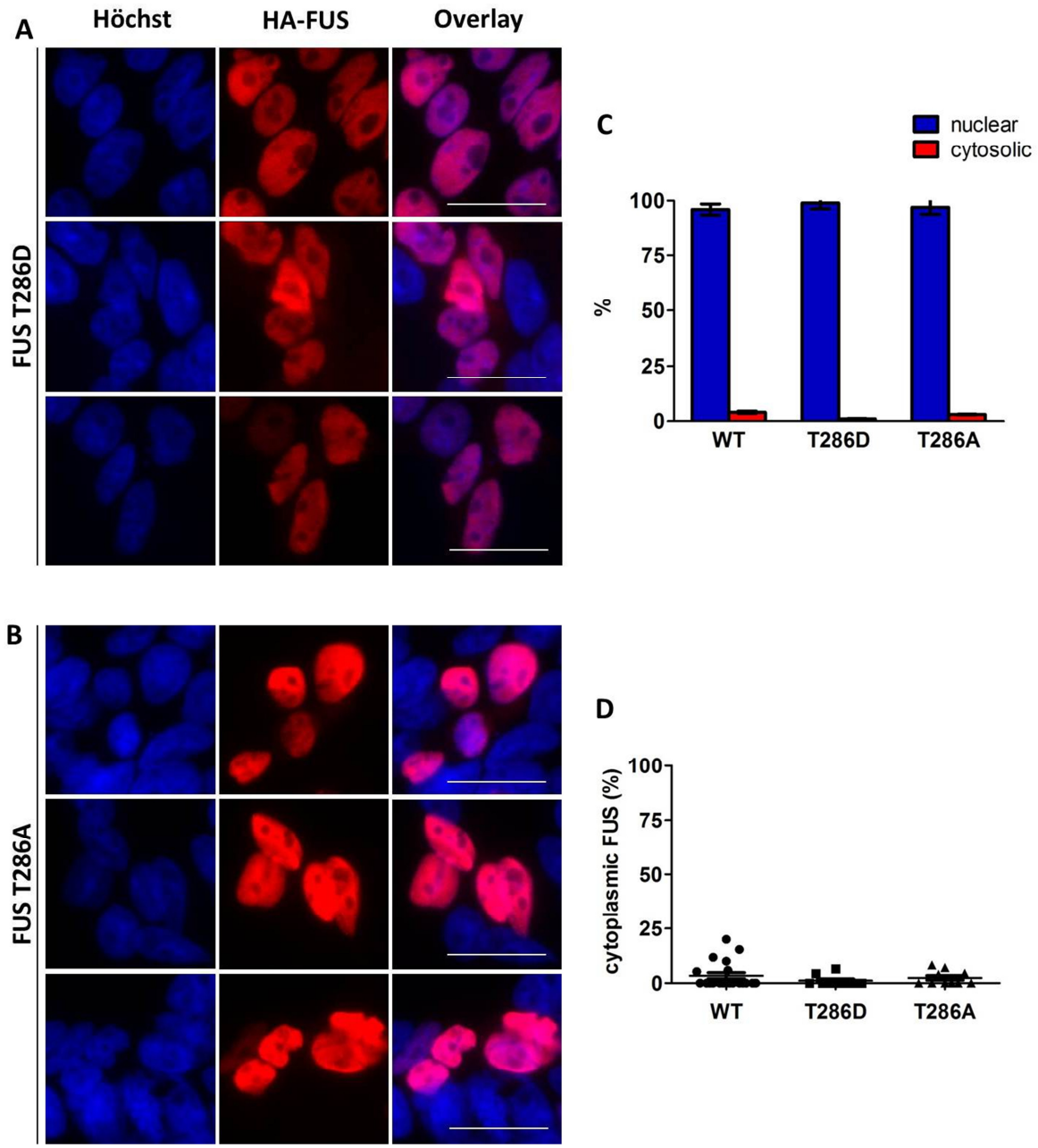

Figure 24. Double immunofluorescence and statistics of HEK293 cells transfected with HA-FUS T286D and FUS T286A.

A and B. Double immunofluorescence. Representative pictures of HEK293 cells transfected with HA-tagged FUS expression vector T286D and T286A for 72 hours. Cells were stained with an HA-specific antibody (red) and with "Höchst" to visualize the nuclei (blue). Stained cells were analysed with a fluorescent microscope. HA-FUS T286D and T286A are located mostly in the nucleus in few cells HA-FUS T286D and T286A are mislocated into the cytoplasm. Scale bar, 25 µm **C. Quantification of transfected cells on the basis of the location of HA-tagged FUS.** Transfection was carried out two times and of each, 5 images were taken randomly and of HA-FUS T286D 185 transfected cells and of HA-FUS T286A 133 transfected cells were counted. Counted cells were divided on the basis of the HA-FUS protein localisation into nuclear and cytoplasmic. Bars represent the mean percentage of cells of HA-FUS in the cytoplasm and nucleus. Error bars indicate standard deviation. **D. Statistical analysis of cytoplasmic HA-tagged FUS.** Counted cells were divided on the basis of the HA-FUS protein localisation into nuclear and cytoplasmic. Transfected cells with a cytoplasmic HA-FUS localisation were analysed with one-way ANOVA and Bonferroni post hoc test. Significance level was set at $p<0.05$ and error bars indicate standard deviation. The difference between HA-FUSwt and HA-FUS T286D and T286A is not significant.

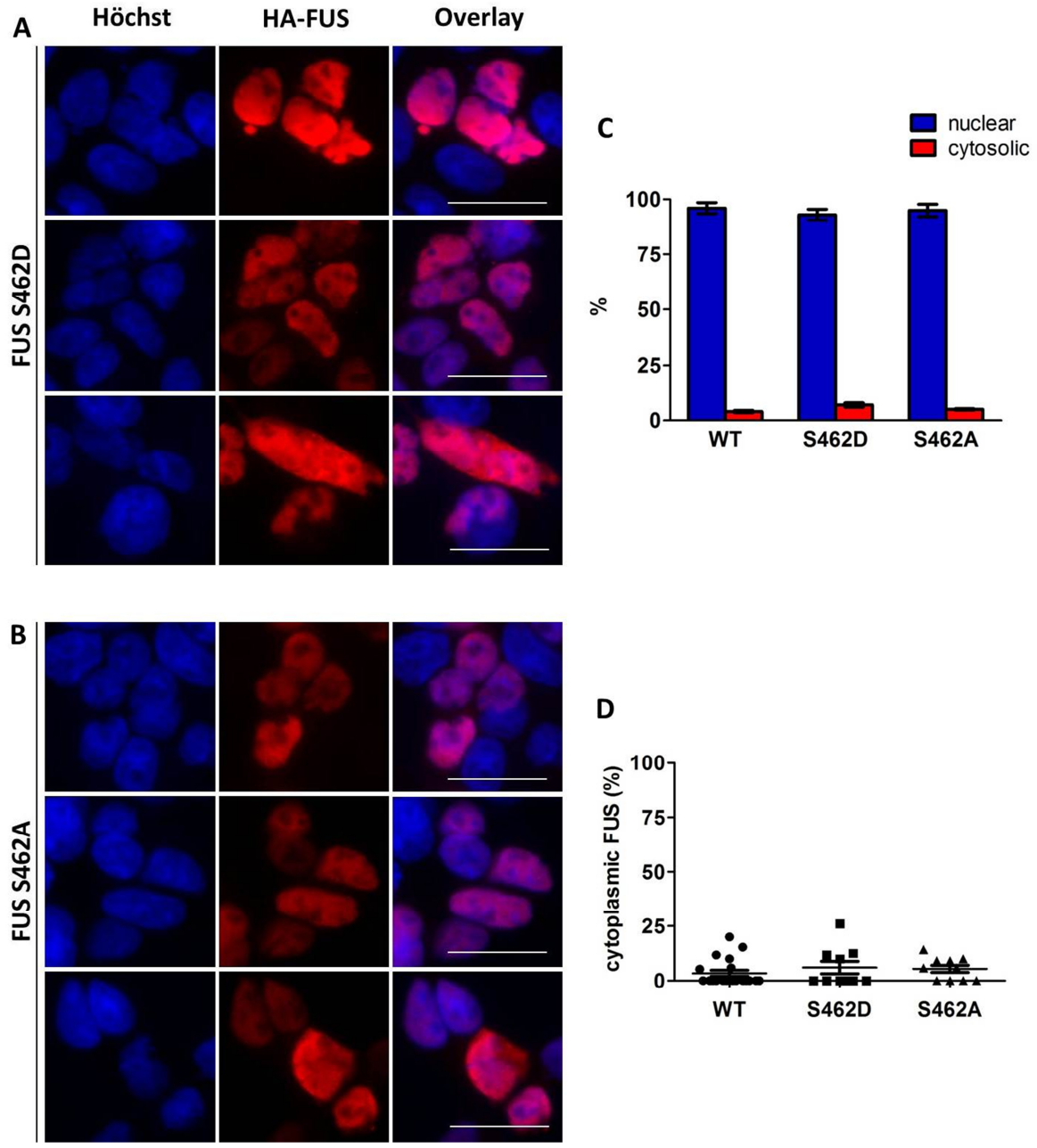

Figure 25. Double immunofluorescence and statistics of HEK293 cells transfected with HA-FUS S462D and FUS S462A.

A and B. Double immunofluorescence. Representative pictures of HEK293 cells transfected with HA-tagged FUS expression vector S462D and S462A for 72 hours. Cells were stained with an HA-specific antibody (red) and with "Höchst" to visualize the nuclei (blue). Stained cells were analysed with a fluorescent microscope. HA-FUS S462D and S462A are located mostly in the nucleus in few cells HA-FUS S462D and S462A are mislocated into the cytoplasm. Scale bar, 25 µm **C. Quantification of transfected cells on the basis of the location of HA-tagged FUS.** Transfection was carried out two times and of each, 5 images were taken randomly and of HA-FUS S462D 172 transfected cells and of HA-FUS S462A 154 transfected cells were counted. Counted cells were divided on the basis of the HA-FUS protein localisation into nuclear and cytoplasmic. Bars represent the mean percentage of cells of HA-FUS in the cytoplasm and nucleus. Error bars indicate standard deviation. **D. Statistical analysis of cytoplasmic HA-tagged FUS.** Counted cells were divided on the basis of the HA-FUS protein localisation into nuclear and cytoplasmic. Transfected cells with a cytoplasmic HA-FUS localisation were analysed with one-way ANOVA and Bonferroni post hoc test. Significance level was set at $p<0.05$ and error bars indicate standard deviation. The difference between HA-FUSwt and HA-FUS S462D and S462A is not significant.

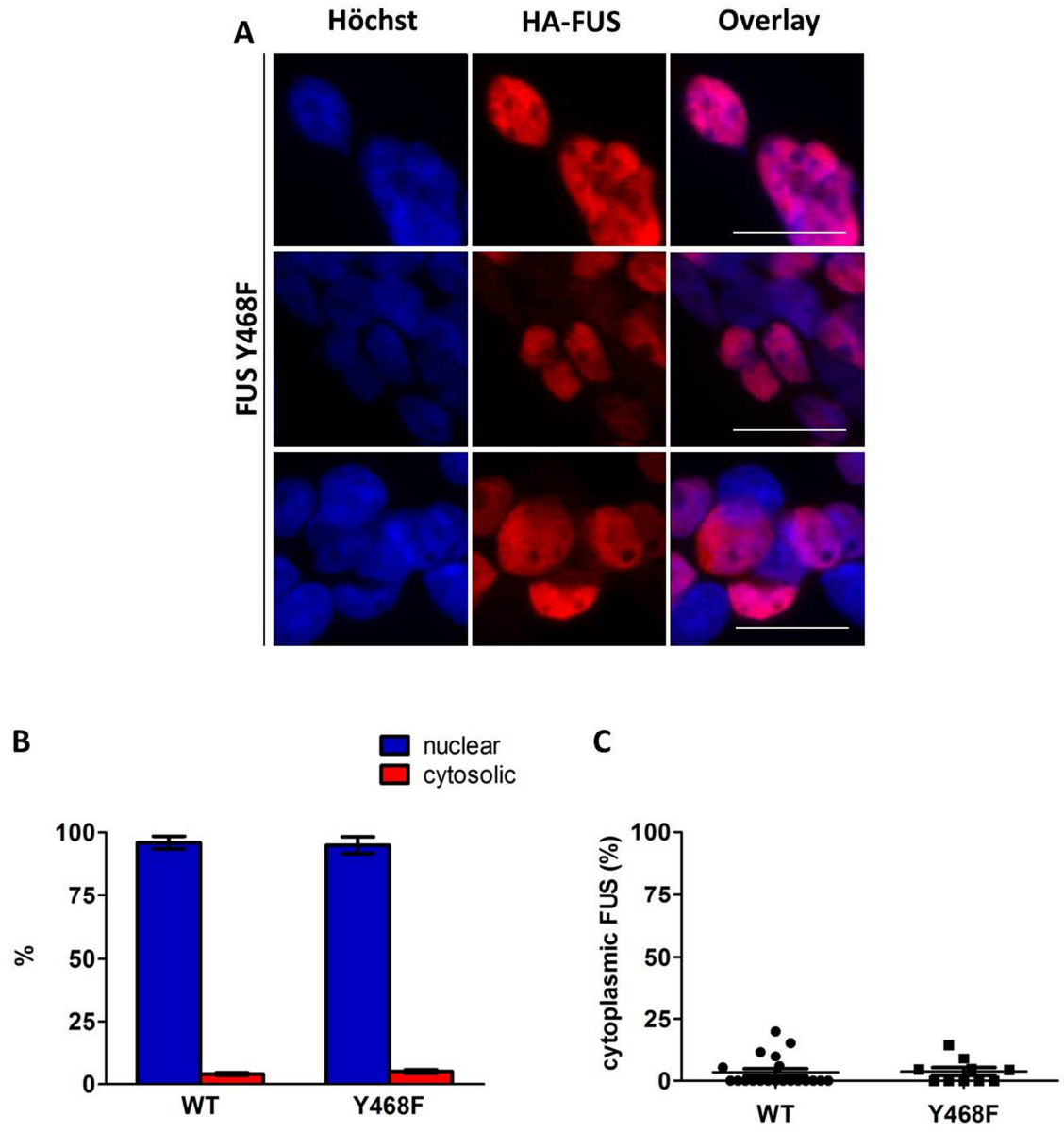

Figure 26. Double immunofluorescence and statistics of HEK293 cells transfected with HA-FUS Y468F.
A. Double immunofluorescence. Representative pictures of HEK293 cells transfected with HA-tagged FUS expression vector Y468F for 72 hours. Cells were stained with an HA-specific antibody (red) and with "Höchst" to visualize the nuclei (blue). Stained cells were analysed with a fluorescent microscope. HA-FUS Y468F is located mostly in the nucleus in few cells HA-FUS Y468F is mislocated into the cytoplasm. Scale bar, 25 µm **B. Quantification of transfected cells on the basis of the location of HA-tagged FUS.** Transfection was carried out two times and of each, 5 images were taken randomly and of HA-FUS Y468F 175 transfected cells were counted. Counted cells were divided on the basis of the HA-FUS protein localisation into nuclear and cytoplasmic. Bars represent the mean percentage of cells of HA-FUS in the cytoplasm and nucleus. Error bars indicate standard deviation. **C. Statistical analysis of cytoplasmic HA-tagged FUS.** Counted cells were divided on the basis of the HA-FUS protein localisation into nuclear and cytoplasmic. Transfected cells with a cytoplasmic HA-FUS localisation were analysed with one-way ANOVA and Bonferroni post hoc test. Significance level was set at $p<0.05$ and error bars indicate standard deviation. The difference between HA-FUSwt and HA-FUS Y468F is not significant.

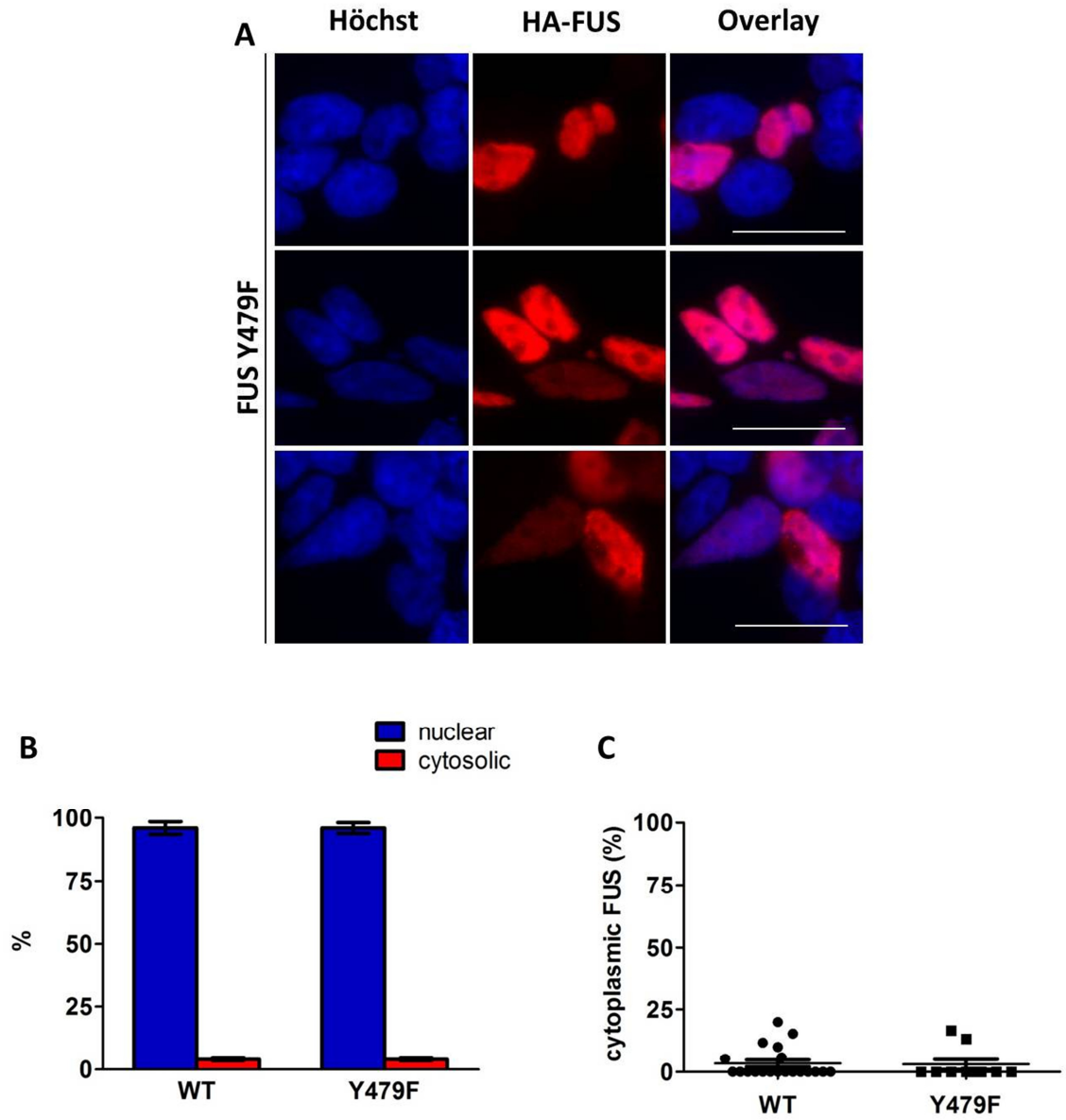

Figure 27. Double immunofluorescence and statistics of HEK293 cells transfected with HA-FUS Y479F.
A. Double immunofluorescence. Representative pictures of HEK293 cells transfected with HA-tagged FUS expression vector Y479F for 72 hours. Cells were stained with an HA-specific antibody (red) and with "Höchst" to visualize the nuclei (blue). Stained cells were analysed with a fluorescent microscope. HA-FUS Y479F is located mostly in the nucleus in few cells HA-FUS Y479F is mislocated into the cytoplasm. Scale bar, 25 μm **B. Quantification of transfected cells on the basis of the location of HA-tagged FUS.** Transfection was carried out two times and of each, 5 images were taken randomly and of HA-FUS Y479F 139 transfected cells were counted. Counted cells were divided on the basis of the HA-FUS protein localisation into nuclear and cytoplasmic. Bars represent the mean percentage of cells of HA-FUS in the cytoplasm and nucleus. Error bars indicate standard deviation. **C. Statistical analysis of cytoplasmic HA-tagged FUS.** Counted cells were divided on the basis of the HA-FUS protein localisation into nuclear and cytoplasmic. Transfected cells with a cytoplasmic HA-FUS localisation were analysed with one-way ANOVA and Bonferroni post hoc test. Significance level was set at $p<0.05$ and error bars indicate standard deviation. The difference between HA-FUSwt and HA-FUS Y479F is not significant.

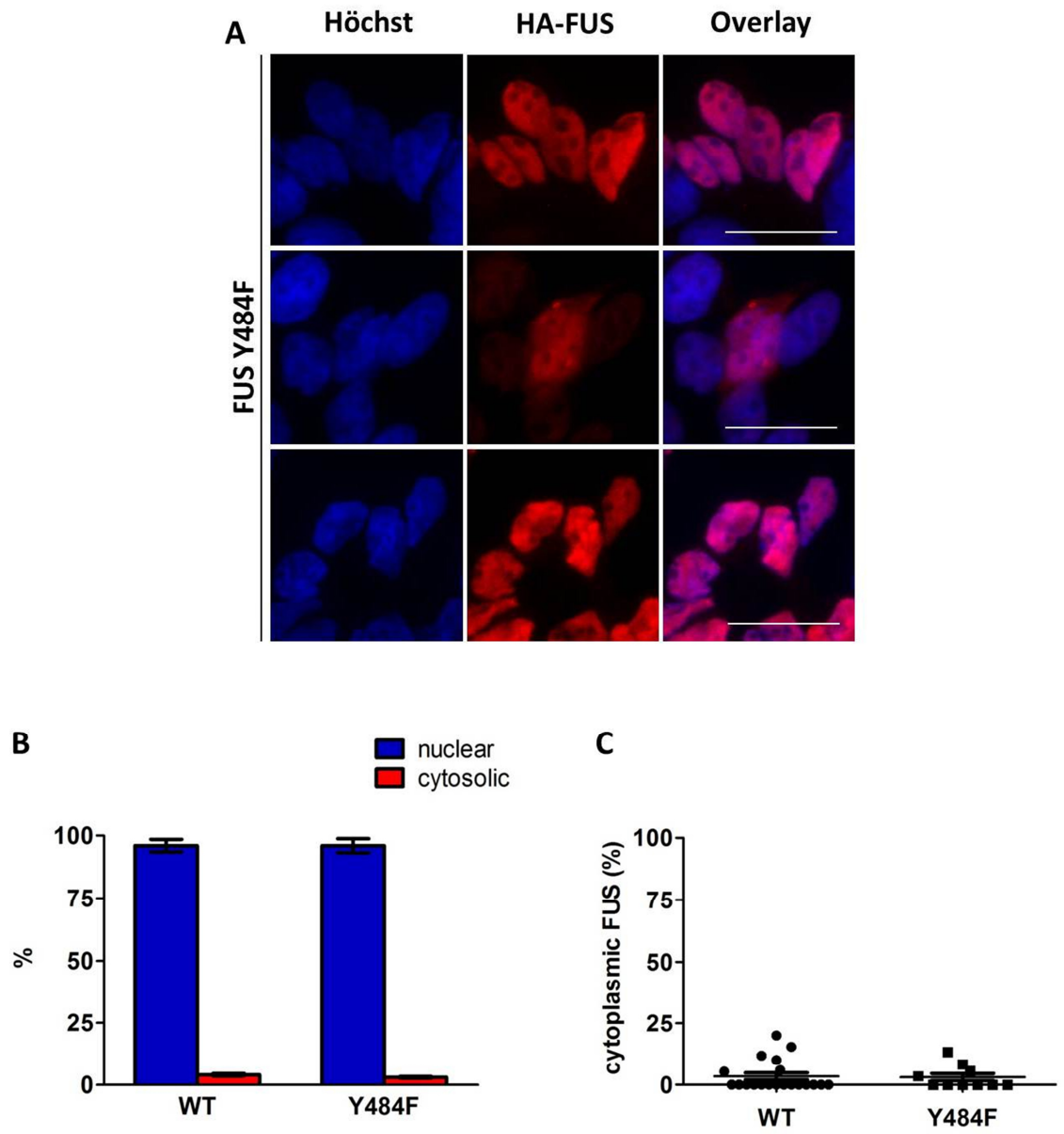

Figure 28. Double immunofluorescence and statistics of HEK293 cells transfected with HA-FUS Y484F.
A. Double immunofluorescence. Representative pictures of HEK293 cells transfected with HA-tagged FUS expression vector Y484F for 72 hours. Cells were stained with an HA-specific antibody (red) and with "Höchst" to visualize the nuclei (blue). Stained cells were analysed with a fluorescent microscope. HA-FUS Y484F is located mostly in the nucleus in few cells HA-FUS Y484F is mislocated into the cytoplasm. Scale bar, 25 µm **B. Quantification of transfected cells on the basis of the location of HA-tagged FUS.** Transfection was carried out two times and of each, 5 images were taken randomly and of HA-FUS Y484F 169 transfected cells were counted. Counted cells were divided on the basis of the HA-FUS protein localisation into nuclear and cytoplasmic. Bars represent the mean percentage of cells of HA-FUS in the cytoplasm and nucleus. Error bars indicate standard deviation. **C. Statistical analysis of cytoplasmic HA-tagged FUS.** Counted cells were divided on the basis of the HA-FUS protein localisation into nuclear and cytoplasmic. Transfected cells with a cytoplasmic HA-FUS localisation were analysed with one-way ANOVA and Bonferroni post hoc test. Significance level was set at $p<0.05$ and error bars indicate standard deviation. The difference between HA-FUSwt and HA-FUS Y484F is not significant.

4.3.2 HeLa cells

To further investigate whether phosphomimicking and dephosphomimicking mutations at S61, S84, S185 and S186 has an effect on the subcellular distribution of FUS independently of the cell type, I transfected HeLa cells with the plasmid encoding wild type FUS and with plasmids with phosphomimicking and dephosphomimicking mutations. Cells were stained as described in 3.2.3 and visualized with a fluorescence microscope.
As a positive control for increased cytoplasmic localization of FUS, I used the expression vector HA-FUS P525L, this point mutation in the PY-NLS signal leads to a severe mislocalization of FUS in HeLa cells (Dormann et al. 2010).

As expected, HA-tagged wild type FUS (HA-FUSwt) is located mostly in the nucleus, while translocation into the cytoplasm could be observed only in 12% of transfected cells (Figure 29A-D).

In further experiments HA-FUSwt is used as reference. As positive control HA-FUS P525L is used. In Figure 30 it is shown that HA-FUS P525L is located in the cytoplasm in all of the transfected cells. This is also apparent in the quantitative analysis of the transfected cells with a 100% localisation of HA-FUS in the cytoplasm.

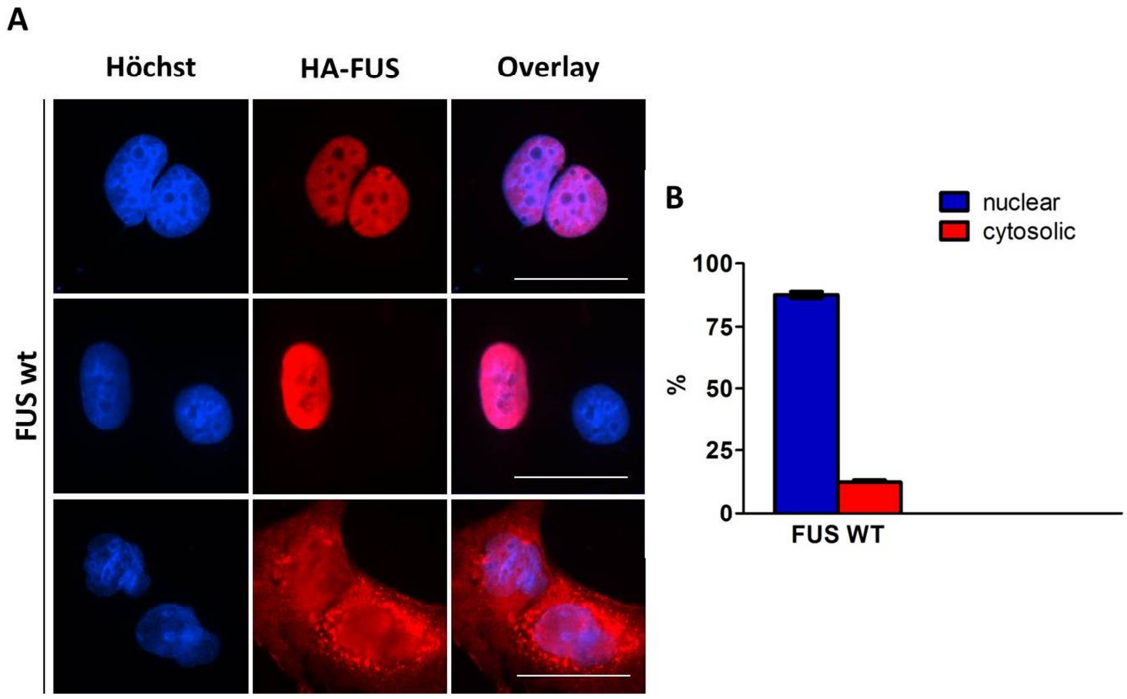

Figure 29. Double immunofluorescence and statistics of HeLa cells transfected with HA-tagged wild type FUS.

A. Double immunofluorescence. Representative pictures of HeLa cells transfected with HA-tagged wild type FUS expression vector for 72 hours. Cells were stained with an HA-specific antibody (red) and with "Höchst" to visualize the nuclei (blue). Stained cells were analysed with a fluorescent microscope. HA-FUSwt is located mostly in the nucleus in few cells HA-FUSwt is mislocated into the cytoplasm. Scale bar, 25 µm **B. Quantification of transfected cells on the basis of the location of HA-tagged FUS.** Transfection was carried out two times and of each, 10 images were taken randomly and of HA-FUSwt 145 transfected cells were counted. Counted cells were divided on the basis of the HA-FUS protein localisation into nuclear and cytoplasmic. Bars represent the mean percentage of cells of HA-FUS in the cytoplasm and nucleus. Error bars indicate standard deviation.

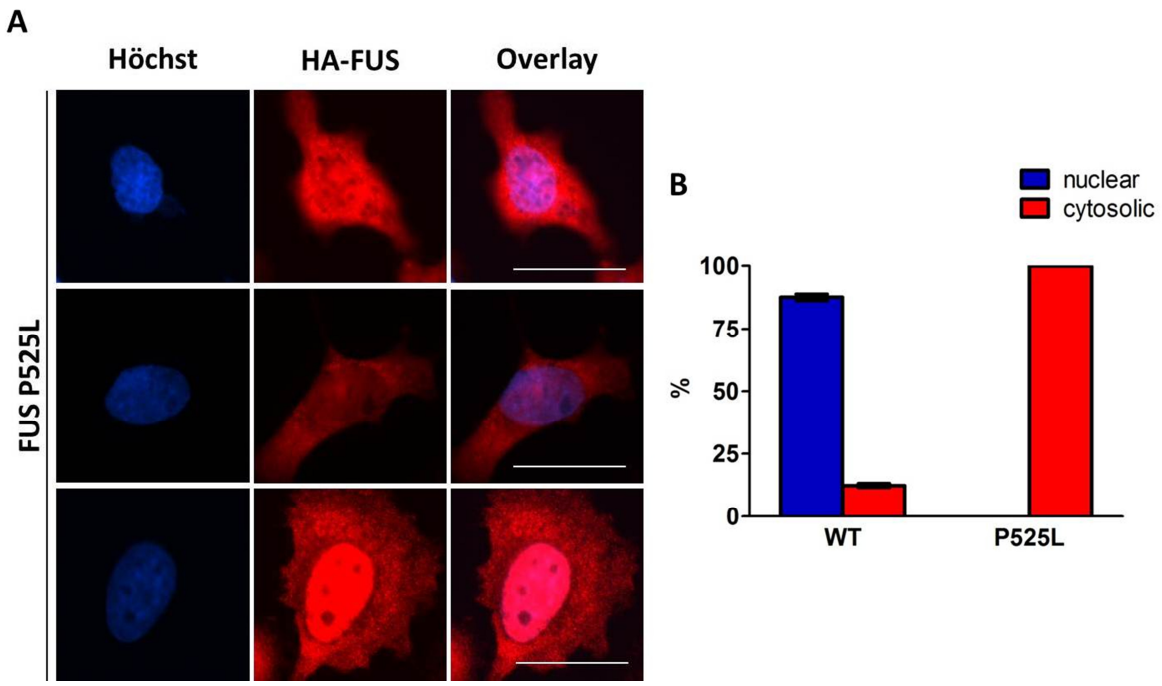

Figure 30. Double immunofluorescence and statistics of HeLa cells transfected with HA-FUS P525L.
A. Double immunofluorescence. Representative pictures of HeLa cells transfected with HA-tagged FUS expression vector P525L for 72 hours. Cells were stained with an HA-specific antibody (red) and with "Höchst" to visualize the nuclei (blue). Stained cells were analysed with a fluorescent microscope. HA-FUS P525L is located in the cytoplasm in all of the transfected cells. Scale bar, 25 µm **B. Quantification of transfected cells on the basis of the location of HA-tagged FUS.** Transfection was carried out two times and of each, 10 images were taken randomly and of HA-FUS P525L 99 transfected cells were counted. Counted cells were divided on the basis of the HA-FUS protein localisation into nuclear and cytoplasmic. Bars represent the mean percentage of cells of HA-FUS in the cytoplasm and nucleus. 100 % of the transfected cells show a mislocalisation of HA-FUS into the cytoplasm. Error bars indicate standard deviation.

In HEK293 cells, HA-FUS S61D is located in the cytoplasm in a significantly higher number of cells compared to HA-FUSwt and the dephosphomimicking partner HA-FUS S61A. However, these findings could not be reproduced in HeLa cells.

As shown in Figure 31 HA-FUS S61D and S61A are located mostly in the nucleus only in around 12% of the transfected cells, HA-FUS S61D and S61A are located in the cytoplasm. The difference between HA-FUSwt and HA-FUS S61D and S61A is not significant

Figure 32 shows representative pictures of HeLa cells transfected with HA-FUS S84D and S84A. Both are located mostly in the nucleus, in 12,6 % of cells transfected with HA-FUS S84D and in 22,8 % of cells transfected with HA-FUS S84A a mislocalisation into the cytoplasm is visible, whereupon the difference in cytoplasmic mislocalisation between those 2 variants is not significant. Although in comparison with wild type FUS, these differences are also not significant.

In HEK293 cells the phospho- and dephosphomimicking variants at S185 and S186 showed a significantly higher mislocalistion of FUS into the cytoplasm.

Transfection of HeLa cells with HA-FUS S185D and S185A led also in around 30% of transfected cell to a significant mislocalisation of HA-FUS into the cytoplasm (Figure 33A-D).

Moreover HA-FUS S186D and S186A are localised in around 30% of the transfected cells in the cytoplasm. In comparison with wild type FUS, only HA-FUS S186D shows a significantly higher mislocalisation of HA-FUS into the cytoplasm (Figure 34A-D).

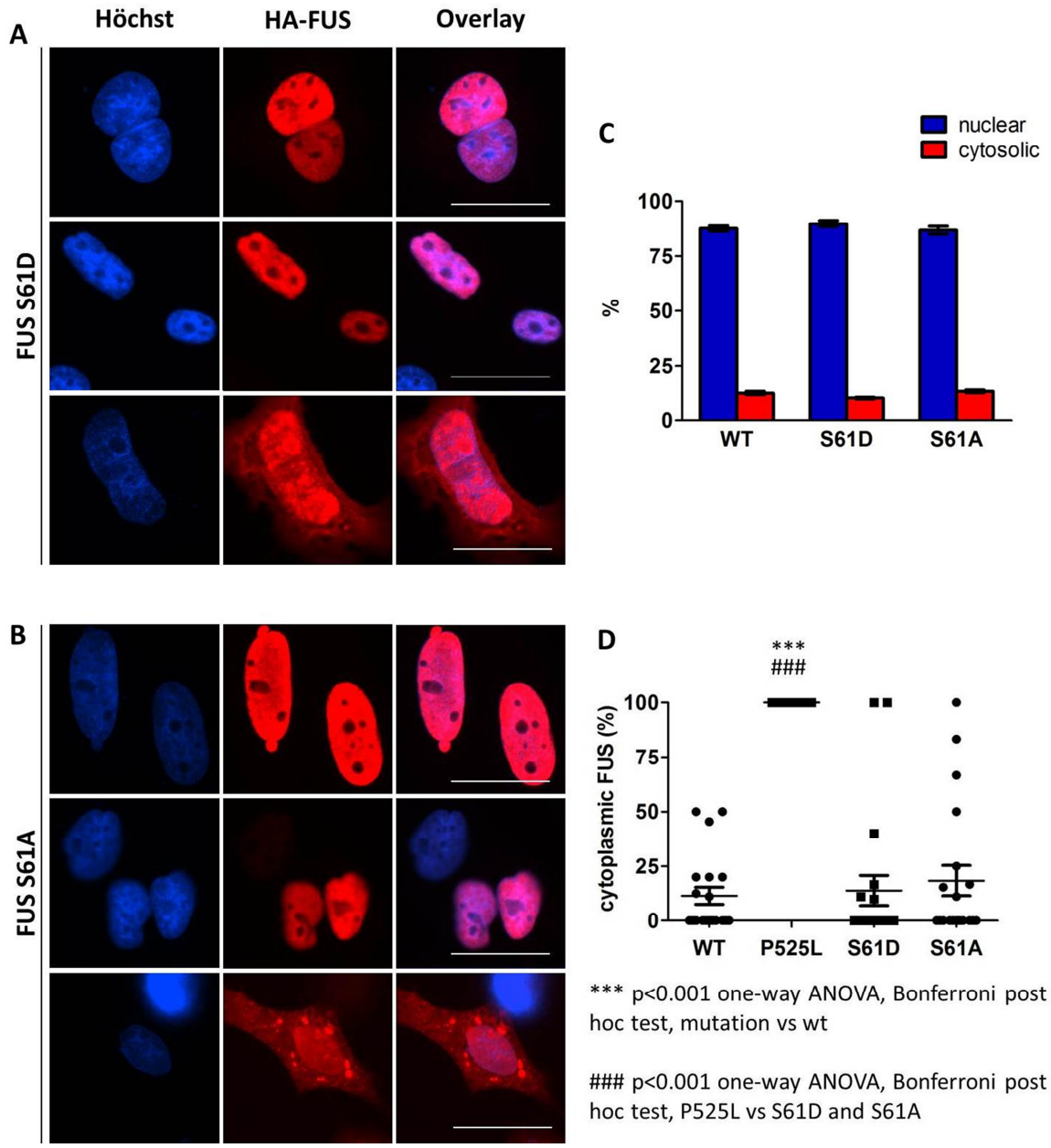

Figure 31. Double immunofluorescence and statistics of HeLa cells transfected with HA-FUS S61D and S61A.

A and B. Double immunofluorescence. Representative pictures of HeLa cells transfected with HA-tagged FUS expression vector S61D and S61A for 72 hours. Cells were stained with an HA-specific antibody (red) and with "Höchst" to visualize the nuclei (blue). Stained cells were analysed with a fluorescent microscope. HA-FUS S61D and S61A are located mostly in the nucleus in few cells HA-FUS S61D and S61A are mislocated into the cytoplasm. Scale bar, 25 μm **C. Quantification of transfected cells on the basis of the location of HA-tagged FUS.** Transfection was carried out two times and of each, 10 images were taken randomly and of HA-FUS S61D 99 transfected cells and of HA-FUS S61A 121 transfected cells were counted. Counted cells were divided on the basis of the HA-FUS protein localisation into nuclear and cytoplasmic. Bars represent the mean percentage of cells of HA-FUS in the cytoplasm and nucleus. Error bars indicate standard deviation. **D. Statistical analysis of cytoplasmic HA-tagged FUS.** Counted cells were divided on the basis of the HA-FUS protein localisation into nuclear and cytoplasmic. Transfected cells with a cytoplasmic HA-FUS localisation were analysed with one-way ANOVA and Bonferroni post hoc test. Significance level was set at $p<0.05$ and error bars indicate standard deviation. The positive control HA-FUS P525L is significantly higher cytoplasmic than HA-FUSwt and phosphomimicking and dephosphomimicking FUS variants. The difference between HA-FUSwt and HA-FUS S61D and S61A is not significant.

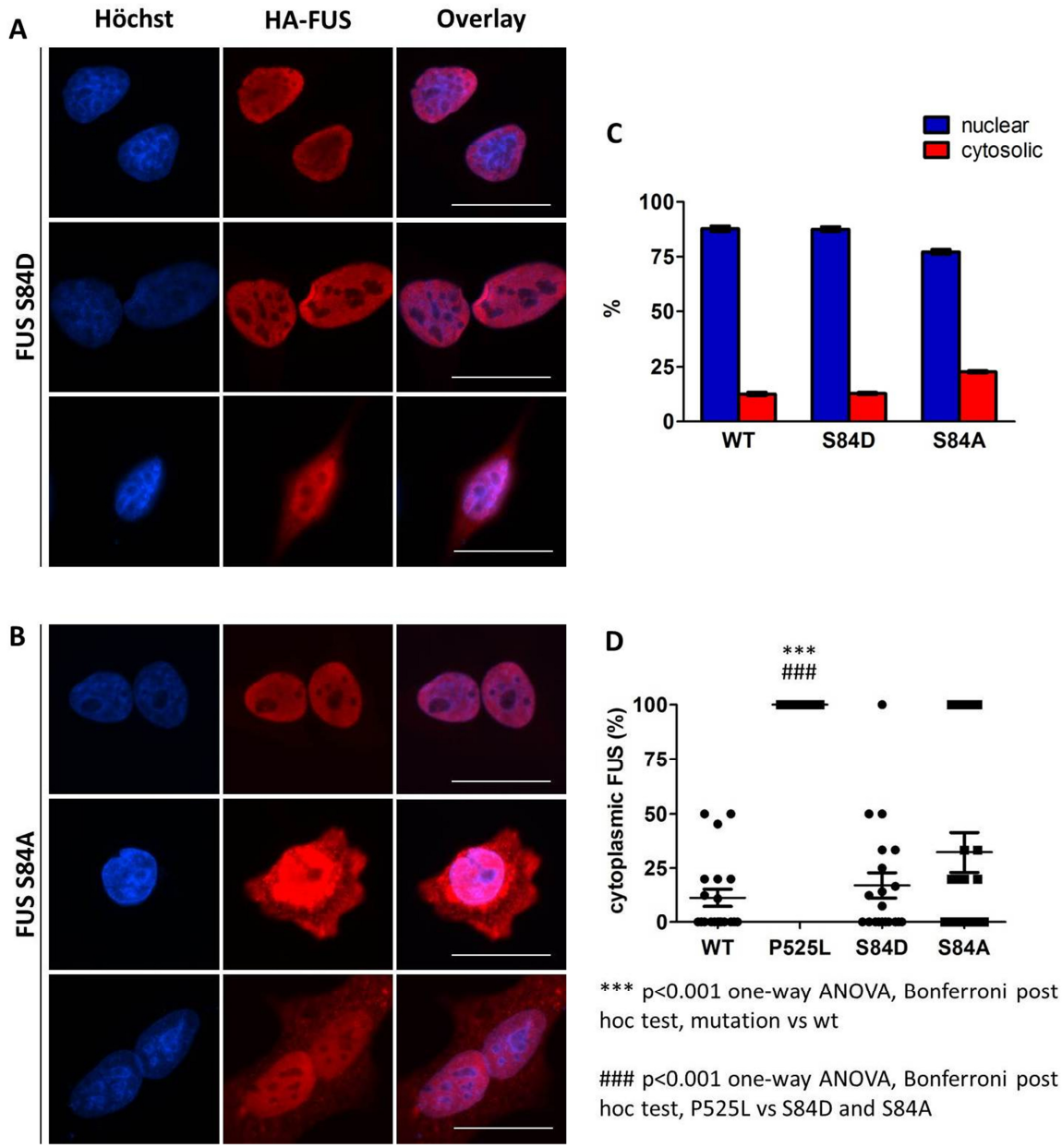

Figure 32. Double immunofluorescence and statistics of HeLa cells transfected with HA-FUS S84D and S84A.

A and B. Double immunofluorescence. Representative pictures of HeLa cells transfected with HA-tagged FUS expression vector S84D and S84A for 72 hours. Cells were stained with an HA-specific antibody (red) and with "Höchst" to visualize the nuclei (blue). Stained cells were analysed with a fluorescent microscope. HA-FUS S84D and S84A are located mostly in the nucleus in few cells HA-FUS S84D and S84A are mislocated into the cytoplasm, although S84A shows a higher mislocalisation than S84D Scale bar, 25 µm **C. Quantification of transfected cells on the basis of the location of HA-tagged FUS.** Transfection was carried out two times and of each, 10 images were taken randomly and of HA-FUS S84D 127 transfected cells and of HA-FUS S84A 101 transfected cells were counted. Counted cells were divided on the basis of the HA-FUS protein localisation into nuclear and cytoplasmic. Bars represent the mean percentage of cells of HA-FUS in the cytoplasm and nucleus. Error bars indicate standard deviation. **D. Statistical analysis of cytoplasmic HA-tagged FUS.** Counted cells were divided on the basis of the HA-FUS protein localisation into nuclear and cytoplasmic. Transfected cells with a cytoplasmic HA-FUS localisation were analysed with one-way ANOVA and Bonferroni post hoc test. Significance level was set at $p<0.05$ and error bars indicate standard deviation. The positive control HA-FUS P525L is significantly higher cytoplasmic than HA-FUSwt and phosphomimicking and dephosphomimicking FUS variants. The difference between HA-FUSwt and HA-FUS S84D and S84A is not significant.

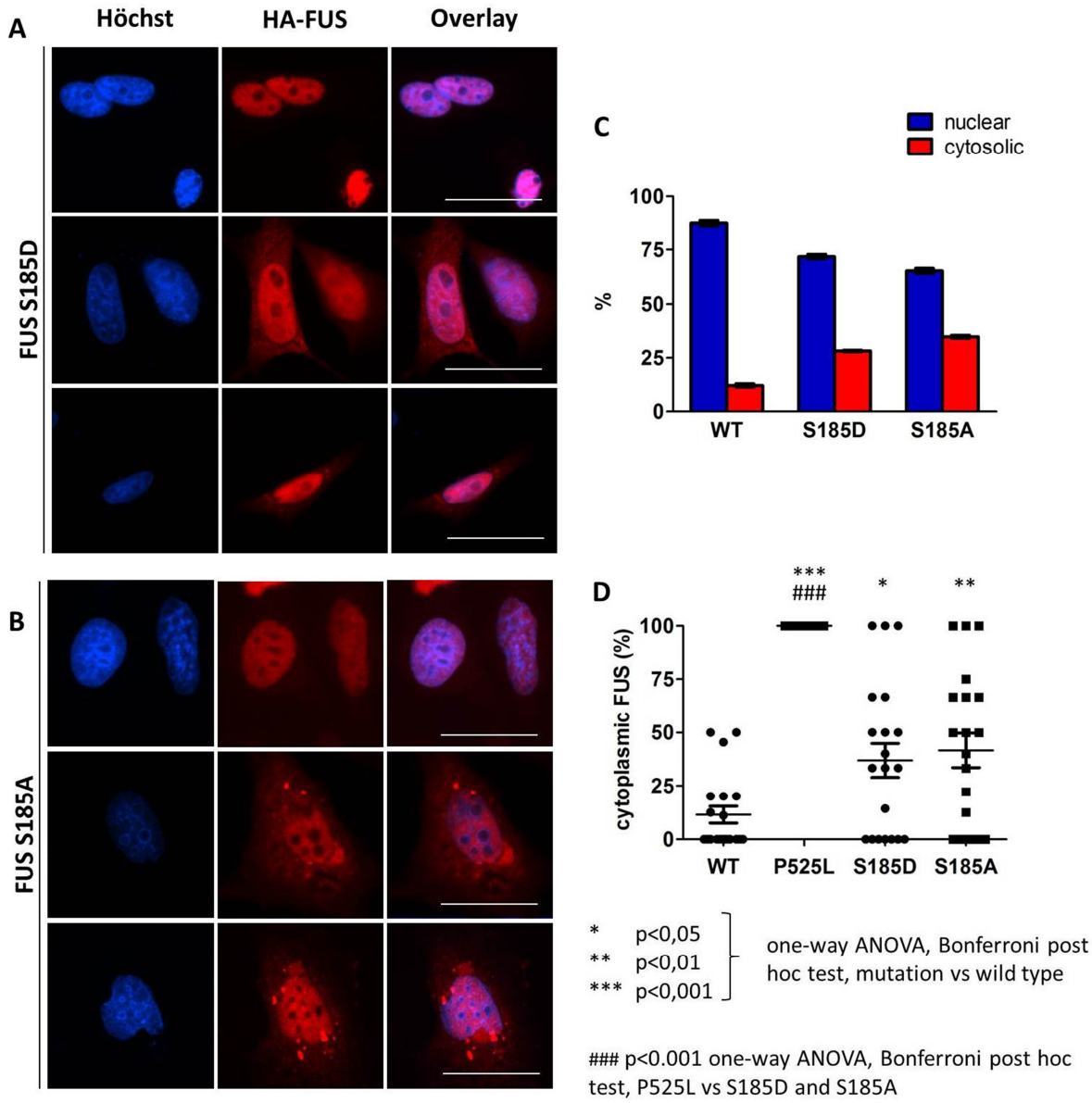

Figure 33. Double immunofluorescence and statistics of HeLa cells transfected with HA-FUS S185D and S185A.

A and B. Double immunofluorescence. Representative pictures of HeLa cells transfected with HA-tagged FUS expression vector S185D and S185A for 72 hours. Cells were stained with an HA-specific antibody (red) and with "Höchst" to visualize the nuclei (blue). Stained cells were analysed with a fluorescent microscope. HA-FUS S185D and S185A are located mostly in the nucleus but in many cells HA-FUS S185D and S185A are mislocated into the cytoplasm. Scale bar, 25 µm **C. Quantification of transfected cells on the basis of the location of HA-tagged FUS.** Transfection was carried out two times and of each, 10 images were taken randomly and of HA-FUS S185D 85 transfected cells and of HA-FUS S185A 95 transfected cells were counted. Counted cells were divided on the basis of the HA-FUS protein localisation into nuclear and cytoplasmic. Bars represent the mean percentage of cells of HA-FUS in the cytoplasm and nucleus. Error bars indicate standard deviation.**D. Statistical analysis of cytoplasmic HA-tagged FUS.** Counted cells were divided on the basis of the HA-FUS protein localisation into nuclear and cytoplasmic. Transfected cells with a cytoplasmic HA-FUS localisation were analysed with one-way ANOVA and Bonferroni post hoc test. Significance level was set at $p<0.05$ and error bars indicate standard deviation. The positive control HA-FUS P525L is significantly higher cytoplasmic than HA-FUSwt and phosphomimicking and dephosphomimicking FUS variants. HA-FUS 185D and S185A show a significantly higher mislocalisation of HA-FUS into the cytoplasm than HA-FUSwt.

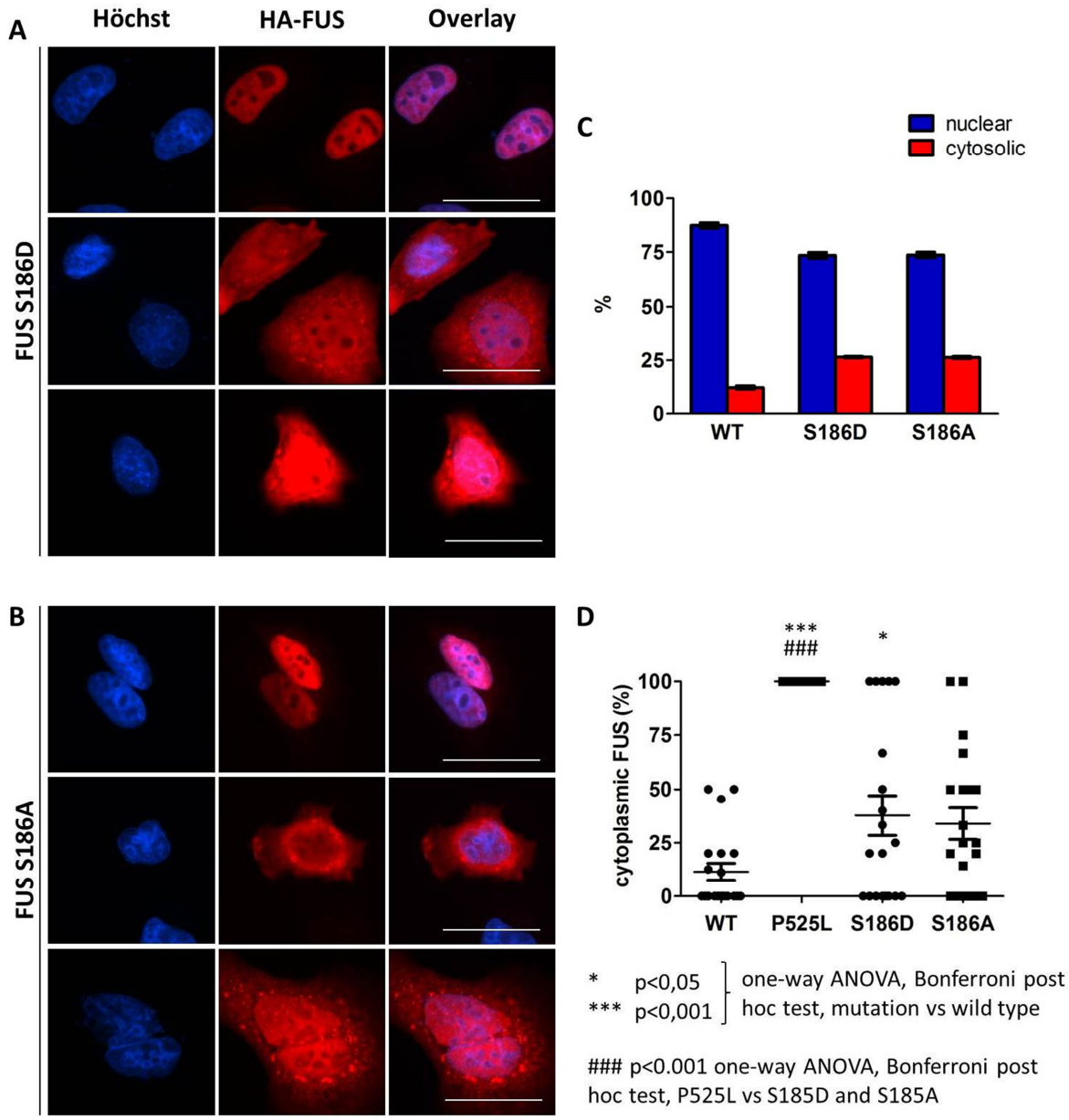

Figure 34. Double immunofluorescence and statistics of HeLa cells transfected with HA-FUS S186D and S186A.

A and B. Double immunofluorescence. Representative pictures of HeLa cells transfected with HA-tagged FUS expression vector S186D and S186A for 72 hours. Cells were stained with an HA-specific antibody (red) and with "Höchst" to visualize the nuclei (blue). Stained cells were analysed with a fluorescent microscope. HA-FUS S186D and S186A are located mostly in the nucleus but in many cells HA-FUS S186D and S186A are mislocated into the cytoplasm. Scale bar, 25 µm **C. Quantification of transfected cells on the basis of the location of HA-tagged FUS.** Transfection was carried out two times and of each, 10 images were taken randomly and of HA-FUS S186D 83 transfected cells and of HA-FUS S186A 99 transfected cells were counted. Counted cells were divided on the basis of the HA-FUS protein localisation into nuclear and cytoplasmic. Bars represent the mean percentage of cells of HA-FUS in the cytoplasm and nucleus. Error bars indicate standard deviation.**D. Statistical analysis of cytoplasmic HA-tagged FUS.** Counted cells were divided on the basis of the HA-FUS protein localisation into nuclear and cytoplasmic. Transfected cells with a cytoplasmic HA-FUS localisation were analysed with one-way ANOVA and Bonferroni post hoc test. Significance level was set at $p<0.05$ and error bars indicate standard deviation. The positive control HA-FUS P525L is significantly higher cytoplasmic than HA-FUSwt and phosphomimicking and dephosphomimicking FUS variants. HA-FUS 186D shows a significantly higher mislocalisation of HA-FUS into the cytoplasm than HA-FUSwt and the dephosphomimetic partner HA-FUS S186A.

5 Discussion

Abnormal aggregation of the protein FUS is a characteristic hallmark lesion in ALS patients with mutations in the *FUS* gene and in a subgroup of FTLD patients (FTLD-FUS). In ALS-*FUS,* mutations in the PY-NLS affect transportin-mediated nuclear import thus leading to abnormal cytoplasmic FUS accumulation (Dormann et al., 2010). Until now, the pathomechanisms which lead to such abnormal protein aggregates in sporadic cases are not understood.

The aim of my thesis was to determine the impact of phosphorylation and dephosphorylation on the subcellular distribution of FUS. Therefore, I produced FUS expression vectors with phosphomimicking and dephosphomimicking mutations and I have evaluated the percentage of cells showing cytoplasmic immunoreactivity.

To see if the investigated amino acid sites may be important amino acids for the function of FUS, I aligned the human FUS sequence with the FUS sequence of mouse, rat and zebrafish (Figure 35). I could determine that the amino acids S26, S84, S183, S185, Y232, S257, S277, T286, S462, Y468, Y479 and Y484 are conserved in nearly all four species. This means that some these amino acids may be important for proper FUS protein folding or function. An interesting feature is that the amino acids Y464, Y479 and Y484, which are conserved in human, mouse and rat, are substituted to phenylalanine, the dephosphomimicking variant of tyrosine, in zebrafish, thus implicating that those amino acids cannot be phosphorylated in zebrafish.

The amino acids S42, S131, S186 are substituted in mouse, rat and zebrafish mainly to glycine and asparagine, those amino acids are chemically different to serine. S61 is substituted to threonine. Threonine and serine have a similar chemical structure, therefore this amino acid change does not have a major impact on the structure or function of the protein thus suggesting that conserving an -OH group in that position might be important to retain FUS function.

With this alignment, I can suggest that nearly all of the investigated site of FUS may play an important role in FUS physiology. Especially S185 where the phosphomimetic as well as dephosphomimetic variant and S84 with a phosphomimetic mutation lead to a mislocalization of FUS into the cytoplasm, both amino acids are conserved in all four species.

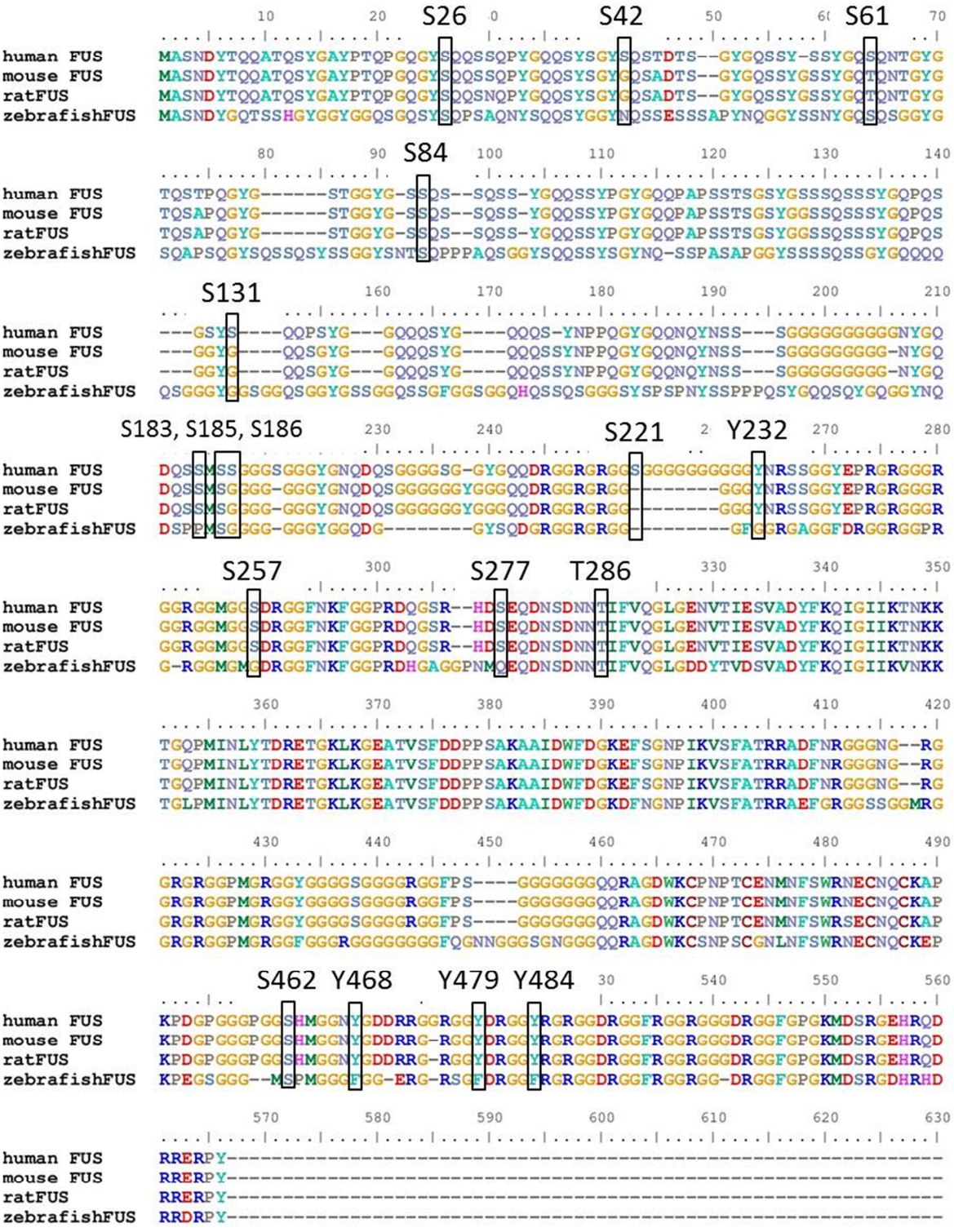

Figure 35. Alignment of FUS sequences.
Alignment of the human, mouse, rat and zebrafish FUS sequence with the software BioEdit. Site S26, S84, S185, T286 and S462 are showing the same amino acid in all four sequences. S183, Y232, S257, S277, T286, S462, Y468, Y479 and Y484 have the same aminoacid in human, mouse and rat. This means that the human FUS sites with the same amino acids also in other sequences are highly conserved and may be important amino acids of the FUS protein. G= glycine, F= phenylalanine, N= asparagine, P=proline, Q=glutamine, S= serine, T= threonine, Y= tyrosine.

In HEK293 cell, phosphomimicking FUS variants at four specific serine sites 61, 84, 185 and 186 are significantly mislocalised into the cytoplasm (Figure 14, Figure 15, Figure 18, Figure 19). Interestingly, while HA-FUS S61A and S84A do not show enhanced cytoplasmic localization, HA-FUS S185A and S186A distribution closely resembles that of their phosphomimicking counterparts (Figure 18, Figure 19).

Under physiological conditions S61and S84 are not phosphorylated (Gardiner et al., 2008), however in cells exposed to ionizing radiation or treated with cytotoxic agents to induce double strand breaks, FUS is phosphorylated by ATM at S61 and S84 (Gardiner et al., 2008). In keeping with this, I might speculate that in FTD an unknown primary insult might trigger FUS phosphorylation on S61 or S84, thus leading to its cytoplasmic localisation.

In contrast, S185 and S186 are two sites, where not the phosphorylation itself but maybe a structural change leads to the mislocalisation of FUS into the cytoplasm. S185 and S186 are located in the glycine rich (Gly-rich) domain of FUS (Figure 3). RNA binding proteins (RBP) have often Gly-rich domain, which are highly unstructured and the function of those Gly-rich domains is rarely understood, it is thought that those unstructured regions are involved in the interaction with other proteins and RNAs. One common thing of unstructured regions is their amino acid composition, most time those regions are enriched in hydrophilic and charged amino acid residues. Furthermore unstructured regions have often a high amount of amino acids which are target for post-translational modifications, such as phosphorylation or arginine methylation. FUS consists of many unstructured regions, like the glycine-serine rich region (in Figure 3 named as Gly-rich region) and the arginine-glycine-glycine (RGG) rich boxes (Rogelj et al., 2011). One third of all *FUS* mutations are located in the Gly-rich region; this leads to the suggestion that this region is a domain of the FUS protein which is important for proper motor neuron maintenance and thus any modification, affecting these specific amino acids S185 and S186 might has a wider impact on the function of FUS.

To confirm that the observed phenomenon in HEK293 cells is not restricted to this specific cell type, I performed the same type of experiment on HeLa cells. Firstly, a quantitatively different result in HEK293 and HeLa cells is obtained for HA-FUSwt. In HEK293 cells, I could observe HA-FUSwt only in 4% of transfected cells in the cytoplasm (Figure 11), however in HeLa cells HA-FUSwt was localised in the cytoplasm in 12% of the transfected cells (Figure 29). Moreover, although all 4 FUS phosphomimicking variants displayed enhanced presence in the cytoplasm, this effect was statistically significant only for HA-FUS S185D and S186D (Figure 31- Figure 34). The difference in HEK293 cells and HeLa cells

could be to some extent explained by the characteristics of those two cell types. HEK293 cells were generated in 1970 from human embryonic cells and transformed with sheared adenovirus 5 DNA. The specific cell type of HEK293 cells is unknown, since they were originated from a tissue containing almost all cell types, such as fibroblasts, endothelial cells and epithelial cells. Through the transformation with the adenovirus the cell morphology and the expression could have been changed (Thomas and Smart, 2005). HeLa cells are an immortal human cell line which was generated in 1950 from cervical cancer cells of Henrietta Lacks. HeLa cells are epithelial cells and since the cell line was generated, they have been used to understand cell physiology and cancer biology (Masters, 2002).

Another possibility to explain the different result in HEK293 and HeLa cells is the different transfection method used, that might itself be a source of cell stress. Namely, I used calcium-phosphate method to transfect HEK293 cells with my specific phospho- and dephosphomimicking variants, while transfection of HeLa cells was performed with Effectene transfection reagent.

To further address this discrepancy, one could perform a more quantitative analysis of the amount of FUS mislocalized in the cytoplasm by subcellular fractionation analyses and Western blot analysis and it would be also important to investigate effect of these mutations in a broader spectrum of cell lines including neuronal cell lines.

During my Masterthesis, I only investigated whether phosphorylation has an effect on the subcellular distribution of FUS. However, it may affect also other physiological conditions, such as RNA binding, solubility or nucleocytoplasmic transport. Phosphorylation, in or next to regions that are important for RNA binding, such as RBD or RGG motif, may have functional consequences, like impaired protein-RNA binding and also impaired protein-protein interactions. The RBD of FET/TET family members consist of 80-90 amino acids, which form four anti-parallel β-strands with two additional α-helices. In this RBD there are two conserved motifs, ribonucleoprotein-1 (RNP-1) and ribonucleoprotein-2 (RNP-2), amino acids in these two motifs are involved in RNA recognition and binding. The RNP-1 of FET/TET proteins comprises a threonine at the fourth position and also other amino acids that could get phosphorylated. The RBD is highly conserved within the FET/TET family and they bind to sequence-specific RNA. Due to that, phosphorylation in this motif may affect FUS-RNA binding (Tan and Manley, 2009). I investigated 6 specific amino acids sites S277, T286, S462, Y468, Y479 and Y484 in the RBD and RGG motif. Phospho- and dephosphomimicking variants of those sites did not led to a significant mislocalisation of FUS

(Figure 23- Figure 29). However, phosphorylation at those sites may be important to modulate RNA binding and therefore, this impact could be investigated in further RNA-binding-experiments, such as RNA electrophoretic mobility shift assay or FISH/ISH co-localisation assay. Moreover, in this region there are also other specific amino acids that can be phosphorylated, during my Masterthesis I only investigated amino acids sites, where phosphorylation has been already described.

Furthermore, phosphorylation can also affect protein solubility (Zhang et al., 2010). The residues of charged hydrophilic amino acids (e.g. arginine, lysine and aspartic acid) on the surface of a protein interact with water molecules and determine the charge of a protein, for example at a pH of 7, aspartic acid carries a negative charge. Normally proteins have a net charge; this depends on the number of charged amino acids and their location within a protein and the pH itself. The pH at which the net charge is zero is called the isoelectric point (pI) (Widmann et al., 2010). For FUS the pI is 9,4, this implicates that at physiological pH it is positively charged and phosphorylation can reduce FUS pI. If proteins have no net charge, they prefer to interact with other proteins and this leads to protein aggregates or protein precipitation (Gitlin et al., 2006, Shaw and Valentine, 2007). Phosphorylation of specific amino acids in FUS could change the net charge of it and thereby lead to protein aggregation in the cytoplasm. Interestingly, analysis of post-mortem FTLD-FUS tissues indicated increased FUS concentration in insoluble protein fractions (Neumann et al., 2009a). Thus, it would be interesting to investigate if phosphorylation has an effect on the solubility of FUS, with sequential protein extraction of transfected cells followed by SDS-Page and western blot.

FUS contains a PY-NLS in its C-terminal domain, which is recognized and bound by the nuclear import receptor transportin (Dormann et al., 2010), this FUS-transportin complex is transported into the nucleus in a Ran-GTPase-dependent manner (Nardozzi et al., 2010). Through a phosphorylation in the NLS of FUS the binding of FUS and transportin could be affected thus impairing the transport into the nucleus. During my Masterthesis, I investigated no site in the NLS of FUS, however, it could be investigated in further experiments if phosphorylation at specific amino acids in the NLS has an impact on the subcellular distribution of FUS. For instance, another interesting amino acid position of FUS would be tyrosine 526 (Y526). Interestingly, it has been reported that the analogue tyrosine in EWS Y656 is phosphorylated and the corresponding dephosphomimetic EWS variant accumulates in the cytoplasm and colocalises with transportin-1 (Leemann-Zakaryan et al., 2011). Thus, it would be interesting to see if phosphorylation or dephosphorylation of Y526 has an effect on the subcellular distribution of FUS. Dormann et al. investigated the subcellular distribution of

HA-FUS Y526A observing a severe mislocalisation of FUS into the cytoplasm (Dormann et al., 2010). However, Y526A cannot be considered as proper dephosphomimicking variant because the structure of tyrosine and alanine are very different. Therefore, it would be interesting to investigate whether the same dramatic effect could be observed with a dephosphomimicking mutation to phenylalanine (F).

ALS-*FUS* is characterized by mutations in the *FUS* gene, most of them are located in the PY-NLS of *FUS* and disrupt the NLS, which leads to a mislocalisation of FUS into the cytoplasm. However, in patients with FTLD-FUS another mechanism must be responsible for FUS pathological redistribution as no mutations could be detected. Furthermore, the occurrence of mutations is not the only difference between ALS-*FU*S and FTLD-FUS. FUS positive inclusions in neurons and glia cells of FTLD-FUS patients are also positive for the other FET/TET proteins, EWS and TAF 15 (Neumann et al., 2011) and their nuclear import receptor transportin (Trn-1) (Neumann et al., 2012) but not inclusions in ALS-*FUS*. This leads to the suggestion that the pathomechanism leading to ALS-*FUS* and FTLD-FUS could be different.

FUS is a member of the FET/TET family, which share structural and functional similarities (Figure 36) and have many sites for post-translational modifications, especially for phosphorylation and arginine methylation.

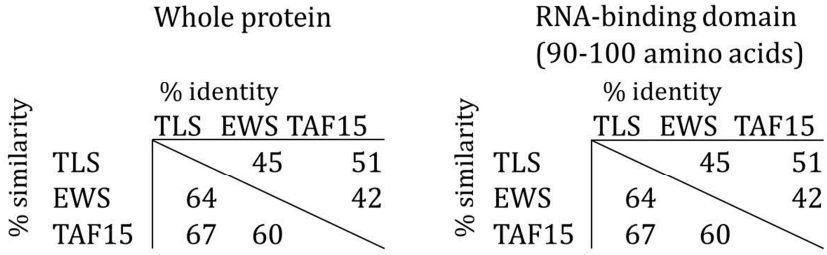

Figure 36. FET/TET proteins: amino acid similarity within the whole proteins and in the RNA-binding domain.
The FET/TET proteins FUS (TLS), EWS and TAF 15 share structural similarities. Reference: modified from Tan et al. 2009

In response to DNA damage, Ewing's Sarcoma protein (EWS) is phosphorylated by c-Jun-N-terminal kinases (JNK) and the p38 mitogen-activated protein kinases at threonine 79. This specific amino acid site is also phosphorylated by ERK (extracellular signal-regulated kinases) in response to mitogens (Klevernic et al., 2009). Furthermore EWS protein contains an IQ (isoleucine-glutamine) motif, which is known as regulatory element for Ca^{2+}

transduction in neuronal proteins, serine 266 in this IQ-motif is phosphorylated by protein kinase C (PKC) which inhibits RNA binding to EWS (Deloulme et al., 1997).
TAF-15, another member of the FET/TET family, has several tyrosine sites which get phosphorylated by v-Src (viral sarcoma) protein tyrosine kinase to modulate transcriptional activity (Lee et al., 2004). These phosphorylation events of EWS and TAF15 have effects on RNA binding, transcription activity and other cellular processes (Tan and Manley, 2009). It would be interesting to investigate EWS, TAF15 and Tpn-1 distribution in HEK293 and HeLa cells expressing the phospho- and dephosphomimicking FUS variants at the sites of interest S61, S84, S185 and S186 and also to investigate effects of similar mutations in corresponding amino acids of TAF15 and EWS on subcellular distribution to further investigate the role of phosphorylation in FTLD-FUS.

To summarize, in my Masterthesis I could identify four promising amino acid positions, whose modification led to FUS cytoplasmic redistribution in a subset of cells. In particular, phosphomimetic mutations of S61 and S84 led to a significant mislocalisation of FUS into the cytoplasm. Phsophorylation at these sites were described after stress conditions, supporting the idea that cellular stress might contribute to FUS accumulation and FUS pathogenesis (Dormann et al. 2010). Both phospho- and dephosphomimetic mutations at S185 and S186 modulated the subcellular distribution in around 50 % of HEK293 cells and in 30 % of HeLa cells most likely by a structural change in the Gly rich domain of FUS. Further experiments including mass-spec analysis of post-mortem brain tissue of FTLD-FUS are needed to further investigate the relevance of FUS phosphorylation in the pathogenesis of FUSopathies.

6 Summary

The neurodegenerative diseases ALS and FTLD are characterized, in a subgroup of cases, by abnormal cytoplasmic aggregates called “inclusions” and containing the protein FUS. In ALS patients, mutations located in the NLS of the *FUS* gene disrupt FUS nuclear import thus leading to FUS mislocalization. However, in sporadic cases the mechanisms of FUS cytoplasmic accumulations are still unknown.

PTMs are chemical modifications which can regulate nucleocytoplasmic transport at different levels. Therefore, the aim of my Masterthesis was to determine the impact of post-translational modifications, especially phosphorylation, on the subcellular distribution of FUS. With site directed mutagenesis, I produced HA-tagged FUS expression vectors with phospho- and dephosphomimicking mutations of 17 specific amino acid sites of FUS, based on described phosphorylation sites. I used those constructs and wild type FUS, as a negative control, to transiently transfect HEK293 cells, followed by immunofluorescence in order to monitor the subcellular distribution of the expressed variant FUS. Only variants at 4 sites displayed significantly enhanced cytoplasmic expression in comparison with wild type FUS, namely serines 61, 84, 185 and 186. In particular, the phosphomimicking FUS variants S61D and S84D were both expressed in the cytoplasm of more cells than the wild type FUS or their dephosphomimicking counterpart. Conversely, both phospho- and dephosphomimicking FUS variants at sites 185 and 186 display enhanced cytoplasmic expression.

In order to corroborate this finding, the expression of those FUS variants was also investigated in HeLa cells, but only phosphomimicking mutation of serine 185 and 186 and dephosphomimicking mutation of serine 185 lead to a significant mislocalisation in to the cytoplasm, compared to wild type FUS.

These results suggest that modifications on specific residues may lead to FUS cytoplasmic localisation in a subgroup of cells thus supporting the possibility that abnormal FUS PTM might be involved in the pathogenesis of FUS-proteinopathies.

7 References

Aman P, Panagopoulos I, Lassen C, Fioretos T, Mencinger M, Toresson H, Hoglund M, Forster A, Rabbitts TH, Ron D, Mandahl N, Mitelman F (1996) Expression patterns of the human sarcoma-associated genes FUS and EWS and the genomic structure of FUS. Genomics 37:1-8.

Andersson MK, Stahlberg A, Arvidsson Y, Olofsson A, Semb H, Stenman G, Nilsson O, Aman P (2008) The multifunctional FUS, EWS and TAF15 proto-oncoproteins show cell type-specific expression patterns and involvement in cell spreading and stress response. BMC cell biology 9:37.

Anthis NJ, Haling JR, Oxley CL, Memo M, Wegener KL, Lim CJ, Ginsberg MH, Campbell ID (2009) Beta integrin tyrosine phosphorylation is a conserved mechanism for regulating talin-induced integrin activation. The Journal of biological chemistry 284:36700-36710.

Baker M, Mackenzie IR, Pickering-Brown SM, Gass J, Rademakers R, Lindholm C, Snowden J, Adamson J, Sadovnick AD, Rollinson S, Cannon A, Dwosh E, Neary D, Melquist S, Richardson A, Dickson D, Berger Z, Eriksen J, Robinson T, Zehr C, Dickey CA, Crook R, McGowan E, Mann D, Boeve B, Feldman H, Hutton M (2006) Mutations in progranulin cause tau-negative frontotemporal dementia linked to chromosome 17. Nature 442:916-919.

Baumer D, Hilton D, Paine SM, Turner MR, Lowe J, Talbot K, Ansorge O (2010) Juvenile ALS with basophilic inclusions is a FUS proteinopathy with FUS mutations. Neurology 75:611-618.

Belly A, Moreau-Gachelin F, Sadoul R, Goldberg Y (2005) Delocalization of the multifunctional RNA splicing factor TLS/FUS in hippocampal neurones: exclusion from the nucleus and accumulation in dendritic granules and spine heads. Neuroscience letters 379:152-157.

Berridge MJ (2012) Cell Signalling Biology. http://www.biochemj.org/csb/010/csb010.pdf; access date: 28.12.2012: Portland Press Limited.

Bertolotti A, Lutz Y, Heard DJ, Chambon P, Tora L (1996) hTAF(II)68, a novel RNA/ssDNA-binding protein with homology to the pro-oncoproteins TLS/FUS and EWS is associated with both TFIID and RNA polymerase II. The EMBO journal 15:5022-5031.

Bird T, Knopman D, VanSwieten J, Rosso S, Feldman H, Tanabe H, Graff-Raford N, Geschwind D, Verpillat P, Hutton M (2003) Epidemiology and genetics of frontotemporal dementia/Pick's disease. Ann Neurol 54 Suppl 5:S29-31.

Boisvert FM, Cote J, Boulanger MC, Richard S (2003) A proteomic analysis of arginine-methylated protein complexes. Molecular & cellular proteomics : MCP 2:1319-1330.

Bruijn LI, Houseweart MK, Kato S, Anderson KL, Anderson SD, Ohama E, Reaume AG, Scott RW, Cleveland DW (1998) Aggregation and motor neuron toxicity of an ALS-linked SOD1 mutant independent from wild-type SOD1. Science 281:1851-1854.

Calvio C, Neubauer G, Mann M, Lamond AI (1995) Identification of hnRNP P2 as TLS/FUS using electrospray mass spectrometry. Rna 1:724-733.

Camats M, Guil S, Kokolo M, Bach-Elias M (2008) P68 RNA helicase (DDX5) alters activity of cis- and trans-acting factors of the alternative splicing of H-Ras. PloS one 3:e2926.

Chansky HA, Barahmand-Pour F, Mei Q, Kahn-Farooqi W, Zielinska-Kwiatkowska A, Blackburn M, Chansky K, Conrad EU, 3rd, Bruckner JD, Greenlee TK, Yang L (2004) Targeting of EWS/FLI-1 by RNA interference attenuates the tumor phenotype of Ewing's sarcoma cells in vitro. Journal of orthopaedic research : official publication of the Orthopaedic Research Society 22:910-917.

Chio A, Mora G, Calvo A, Mazzini L, Bottacchi E, Mutani R, Parals (2009) Epidemiology of ALS in Italy: a 10-year prospective population-based study. Neurology 72:725-731.

Cohen P (2000) The regulation of protein function by multisite phosphorylation--a 25 year update. Trends in biochemical sciences 25:596-601.

Crozat A, Aman P, Mandahl N, Ron D (1993) Fusion of CHOP to a novel RNA-binding protein in human myxoid liposarcoma. Nature 363:640-644.

Cruts M, Kumar-Singh S, Van Broeckhoven C (2006) Progranulin mutations in ubiquitin-positive frontotemporal dementia linked to chromosome 17q21. Current Alzheimer research 3:485-491.

DeJesus-Hernandez M, Mackenzie IR, Boeve BF, Boxer AL, Baker M, Rutherford NJ, Nicholson AM, Finch NA, Flynn H, Adamson J, Kouri N, Wojtas A, Sengdy P, Hsiung GY, Karydas A, Seeley WW, Josephs KA, Coppola G, Geschwind DH, Wszolek ZK, Feldman H, Knopman DS, Petersen RC, Miller BL, Dickson DW, Boylan KB, Graff-Radford NR, Rademakers R (2011) Expanded GGGGCC hexanucleotide repeat in noncoding region of C9ORF72 causes chromosome 9p-linked FTD and ALS. Neuron 72:245-256.

Deloulme JC, Prichard L, Delattre O, Storm DR (1997) The prooncoprotein EWS binds calmodulin and is phosphorylated by protein kinase C through an IQ domain. The Journal of biological chemistry 272:27369-27377.

Diehl-Schmid J, Neumann M, Laws SM, Perneczky R, Grimmer T, Danek A, Kurz A, Riemenschneider M, Forstl H (2009) [Frontotemporal lobar degeneration]. Fortschr Neurol Psychiatr 77:295-304.

Dormann D, Madl T, Valori CF, Bentmann E, Tahirovic S, Abou-Ajram C, Kremmer E, Ansorge O, Mackenzie IR, Neumann M, Haass C (2012) Arginine methylation next to the PY-NLS modulates Transportin binding and nuclear import of FUS. The EMBO journal 31:4258-4275.

Dormann D, Rodde R, Edbauer D, Bentmann E, Fischer I, Hruscha A, Than ME, Mackenzie IR, Capell A, Schmid B, Neumann M, Haass C (2010) ALS-associated fused in sarcoma (FUS) mutations disrupt Transportin-mediated nuclear import. The EMBO journal 29:2841-2857.

Du K, Arai S, Kawamura T, Matsushita A, Kurokawa R (2011) TLS and PRMT1 synergistically coactivate transcription at the survivin promoter through TLS arginine methylation. Biochemical and biophysical research communications 404:991-996.

Ferraiuolo L, Kirby J, Grierson AJ, Sendtner M, Shaw PJ (2011) Molecular pathways of motor neuron injury in amyotrophic lateral sclerosis. Nature reviews Neurology 7:616-630.

Fujii R, Okabe S, Urushido T, Inoue K, Yoshimura A, Tachibana T, Nishikawa T, Hicks GG, Takumi T (2005) The RNA binding protein TLS is translocated to dendritic spines by mGluR5 activation and regulates spine morphology. Current biology : CB 15:587-593.

Fujii R, Takumi T (2005) TLS facilitates transport of mRNA encoding an actin-stabilizing protein to dendritic spines. Journal of cell science 118:5755-5765.

Gardiner M, Toth R, Vandermoere F, Morrice NA, Rouse J (2008) Identification and characterization of FUS/TLS as a new target of ATM. The Biochemical journal 415:297-307.

Gitlin I, Carbeck JD, Whitesides GM (2006) Why are proteins charged? Networks of charge-charge interactions in proteins measured by charge ladders and capillary electrophoresis. Angewandte Chemie 45:3022-3060.

Gregory RI, Yan KP, Amuthan G, Chendrimada T, Doratotaj B, Cooch N, Shiekhattar R (2004) The Microprocessor complex mediates the genesis of microRNAs. Nature 432:235-240.

Hallier M, Lerga A, Barnache S, Tavitian A, Moreau-Gachelin F (1998) The transcription factor Spi-1/PU.1 interacts with the potential splicing factor TLS. The Journal of biological chemistry 273:4838-4842.

Hodges JR, Davies R, Xuereb J, Kril J, Halliday G (2003) Survival in frontotemporal dementia. Neurology 61:349-354.

Hoell JI, Larsson E, Runge S, Nusbaum JD, Duggimpudi S, Farazi TA, Hafner M, Borkhardt A, Sander C, Tuschl T (2011) RNA targets of wild-type and mutant FET family proteins. Nature structural & molecular biology 18:1428-1431.

Hsu PP, Kang SA, Rameseder J, Zhang Y, Ottina KA, Lim D, Peterson TR, Choi Y, Gray NS, Yaffe MB, Marto JA, Sabatini DM (2011) The mTOR-regulated phosphoproteome reveals a mechanism of mTORC1-mediated inhibition of growth factor signaling. Science 332:1317-1322.

Husi H, Ward MA, Choudhary JS, Blackstock WP, Grant SG (2000) Proteomic analysis of NMDA receptor-adhesion protein signaling complexes. Nature neuroscience 3:661-669.

Hutton M, Perez-Tur J, Hardy J (1998) Genetics of Alzheimer's disease. Essays in biochemistry 33:117-131.

Iko Y, Kodama TS, Kasai N, Oyama T, Morita EH, Muto T, Okumura M, Fujii R, Takumi T, Tate S, Morikawa K (2004) Domain architectures and characterization of an RNA-binding protein, TLS. The Journal of biological chemistry 279:44834-44840.

Ishigaki S, Masuda A, Fujioka Y, Iguchi Y, Katsuno M, Shibata A, Urano F, Sobue G, Ohno K (2012) Position-dependent FUS-RNA interactions regulate alternative splicing events and transcriptions. Scientific reports 2:529.

Jorgensen C, Sherman A, Chen GI, Pasculescu A, Poliakov A, Hsiung M, Larsen B, Wilkinson DG, Linding R, Pawson T (2009) Cell-specific information processing in segregating populations of Eph receptor ephrin-expressing cells. Science 326:1502-1509.

Kameoka S, Duque P, Konarska MM (2004) p54(nrb) associates with the 5' splice site within large transcription/splicing complexes. The EMBO journal 23:1782-1791.

Klevernic IV, Morton S, Davis RJ, Cohen P (2009) Phosphorylation of Ewing's sarcoma protein (EWS) and EWS-Fli1 in response to DNA damage. The Biochemical journal 418:625-634.

Kwiatkowski TJ, Jr., Bosco DA, Leclerc AL, Tamrazian E, Vanderburg CR, Russ C, Davis A, Gilchrist J, Kasarskis EJ, Munsat T, Valdmanis P, Rouleau GA, Hosler BA, Cortelli P, de Jong PJ, Yoshinaga Y, Haines JL, Pericak-Vance MA, Yan J, Ticozzi N, Siddique T, McKenna-Yasek D, Sapp PC, Horvitz HR, Landers JE, Brown RH, Jr. (2009) Mutations in the FUS/TLS gene on chromosome 16 cause familial amyotrophic lateral sclerosis. Science 323:1205-1208.

Lagier-Tourenne C, Polymenidou M, Cleveland DW (2010) TDP-43 and FUS/TLS: emerging roles in RNA processing and neurodegeneration. Human molecular genetics 19:R46-64.

Lagier-Tourenne C, Polymenidou M, Hutt KR, Vu AQ, Baughn M, Huelga SC, Clutario KM, Ling SC, Liang TY, Mazur C, Wancewicz E, Kim AS, Watt A, Freier S, Hicks GG, Donohue JP, Shiue L, Bennett CF, Ravits J, Cleveland DW, Yeo GW (2012) Divergent roles of ALS-linked proteins FUS/TLS and TDP-43 intersect in processing long pre-mRNAs. Nature neuroscience 15:1488-1497.

Lanson NA, Jr., Pandey UB (2012) FUS-related proteinopathies: lessons from animal models. Brain research 1462:44-60.

Law WJ, Cann KL, Hicks GG (2006) TLS, EWS and TAF15: a model for transcriptional integration of gene expression. Briefings in functional genomics & proteomics 5:8-14.

Lee HJ, Kim S, Pelletier J, Kim J (2004) Stimulation of hTAFII68 (NTD)-mediated transactivation by v-Src. FEBS letters 564:188-198.
Leemann-Zakaryan RP, Pahlich S, Grossenbacher D, Gehring H (2011) Tyrosine Phosphorylation in the C-Terminal Nuclear Localization and Retention Signal (C-NLS) of the EWS Protein. Sarcoma 2011:218483.
Lerga A, Hallier M, Delva L, Orvain C, Gallais I, Marie J, Moreau-Gachelin F (2001) Identification of an RNA binding specificity for the potential splicing factor TLS. The Journal of biological chemistry 276:6807-6816.
Mackenzie IR, Ansorge O, Strong M, Bilbao J, Zinman L, Ang LC, Baker M, Stewart H, Eisen A, Rademakers R, Neumann M (2011a) Pathological heterogeneity in amyotrophic lateral sclerosis with FUS mutations: two distinct patterns correlating with disease severity and mutation. Acta Neuropathol 122:87-98.
Mackenzie IR, Munoz DG, Kusaka H, Yokota O, Ishihara K, Roeber S, Kretzschmar HA, Cairns NJ, Neumann M (2011b) Distinct pathological subtypes of FTLD-FUS. Acta Neuropathol 121:207-218.
Mackenzie IR, Neumann M, Bigio EH, Cairns NJ, Alafuzoff I, Kril J, Kovacs GG, Ghetti B, Halliday G, Holm IE, Ince PG, Kamphorst W, Revesz T, Rozemuller AJ, Kumar-Singh S, Akiyama H, Baborie A, Spina S, Dickson DW, Trojanowski JQ, Mann DM (2009) Nomenclature for neuropathologic subtypes of frontotemporal lobar degeneration: consensus recommendations. Acta Neuropathol 117:15-18.
Mackenzie IR, Neumann M, Bigio EH, Cairns NJ, Alafuzoff I, Kril J, Kovacs GG, Ghetti B, Halliday G, Holm IE, Ince PG, Kamphorst W, Revesz T, Rozemuller AJ, Kumar-Singh S, Akiyama H, Baborie A, Spina S, Dickson DW, Trojanowski JQ, Mann DM (2010a) Nomenclature and nosology for neuropathologic subtypes of frontotemporal lobar degeneration: an update. Acta Neuropathol 119:1-4.
Mackenzie IR, Rademakers R, Neumann M (2010b) TDP-43 and FUS in amyotrophic lateral sclerosis and frontotemporal dementia. Lancet neurology 9:995-1007.
Masters JR (2002) HeLa cells 50 years on: the good, the bad and the ugly. Nature reviews Cancer 2:315-319.
Mayya V, Lundgren DH, Hwang SI, Rezaul K, Wu L, Eng JK, Rodionov V, Han DK (2009) Quantitative phosphoproteomic analysis of T cell receptor signaling reveals system-wide modulation of protein-protein interactions. Sci Signal 2:ra46.
Meissner M, Lopato S, Gotzmann J, Sauermann G, Barta A (2003) Proto-oncoprotein TLS/FUS is associated to the nuclear matrix and complexed with splicing factors PTB, SRm160, and SR proteins. Experimental cell research 283:184-195.
Mitchell JD, Borasio GD (2007) Amyotrophic lateral sclerosis. Lancet 369:2031-2041.
Nardozzi JD, Lott K, Cingolani G (2010) Phosphorylation meets nuclear import: a review. Cell communication and signaling : CCS 8:32.
Neumann M, Bentmann E, Dormann D, Jawaid A, DeJesus-Hernandez M, Ansorge O, Roeber S, Kretzschmar HA, Munoz DG, Kusaka H, Yokota O, Ang LC, Bilbao J, Rademakers R, Haass C, Mackenzie IR (2011) FET proteins TAF15 and EWS are selective markers that distinguish FTLD with FUS pathology from amyotrophic lateral sclerosis with FUS mutations. Brain : a journal of neurology 134:2595-2609.
Neumann M, Rademakers R, Roeber S, Baker M, Kretzschmar HA, Mackenzie IR (2009a) A new subtype of frontotemporal lobar degeneration with FUS pathology. Brain : a journal of neurology 132:2922-2931.
Neumann M, Roeber S, Kretzschmar HA, Rademakers R, Baker M, Mackenzie IR (2009b) Abundant FUS-immunoreactive pathology in neuronal intermediate filament inclusion disease. Acta Neuropathol 118:605-616.
Neumann M, Sampathu DM, Kwong LK, Truax AC, Micsenyi MC, Chou TT, Bruce J, Schuck T, Grossman M, Clark CM, McCluskey LF, Miller BL, Masliah E, Mackenzie

IR, Feldman H, Feiden W, Kretzschmar HA, Trojanowski JQ, Lee VM (2006) Ubiquitinated TDP-43 in frontotemporal lobar degeneration and amyotrophic lateral sclerosis. Science 314:130-133.

Neumann M, Valori CF, Ansorge O, Kretzschmar HA, Munoz DG, Kusaka H, Yokota O, Ishihara K, Ang LC, Bilbao JM, Mackenzie IR (2012) Transportin 1 accumulates specifically with FET proteins but no other transportin cargos in FTLD-FUS and is absent in FUS inclusions in ALS with FUS mutations. Acta Neuropathol 124:705-716.

Pawson T (2002) Regulation and targets of receptor tyrosine kinases. European journal of cancer 38 Suppl 5:S3-10.

Perrotti D, Iervolino A, Cesi V, Cirinna M, Lombardini S, Grassilli E, Bonatti S, Claudio PP, Calabretta B (2000) BCR-ABL prevents c-jun-mediated and proteasome-dependent FUS (TLS) proteolysis through a protein kinase CbetaII-dependent pathway. Molecular and cellular biology 20:6159-6169.

Powers CA, Mathur M, Raaka BM, Ron D, Samuels HH (1998) TLS (translocated-in-liposarcoma) is a high-affinity interactor for steroid, thyroid hormone, and retinoid receptors. Molecular endocrinology 12:4-18.

Rabbitts TH, Forster A, Larson R, Nathan P (1993) Fusion of the dominant negative transcription regulator CHOP with a novel gene FUS by translocation t(12;16) in malignant liposarcoma. Nature genetics 4:175-180.

Rademakers R, Stewart H, Dejesus-Hernandez M, Krieger C, Graff-Radford N, Fabros M, Briemberg H, Cashman N, Eisen A, Mackenzie IR (2010) Fus gene mutations in familial and sporadic amyotrophic lateral sclerosis. Muscle & nerve 42:170-176.

Rappsilber J, Friesen WJ, Paushkin S, Dreyfuss G, Mann M (2003) Detection of arginine dimethylated peptides by parallel precursor ion scanning mass spectrometry in positive ion mode. Analytical chemistry 75:3107-3114.

Rappsilber J, Ryder U, Lamond AI, Mann M (2002) Large-scale proteomic analysis of the human spliceosome. Genome research 12:1231-1245.

Renton AE, Majounie E, Waite A, Simon-Sanchez J, Rollinson S, Gibbs JR, Schymick JC, Laaksovirta H, van Swieten JC, Myllykangas L, Kalimo H, Paetau A, Abramzon Y, Remes AM, Kaganovich A, Scholz SW, Duckworth J, Ding J, Harmer DW, Hernandez DG, Johnson JO, Mok K, Ryten M, Trabzuni D, Guerreiro RJ, Orrell RW, Neal J, Murray A, Pearson J, Jansen IE, Sondervan D, Seelaar H, Blake D, Young K, Halliwell N, Callister JB, Toulson G, Richardson A, Gerhard A, Snowden J, Mann D, Neary D, Nalls MA, Peuralinna T, Jansson L, Isoviita VM, Kaivorinne AL, Holtta-Vuori M, Ikonen E, Sulkava R, Benatar M, Wuu J, Chio A, Restagno G, Borghero G, Sabatelli M, Heckerman D, Rogaeva E, Zinman L, Rothstein JD, Sendtner M, Drepper C, Eichler EE, Alkan C, Abdullaev Z, Pack SD, Dutra A, Pak E, Hardy J, Singleton A, Williams NM, Heutink P, Pickering-Brown S, Morris HR, Tienari PJ, Traynor BJ (2011) A hexanucleotide repeat expansion in C9ORF72 is the cause of chromosome 9p21-linked ALS-FTD. Neuron 72:257-268.

Rigbolt KT, Prokhorova TA, Akimov V, Henningsen J, Johansen PT, Kratchmarova I, Kassem M, Mann M, Olsen JV, Blagoev B (2011) System-wide temporal characterization of the proteome and phosphoproteome of human embryonic stem cell differentiation. Sci Signal 4:rs3.

Rogelj B, Easton LE, Bogu GK, Stanton LW, Rot G, Curk T, Zupan B, Sugimoto Y, Modic M, Haberman N, Tollervey J, Fujii R, Takumi T, Shaw CE, Ule J (2012) Widespread binding of FUS along nascent RNA regulates alternative splicing in the brain. Scientific reports 2:603.

Rogelj B, Godin KS, Shaw CE, Ule J (2011) THE FUNCTION OF GLYCINE-RICH REGIONS IN TDP-43, FUS AND RELATED RNA-BINDING PROTEINS.

http://www2.mrc-lmb.cam.ac.uk/groups/jule/publications/pub5.pdf; access date: 24.12.2012: Landes Bioscience and Springer Science.
Rosso SM, Donker Kaat L, Baks T, Joosse M, de Koning I, Pijnenburg Y, de Jong D, Dooijes D, Kamphorst W, Ravid R, Niermeijer MF, Verheij F, Kremer HP, Scheltens P, van Duijn CM, Heutink P, van Swieten JC (2003) Frontotemporal dementia in The Netherlands: patient characteristics and prevalence estimates from a population-based study. Brain : a journal of neurology 126:2016-2022.
Selamat W, Jamari I, Wang Y, Takumi T, Wong F, Fujii R (2009) TLS interaction with NMDA R1 splice variant in retinal ganglion cell line RGC-5. Neuroscience letters 450:163-166.
Shaw BF, Valentine JS (2007) How do ALS-associated mutations in superoxide dismutase 1 promote aggregation of the protein? Trends in biochemical sciences 32:78-85.
Shoesmith CL, Findlater K, Rowe A, Strong MJ (2007) Prognosis of amyotrophic lateral sclerosis with respiratory onset. Journal of neurology, neurosurgery, and psychiatry 78:629-631.
Skibinski G, Parkinson NJ, Brown JM, Chakrabarti L, Lloyd SL, Hummerich H, Nielsen JE, Hodges JR, Spillantini MG, Thusgaard T, Brandner S, Brun A, Rossor MN, Gade A, Johannsen P, Sorensen SA, Gydesen S, Fisher EM, Collinge J (2005) Mutations in the endosomal ESCRTIII-complex subunit CHMP2B in frontotemporal dementia. Nature genetics 37:806-808.
Tan AY, Manley JL (2009) The TET family of proteins: functions and roles in disease. Journal of molecular cell biology 1:82-92.
Tan AY, Manley JL (2010) TLS inhibits RNA polymerase III transcription. Molecular and cellular biology 30:186-196.
Thermo Fisher Scientific (2012) Post-translational modifications. http://www.piercenet.com/browse.cfm?fldID=7CE3FCF5-0DA0-4378-A513-2E35E5E3B49B; access date: 30.11.2012.
Thomas P, Smart TG (2005) HEK293 cell line: a vehicle for the expression of recombinant proteins. Journal of pharmacological and toxicological methods 51:187-200.
Tradewell ML, Yu Z, Tibshirani M, Boulanger MC, Durham HD, Richard S (2012) Arginine methylation by PRMT1 regulates nuclear-cytoplasmic localization and toxicity of FUS/TLS harbouring ALS-linked mutations. Human molecular genetics 21:136-149.
Ubersax JA, Ferrell JE, Jr. (2007) Mechanisms of specificity in protein phosphorylation. Nature reviews Molecular cell biology 8:530-541.
Uranishi H, Tetsuka T, Yamashita M, Asamitsu K, Shimizu M, Itoh M, Okamoto T (2001) Involvement of the pro-oncoprotein TLS (translocated in liposarcoma) in nuclear factor-kappa B p65-mediated transcription as a coactivator. The Journal of biological chemistry 276:13395-13401.
Urwin H, Josephs KA, Rohrer JD, Mackenzie IR, Neumann M, Authier A, Seelaar H, Van Swieten JC, Brown JM, Johannsen P, Nielsen JE, Holm IE, Consortium FR, Dickson DW, Rademakers R, Graff-Radford NR, Parisi JE, Petersen RC, Hatanpaa KJ, White CL, 3rd, Weiner MF, Geser F, Van Deerlin VM, Trojanowski JQ, Miller BL, Seeley WW, van der Zee J, Kumar-Singh S, Engelborghs S, De Deyn PP, Van Broeckhoven C, Bigio EH, Deng HX, Halliday GM, Kril JJ, Munoz DG, Mann DM, Pickering-Brown SM, Doodeman V, Adamson G, Ghazi-Noori S, Fisher EM, Holton JL, Revesz T, Rossor MN, Collinge J, Mead S, Isaacs AM (2010) FUS pathology defines the majority of tau- and TDP-43-negative frontotemporal lobar degeneration. Acta Neuropathol 120:33-41.
van Langenhove T, van der Zee J, van Broeckhoven C (2012) The molecular basis of the frontotemporal lobar degeneration-amyotrophic lateral sclerosis spectrum. Annals of medicine 44:817-828.

Vance C, Rogelj B, Hortobagyi T, De Vos KJ, Nishimura AL, Sreedharan J, Hu X, Smith B, Ruddy D, Wright P, Ganesalingam J, Williams KL, Tripathi V, Al-Saraj S, Al-Chalabi A, Leigh PN, Blair IP, Nicholson G, de Belleroche J, Gallo JM, Miller CC, Shaw CE (2009) Mutations in FUS, an RNA processing protein, cause familial amyotrophic lateral sclerosis type 6. Science 323:1208-1211.

Watts GD, Wymer J, Kovach MJ, Mehta SG, Mumm S, Darvish D, Pestronk A, Whyte MP, Kimonis VE (2004) Inclusion body myopathy associated with Paget disease of bone and frontotemporal dementia is caused by mutant valosin-containing protein. Nature genetics 36:377-381.

Widmann M, Trodler P, Pleiss J (2010) The isoelectric region of proteins: a systematic analysis. PloS one 5:e10546.

Worms PM (2001) The epidemiology of motor neuron diseases: a review of recent studies. Journal of the neurological sciences 191:3-9.

Wu F, Wang P, Zhang J, Young LC, Lai R, Li L (2010) Studies of phosphoproteomic changes induced by nucleophosmin-anaplastic lymphoma kinase (ALK) highlight deregulation of tumor necrosis factor (TNF)/Fas/TNF-related apoptosis-induced ligand signaling pathway in ALK-positive anaplastic large cell lymphoma. Molecular & cellular proteomics : MCP 9:1616-1632.

Wu S, Green MR (1997) Identification of a human protein that recognizes the 3' splice site during the second step of pre-mRNA splicing. The EMBO journal 16:4421-4432.

Yan J, Deng HX, Siddique N, Fecto F, Chen W, Yang Y, Liu E, Donkervoort S, Zheng JG, Shi Y, Ahmeti KB, Brooks B, Engel WK, Siddique T (2010) Frameshift and novel mutations in FUS in familial amyotrophic lateral sclerosis and ALS/dementia. Neurology 75:807-814.

Yang L, Embree LJ, Hickstein DD (2000) TLS-ERG leukemia fusion protein inhibits RNA splicing mediated by serine-arginine proteins. Molecular and cellular biology 20:3345-3354.

Yang L, Embree LJ, Tsai S, Hickstein DD (1998) Oncoprotein TLS interacts with serine-arginine proteins involved in RNA splicing. The Journal of biological chemistry 273:27761-27764.

Zhang YJ, Gendron TF, Xu YF, Ko LW, Yen SH, Petrucelli L (2010) Phosphorylation regulates proteasomal-mediated degradation and solubility of TAR DNA binding protein-43 C-terminal fragments. Molecular neurodegeneration 5:33.

Zinszner H, Sok J, Immanuel D, Yin Y, Ron D (1997) TLS (FUS) binds RNA in vivo and engages in nucleo-cytoplasmic shuttling. Journal of cell science 110 (Pt 15):1741-1750.

8 Index

8.1 List of figures

8.2 List of tables

9 Glossary

%	percentage
°C	degree Celsius
µg	microgram
µl	microlitre
µm	micrometre
A	alanine
AD	Alzheimer disease
ALS	Amyotrophic lateral sclerosis
ALS-FUS	ALS with inclusions positive for the protein FUS
ALS-SOD	ALS with inclusions positive for the protein SOD-1
ALS-TDP	ALS with inclusions positive for the protein TDP-43
Ca^{2+}	calcium
$CaCl_2$	calcium chloride
CO_2	carbon dioxide
D	aspartic acid
DAPI	4',6-diamidino-2-phenylindole
dH_2O	distilled water
Dpn	Diplococcus pneumoniae
EDTA	Ethylenediaminetetraacetic acid
F	phenylalanine
FALS	ALS with positive family history
FBS/FCS	fetal bovine serum / fetal calf serum
FTD	Frontotemporal dementia
FTLD	Frontotemporal lobar degeneration
FTLD-FUS	FTLD with inclusions positive for the protein FUS
FTLD-TDP	FTLD with inclusions positive for the protein TDP-43
FTLD-UPS	FTLD with unknown protein inclusions
FUS	fused in sarcoma
g	gram
HA-FUSwt	HA-tagged wild type FUS
HA-tag	Human influenza hemagglutinin
HBS	HEPES buffered saline
HEK293	human embryonic kidney cells

HeLa	human cervical carcinoma cells taken from Henrietta Lacks
HEPES	2-(4-(2-Hydroxyethyl)- 1-piperazinyl)-ethansulfonsäure
K^+	potassium
l	litre
LB	lysogeny broth
M	molar
mg	milligram
Mg^{2+}	magnesium
min	minutes
ml	millilitre
mM	millimolar
Na^+	sodium
Na_2HPO_4	disodium hydrogen phosphate
NaCl	sodium chloride
ng	nanogram
nM	nanomolar
nm	nanometre
PBS	Phosphate buffered saline
pH	potentia Hydrogenii; power of hydrogen
rpm	revolutions per minute
S	serine
SALS	sporadic ALS
T	threonine
TDP	TAR-DNA binding protein
TLS	translocated in liposarcoma
WT	wild type
Y	tyrosine